

**MUTATIONAL ANALYSIS OF THE ACTIVE SITE
RESIDUES ASPARTATE 313 AND TYROSINE 435 OF
CHITINASE A FROM A MARINE BACTERIUM**

Vibrio harveyi



Natchanok Sritho

A Thesis Submitted in Partial Fulfillment of the Requirements for the

Degree of Master of Science in Biochemistry

Suranaree University of Technology

Academic Year 2009

การวิเคราะห์การกลายพันธุ์ของกรดอะมิโนที่บริเวณเร่ง Aspartate 313 และ
Tyrosine 435 ของเอนไซม์ไลติเนส เอ จากเชื้อแบคทีเรียในทะเล
Vibrio harveyi



นางสาวนารถชนก ศรีโท

วิทยานิพนธ์นี้เป็นส่วนหนึ่งของการศึกษาตามหลักสูตรปริญญาวิทยาศาสตรมหาบัณฑิต
สาขาวิชาชีวเคมี
มหาวิทยาลัยเทคโนโลยีสุรนารี
ปีการศึกษา 2552

**MUTATIONAL ANALYSIS OF THE ACTIVE SITE RESIDUES
ASPARTATE 313 AND TYROSINE 435 OF CHITINASE A
FROM A MARINE BACTERIUM *Vibrio harveyi***

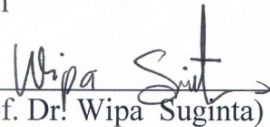
Suranaree University of Technology has approved this thesis submitted in partial fulfillment of the requirements for a Master's Degree.

Thesis Examining Committee



(Assoc. Prof. Dr. Malee Tangsathitkulchai)

Chairperson



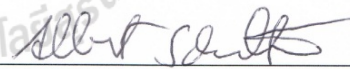
(Assoc. Prof. Dr. Wipa Suginta)

Member (Thesis Advisor)



(Assoc. Prof. Dr. James R. Ketudat Cairns)

Member



(Assoc. Prof. Dr. Albert Schulte)

Member



(Dr. Panida Khunkaewla)

Member



(Assoc. Prof. Dr. Prapun Manyum)



(Prof. Dr. Sukit Limpijumnong)

Vice Rector for Academic Affairs

Dean of Institute of Science

นารถชนก ศรีโท : การวิเคราะห์การกลายพันธุ์ของกรดอะมิโนที่บริเวณเร่ง Aspartate 313 และ Tyrosine 435 ของเอนไซม์ไคตินเนส เอ จากเชื้อแบคทีเรียในทะเล *Vibrio harveyi* (MUTATIONAL ANALYSIS OF THE ACTIVE SITE RESIDUES ASPARTATE 313 AND TYROSINE 435 OF CHITINASE A FROM A MARINE BACTERIUM *Vibrio harveyi*) อาจารย์ที่ปรึกษา : รองศาสตราจารย์ ดร.วิภา สุจินต์, 139 หน้า.

ไคตินเนส เอ จากเชื้อแบคทีเรียในทะเล *Vibrio harveyi* เป็นเอนไซม์ในกลุ่มไกลโคซิลไฮโดรเลส เร่งปฏิกิริยาการย่อยสลายไคติน จากโครงสร้าง 3 มิติพบว่า กรดอะมิโน aspartate 313 และ tyrosine 435 อยู่ที่ตำแหน่งจับ -1 และ +2 เพื่อเข้าจับบทบาทและหน้าที่ของกรดอะมิโนดังกล่าว จึงทำการกลายพันธุ์แบบเฉพาะตำแหน่ง ได้แก่ โพรตีนกลายพันธุ์ D313A D313N Y435A และ Y435W โพรตีนดั้งเดิม มี pH ที่เหมาะสมที่ 6 การกลายพันธุ์ที่ตำแหน่ง Asp313 ทุกช่วง pH มีผลต่อค่า k_{cat} และค่า k_{cat}/K_m แต่ไม่มีผลต่อการเปลี่ยนแปลงค่า K_m จากการศึกษาความสามารถในการย่อยสลายตัวถูกย่อยและรูปแบบการย่อยสลายตัวถูกย่อยไคตินด้วยวิธี TLC ของ โพรตีนกลายพันธุ์ D313A/N ทั้งสองนี้ทำให้การทำงานของเอนไซม์ไคตินเนส เอ ลดลง สำหรับการกลายพันธุ์ที่ตำแหน่ง Tyr435 พบว่ามีการเพิ่มขึ้นของการเร่งปฏิกิริยาและการจับกับตัวถูกย่อยทั้งหมด โดยทำการทดลองจากโพรตีนกลายพันธุ์ Y435A กับเทคนิคทางชีวเคมีต่างๆ ในขณะที่การกลายพันธุ์ของ Tyr435 ด้วย Trp พบว่าการเร่งปฏิกิริยาและการจับกับตัวถูกย่อยลดลง จึงสามารถสรุปผลการทดลองได้ว่ากรดอะมิโน Asp313 มีความสำคัญในการช่วยย่อยสลายตัวถูกย่อยโดยทำหน้าที่ช่วยให้สารตัวกลาง oxazolanium มีความเสถียร ส่วนกรดอะมิโน Tyr 435 ทำหน้าที่ในการเป็นตัวกั้นที่จุดปลายของน้ำตาลด้านปลายรีดิวซ์

สาขาวิชาชีวเคมี
ปีการศึกษา 2552

ลายมือชื่อนักศึกษา นารถชนก
ลายมือชื่ออาจารย์ที่ปรึกษา วิภา สุจินต์

NATCHANOK SRITHO : MUTATIONAL ANALYSIS OF THE ACTIVE
SITE RESIDUES ASPARTATE 313 AND TYROSINE 435 OF CHITINASE
A FROM A MARINE BACTERIUM *Vibrio harveyi*. THESIS ADVISOR :
ASSOC. PROF. WIPA SUGINTA, Ph.D. 139 PP.

CHITINASE A VIBRIO SITE-DIRECTED MUTAGENESIS KINETICS CHITIN

Chitinase A (EC 3.2.1.14) from *Vibrio harveyi* belongs to glycosyl hydrolase family-18. The X-ray structure of chitinase A in complex with GlcNAc₆ displays Asp313 at subsite -1 and Tyr435 at subsite +2. Site-directed mutagenesis at residues Asp313 and Tyr435 generated four mutants namely D313A, D313N, Y435A, and Y435W. The pH activity profiles revealed the optimum pH of the wild-type enzyme as 6.0 and the pK_a values of the two ionizable groups of 4 and 8. Mutation of Asp313 severely affected the k_{cat} and the k_{cat}/K_m over the entire range of pH, although it did not significantly change the K_m values. The dramatic effects of the Asp313 mutations on the hydrolytic and binding activities of *V. harveyi* chitinase A further confirmed the important role of this residue in stabilization of the transition state through the “substrate-assisted” mechanism. Regarding Tyr435 mutations, the Y435A mutant enzyme showed increased catalytic activity, suggesting that Ala substitution might partially remove the steric clash around the reducing subsites, thereby allowing the sugar chain to move beyond or to access the reducing end subsites more straightforwardly.

School of Biochemistry

Academic Year 2009

Student's Signature Natchanok.

Advisor's Signature Wipa Suginta

ACKNOWLEDGEMENTS

I would like to express my deepest gratitude to my thesis advisor, Assoc. Prof. Dr. Wipa Suginta for providing me a financial support throughout my study and a great opportunity for me to work on the chitinase project. I am grateful for her timely and invaluable guidance.

My gratitude also extends to Assoc. Prof. Dr. Albert Schulte and Dr. Panida Khunkaewla for investing their time and providing valuable advice to improve my thesis preparation.

I would like to thank Dr. Chomphunuch Songsiriritthigul at the Synchrotron Light Research Institute (SLRI), Thailand who helps to demonstrate the TLC technique.

I special like to thank Miss Supansa Pantoom for all her guidance on several key biochemical techniques.

I would like to thank all members of the School of Biochemistry and especially to the members of the Biochemistry and Electrochemistry Research Unit at Suranaree University of Technology who helped me along the course of the work.

Finally, special thanks are given to my family for their support, infinite love and care throughout my life.

Natchanok Sritho

CONTENTS

	Page
ABSTRACT IN THAI.....	I
ABSTRACT IN ENGLISH	II
ACKNOWLEDGEMENTS.....	III
CONTENTS.....	IV
LIST OF TABLES.....	IX
LIST OF FIGURES	X
LIST OF ABBREVIATIONS.....	XV
CHAPTER	
I INTRODUCTION.....	1
1.1 Chitin Structure and Applications.....	1
1.2 Overview of Chitinases	3
1.3 Classification of Chitinases.....	6
1.4 The Catalytic Mechanism of Chitinases	9
1.5 Multiple Forms of Bacterial Family 18 Chitinases.....	11
1.6 Structural Analysis of Bacteria Family 18 Chitinases	13
1.6.1 Structural Analysis of Chitinase A.....	13
1.6.2 Structural Analysis of Chitinase B.....	16
1.6.3 Structural Analysis of Chitinase A1.....	18
1.6.4 Structural Analysis of Chitinase C.....	20

CONTENTS (Continued)

	Page
1.7 Measurement of Chitinase Activities Measurement of Chitinase Activities	21
1.8 Background of Chitinase A from <i>V. harveyi</i>	23
1.8.1 Expression of <i>V. harveyi</i> Chitinase A	23
1.8.2 Function and Characterization of Chitinase A from <i>V. harveyi</i>	24
1.8.3 Mutational Analysis of the Active Site Residues.....	24
1.8.4 Substrate Binding Modes Anomer Selectivity.....	26
1.8.5 Mutational Analysis of the Surface-Exposed Residues	28
1.8.6 Structural Determination of <i>V. harveyi</i> Chitinase A	29
1.7 Research Objectives	35
II MAERIALS AND METHODS	36
2.1 Bacterial Strains and Vector.....	36
2.2 Chemicals and Reagents	37
2.3 Instrumentation	38
2.4 General Methods	38
2.4.1 Site-Directed Mutagenesis	38
2.4.2 Expression of Recombinant Chitinase A in <i>E. coli</i> M15	41
2.4.3 Purification of Recombinant Chitinase A Variants.....	41
2.4.4 Determination of Protein Concentration by Bradford's Method	42
2.4.5 Sodium Dodecyl Sulfate Polyacrylamide Gel Electrophoresis.....	42

CONTENTS (Continued)

	Page
2.4.6 Thin-Layer Chromatography (TLC) Analysis of the Hydrolytic Products	43
2.4.7 Determination of Chitinase A Activity	44
2.4.8 Determination of Specific Hydrolyzing Activity	44
2.4.9 Chitin Binding Assay and Determination of Equilibrium Adsorption Isotherm.....	46
2.4.10 Steady-State Kinetics	46
2.4.11 Determination of Asp313 Mutations on pH Activity Profile.....	47
III RESULTS	49
3.1 Structure Analysis and Site Directed Mutation	49
3.2 Structural Comparisons of <i>V. harveyi</i> Chitinase A and <i>S. marcescens</i> Chitinase A.....	53
3.3 Structural Comparisons of <i>V. harveyi</i> Chitinase A and <i>S. marcescens</i> Chitinase B	55
3.4 Structural Comparisons of <i>V. harveyi</i> Chitinase A and <i>S. marcescens</i> Chitinase A1	57
3.5 Expression and Purification of the Recombinant Chitinase A and it Asp313 and Tyr435 Mutants	59
3.6 Effects of pH Asp313 Mutations on the pH Activity Profile.....	61

CONTENTS (Continued)

	Page
3.7 Effects of Mutations on the Specific Hydrolyzing Activities of Wild-type Chitinase A and Mutants	64
3.8 TLC Analysis of the Hydrolytic Products of Wild-type Chitinase A and Mutants	66
3.8.1 TLC Analysis of GlcNAc ₂ Hydrolysis	66
3.8.2 TLC Analysis of GlcNAc ₃ Hydrolysis	68
3.8.3 TLC Analysis of GlcNAc ₄ Hydrolysis	70
3.8.4 TLC Analysis of GlcNAc ₅ Hydrolysis	72
3.8.5 TLC Analysis of GlcNAc ₆ Hydrolysis	74
3.8.6 TLC Analysis of Colloidal Chitin Hydrolysis	76
3.8.7 TLC Analysis of Glycol Chitin Hydrolysis	78
3.9 Steady-State Kinetics of Chitinase A and Mutants	80
3.9.1 Steady-State Kinetics of <i>p</i> NP-GlcNAc ₂ Hydrolysis	80
3.9.2 Steady-State Kinetics of GlcNAc ₃ Hydrolysis	82
3.9.3 Steady-State Kinetics of GlcNAc ₄ Hydrolysis	84
3.9.4 Steady-State Kinetics of GlcNAc ₅ Hydrolysis	86
3.9.5 Steady-State Kinetics of GlcNAc ₆ Hydrolysis	88
3.9.6 Steady-State Kinetics of Colloidal Chitin Hydrolysis	90
3.9.6 Steady-State Kinetics of Glycol Chitin Hydrolysis	92
3.10 Effects of Mutations on the Chitin Binding Activities	94

CONTENTS (Continued)

	Page
IV DISCUSSION	101
4.1 Site-Directed Mutagenesis of DxxDxDxE Motif of family 18 Chitinases	101
4.2 Influence of the Asp313 Mutants on the pH Activity Profile	103
4.3 Reaction Patterns of the Chitinase A and its Mutants.....	105
4.4 The Effects of Mutations on the Specific Hydrolyzing Activity	106
4.5 The Effects of Mutations on Chitin Binding Activity	107
V CONCLUSION	110
REFERENCES	111
APPENDICES	124
APPENDIX A SOLUTION AND REAGENT PREPARATION	125
APPENDIX B STRANDA DE CURVEDS.....	136
APPENDIX C ABSTRACT SUBMIT	138
CURRICULUM VITAE.....	139

LIST OF TABLES

Table	Page
1.1 Role of chitinases in different organisms.....	5
2.1 Primers for site-directed mutagenesis.....	39
3.1 Specific hydrolyzing activity of chitinase A and its mutants	65
3.2 Kinetic parameters of <i>p</i> NP-GlcNAc ₂ hydrolysis.....	81
3.3 Kinetic parameters of GlcNAc ₃ hydrolysis.....	83
3.4 Kinetic parameters of GlcNAc ₄ hydrolysis.....	85
3.5 Kinetic parameters of GlcNAc ₅ hydrolysis.....	87
3.6 Kinetic parameters of GlcNAc ₆ hydrolysis	89
3.7 Kinetic parameters of colloidal chitin hydrolysis	93
3.8 Kinetic parameters of glycol chitin hydrolysis	95
3.9 Binding of crystalline chitin by chitinase A wild-type and mutants.....	96
3.10 Binding of colloidal chitin by chitinase A wild-type and mutants	98
3.11 Binding of chitosan by chitinase A wild-type and mutants	100
4.1 Site-directed mutagenesis on DxxDxDxE motif of family 18 chitinases	102

LIST OF FIGURES

Figure	Page
1.1	Chemical structures of cellulose and chitin 1
1.2	Arrangement of the α -chitin, β -chitin and γ -chitin 2
1.3	Preparation of chitin derivatives and chitosan from chitin 3
1.4	Schematic drawing of the cleaved patterns of chitinolytic enzymes 6
1.5	A ribbon representation of the main structural characteristics of the catalytic domains of the family 18 and 19 chitinases 8
1.6	The two conformations of catalyzed chitin chains by chitinases 9
1.7	The catalytic mechanism of family 18 and 19 chitinases 11
1.8	Modular architecture of chitinases A, A1, B, C1 C2 and D1 13
1.9	A structure of chitinase A from <i>S.marcescens</i> 14
1.10	The 3D structure of <i>S. marcescens</i> chitinase A mutant E315L with the GlcNac ₆ 15
1.11	The model for crystalline β -chitin hydrolysis by chitinase A 16
1.12	A structure of chitinase B from <i>S.marcescens</i> 16
1.13	The surface structure of chitinase B from <i>S.marcescens</i> 17
1.14	Chain-folding topology and structure of the CatD of chitinase A1 of <i>B. circulans</i> 18
1.15	The solution structure of ChBD and FnIIID of chitinase A1 of <i>B. circulans</i> 19

LIST OF FIGURES (Continued)

Figure	Page
1.16 The catalytic domain of chitinase A1 from <i>B. circulans</i> complexed with GlcNAc ₇	20
1.17 The stick model of the putative binding cleft of <i>V. harveyi</i> chitinase A was superimposed on that of <i>S. marcescens</i> chitinase A mutant E315L with the GlcNAc ₆	25
1.18 The possible models of chitinoligosaccharide bindings to the multiple binding subsites of <i>V. harveyi</i> chitinase A	27
1.19 The representation of the 3D structure of <i>V. harveyi</i> chitinase A was constructed based on the X-ray structure of <i>S. marcescens</i> chitinase A E315L mutant	29
1.20 The structure of catalytically inactive mutant E315M complexed with GlcNAc ₆ of <i>V. harveyi</i> chitinase A	30
1.21 Surface representation of mutant E315M showing the positions of the regularly-spaced, surface-exposed hydrophobic residues	31
1.22 Structural comparisons of GlcNAc ₅ and GlcNAc ₆ in the catalytic cleft of mutant E315M	32
1.23 Specific interactions within the substrate-binding cleft of mutant E315M interactions of GlcNAc ₅ and GlcNAc ₆	33
1.24 The schematic diagram highlighting the proposed catalytic mechanism of <i>V. harveyi</i> chitinase A	34
2.1 Mapping of pQE-60 vector	36

LIST OF FIGURES (Continued)

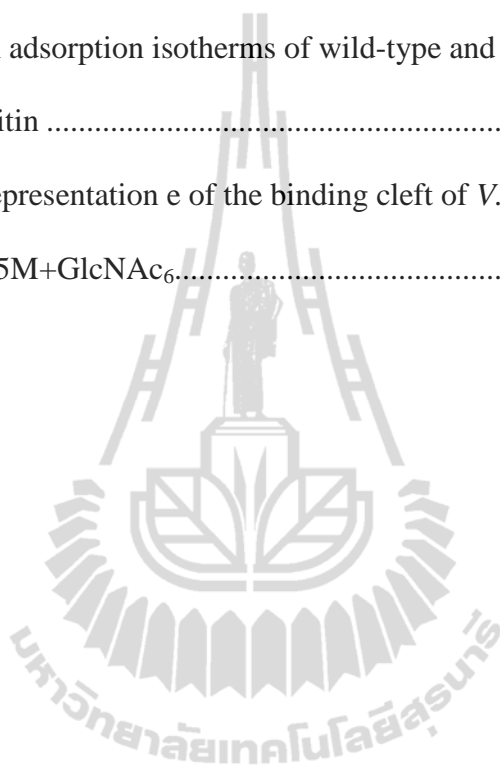
Figure	Page
2.2	Schematic of the Quickchange® Site-Directed Mutagenesis Kit..... 40
3.1	Surface representation of the 3D-structure of <i>V. harveyi</i> chitinase A E315M mutant bound with GlcNAc ₆ 50
3.2	Superimposition of the interactions of the binding residues of wild-type and E315M+GlcNAc ₆ complex in the active cleft 52
3.3	Superimposition of <i>V. harveyi</i> chitinase A and <i>S. marcescens</i> chitinase A structure 54
3.4	Superimposition of <i>V. harveyi</i> chitinase A and <i>S. marcescens</i> chitinase B structure 56
3.5	Superimposition of <i>V. harveyi</i> chitinase A and <i>B. circulans</i> chitinase A1 structure 58
3.6	Purification of the recombinant chitinase A and mutants using Ni-NTA agarose affinity chromatography..... 60
3.7	SDS-PAGE analysis of purified chitinase A and its mutants 61
3.8	Effects of mutations on the pH activity profiles of <i>V. harveyi</i> chitinase A 63
3.9	Time course of GlcNAc ₂ hydrolysis by <i>V. harveyi</i> chitinase A mutants as analyzed by TLC..... 67
3.10	Time course of GlcNAc ₃ hydrolysis by <i>V. harveyi</i> chitinase A mutants as analyzed by TLC..... 69
3.11	Time course of GlcNAc ₄ hydrolysis by <i>V. harveyi</i> chitinase A mutants as analyzed by TLC..... 71

LIST OF FIGURES (Continued)

Figure	Page
3.12 Time course of GlcNAc ₅ hydrolysis by <i>V. harveyi</i> chitinase A mutants as analyzed by TLC.....	73
3.13 Time course of GlcNAc ₆ hydrolysis by <i>V. harveyi</i> chitinase A mutants as analyzed by TLC.....	75
3.14 Time course of colloidal chitin hydrolysis by <i>V. harveyi</i> chitinase A mutants as analyzed by TLC.....	77
3.15 Time course of glycol chitin hydrolysis by <i>V. harveyi</i> chitinase A mutants as analyzed by TLC.....	79
3.16 The Michaelis-Menten plot of <i>p</i> NP-GlcNAc ₂ hydrolysis	81
3.17 The Michaelis-Menten plot of GlcNAc ₃ hydrolysis	83
3.18 The Michaelis-Menten plot of GlcNAc ₄ hydrolysis	85
3.19 The Michaelis-Menten plot of GlcNAc ₅ hydrolysis	87
3.20 The Michaelis-Menten plot of GlcNAc ₆ hydrolysis	89
3.21 The Michaelis-Menten plot of colloidal chitin hydrolysis.....	91
3.22 The Michaelis-Menten plot of glycol chitin hydrolysis.....	93
3.23 Binding of chitinase A and mutants to insoluble chitin.....	94
3.24 Equilibrium adsorption isotherms of wild-type and mutant chitinases A to crystalline chitin.....	96
3.25 Equilibrium adsorption isotherms of wild-type and mutant chitinases A to colloidal chitin	98

LIST OF FIGURES (Continued)

Figure	Page
3.26 Equilibrium adsorption isotherms of wild-type and mutant chitinases A to colloidal chitin	100
4.1 A surface representation of the binding cleft of <i>V. harveyi</i> chitinase A mutant E315M+GlcNAc ₆	109



LIST OF ABBREVIATIONS

BSA	=	Bovine Serum Albumin
(m, μ) g	=	(milli, micro) Gram
(m, μ) L	=	(milli, micro) Liter
(m, μ) M	=	(milli, micro) Molar
$^{\circ}\text{C}$	=	Degree Celsius
\AA	=	Angstrom
CatD	=	Catalytic Domain
ChBD	=	Chitin-Binding Domain
cm	=	Centimeter
DNS	=	3, 5-Dinitrosalicylic Acid
E_b	=	Bound Enzyme Concentration
EDTA	=	Ethylenediamine Tatre-acetic Acid
E_f	=	Free Enzyme Concentration
E_t	=	Total Enzyme Concentration
FnIIID	=	Fibronectin Type III-like Domain
GlcNAc	=	<i>N</i> -acetyl-D-glucosamine
h	=	Hour
IPTG	=	Isopropyl- β -D-thiogalactoside
K_{cat}	=	Turnover Number
K_d	=	Dissociation Constants

LIST OF ABBREVIATIONS (Continued)

kDa	=	Kilo Dalton
LB	=	Luria-Bertani Medium
min	=	Minute
M_r	=	Relative Molecular Mass
Ni-NTA	=	Nickel-Nitrilotriacetic Acid
nm	=	Nanometers
NRE	=	Non-Reducing End
OD	=	Optical density
PAGE	=	Polyacrylamide Gel Electrophoresis
PCR	=	Polymerase Chain Reaction
<i>p</i> NP	=	<i>p</i> -Nitrophenolate
RE	=	Reducing End
rpm	=	Rotation per Minute
s	=	Second
SDS	=	Sodium Dodecyl Sulfate
TEMED	=	Tetramethylenediamine
TLC	=	Thin-Layer Chromatography
Tris	=	Tris-(hydroxymethyl)-aminoethane
UV	=	Ultraviolet
V	=	Volt
v/v	=	Volume/Volume
w/v	=	Weight/Volume

CHAPTER I

INTRODUCTION

1.1 Chitin Structure and Applications

Chitin ($C_8H_{13}O_5N$)_n is a long-chain insoluble polysaccharide consists of *N*-acetyl-D-glucosamine (GlcNAc) residues connected via β -1, 4 glycosidic bonds. Hence, it may also be described as cellulose with one hydroxyl group on each monomer replaced by an acetylamin group, as shown in Figure 1.1 (Cohen-Kupiec and Chet, 1998; Gooday, 1990). Chitin is the main component of the cell walls of fungi, the shells and radulae of molluscs and of the exoskeletons of arthropods, especially crustaceans and insects.

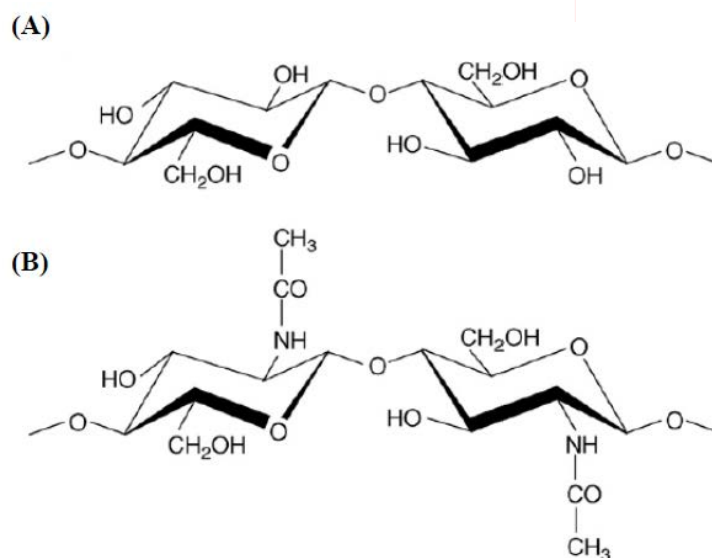


Figure 1.1 Chemical structures of (A) cellulose and (B) chitin (Eijsink *et al.*, 2008).

X-ray diffraction analysis suggested that chitin occurs in three crystalline forms, mainly alpha-, beta- and gamma-chitin, which differ in the arrangement of the molecular chains within the crystal cell. The α -chitin is characterized by anti-parallel chains and is the most abundant in nature. It occurs in the shells of crustaceans, in skeletons of mollusks and krill, insects and in the cell walls of fungi (Gardner and Blackwell, 1975). The β -chitin has parallel chains and which are in squid pens, in the extracellular spines of the euryhaline diatom (Herth and Barthlott, 1979), and in pogonophore tubes (Blackwell, 1969). The γ -chitin, has a mixture of two to one parallel to anti-parallel (Seidl, 2008), and is found in the cocoons of insects (Rudall and Kenchington, 1973) (Figure 1.2).

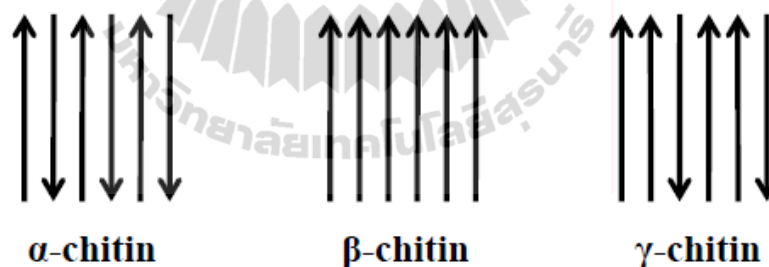


Figure 1.2 Arrangement of the α -chitin, β -chitin and γ -chitin.

Chitin has a broad range of applications in biochemical, food and various chemical industries. It has antimicrobial, anticholesterol and antitumor activities (Gooday, 1999; Patil *et al.*, 2000). Chitin and its related materials are also used in wastewater treatment (Flach *et al.*, 1992), drug delivery (Kadowaki *et al.*, 1997), wound healing and dietary fiber (Dixon, 1995; Muzzarelli, 1977; Muzzarelli *et al.*, 1999). A serious pollution from chitin wastes released from seafood industries leads

to an interest to bioconvert chitin to utilizable carbohydrates. The chitin-derived products such as chitosans, derivatives of chitin/chitosan, oligosaccharides and glucosamine, have been prepared by chemical and enzymatic methods as shown in Figure 1.3. However, the chitin hydrolyzed by chemical occurs via a series of chemical reactions-generate unwanted by-products. On the other hand, enzymatic hydrolysis of chitin usually takes place under mild conditions, in which the selectivity of the end products depends on the substrate specificity of chitinolytic enzymes.

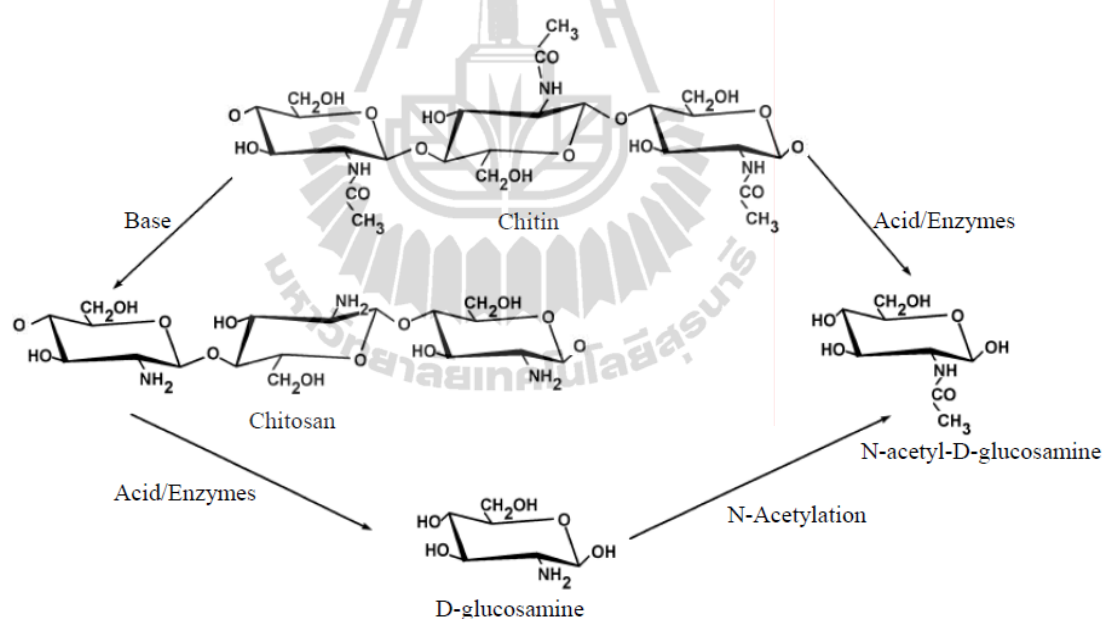


Figure 1.3 Preparation of chitin derivatives and chitosan from chitin (modified from Shahidi *et al.*, 1999).

1.2 Overview of Chitinases

Chitinase was first observed by Bernard in 1911, when he isolated a thermostable and diffusible chitinolytic fraction from orchid pulp. A further report was on a

chitinase in snail by Karrer and Hoffma (Flach *et al.*, 1992). In recent years, there has been a lot of research for enhanced production of chitinases from microorganisms using DNA technology.

Chitinases (EC3.2.1.14) are a group of hydrolytic enzymes that catalyze depolymerisation of chitin. Chitin degradation is initiated by chitinases to chitooligosacchride chains which are subsequently degraded to metabolizable GlcNAc monomer by chitobiasis or β -*N*-acetylglucosaminidases (EC3.2.1.52). Chitinases are typically found in organisms that possess chitin as a structural constituent, such as fungi, yeast, crustaceans and insects. It is, however, also present in organisms that do not synthesize chitin such as bacteria, plants and vertebrates (Jeuniaux, 1966). The physiological functions of chitinases depend on their sources as shown in Table 1.1.

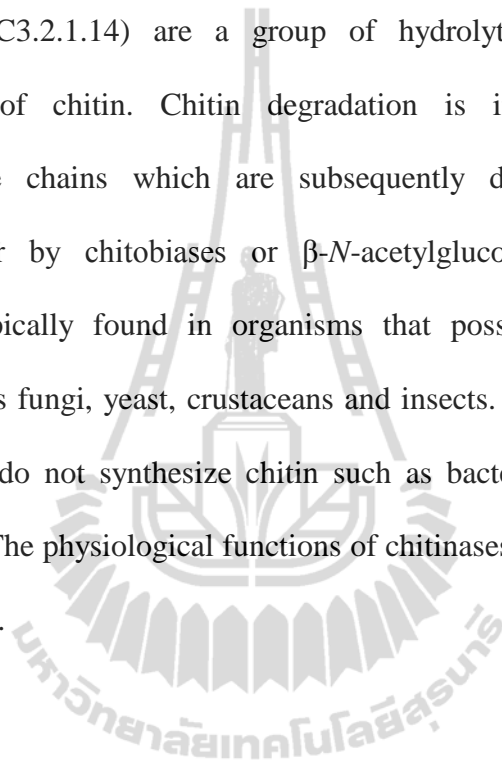


Table 1.1 Roles of chitinases in different organisms.

Organism	Roles of chitinases	References
Bacteria	Required for breaking down chitin, which generally serves as a carbon and nitrogen nutritional source.	Cottrell <i>et al.</i> , 1999; Gooday, 1990
Viruses	Involve in pathogenesis.	Patil <i>et al.</i> , 2000
Fungi	Involve in cell division, differentiation and nutritional roles related to mycoparasitic activity.	Gooday <i>et al.</i> , 1992; Kuranda <i>et al.</i> , 1991
Plants	Play a defense mechanism against fungal and bacterial pathogens by degradation of their cell walls. Specific isoforms may play a role in embryo development, pollination and sexual reproduction.	Jach <i>et al.</i> , 1995; Taira <i>et al.</i> , 2002
Insects	Involve in developmental process of cuticle degradation at different larval stages.	Taira <i>et al.</i> , 2002
Protozoa	Participate in life cycle of parasites. For example, malarial parasites produce chitinases to penetrate the chitin containing peritrophic matrix of the mosquito midgut.	Langer <i>et al.</i> , 2002
Yeast	Has an essential function in cell separation during budding of the chitinous yeast <i>Saccharomyces cerevisiae</i> .	Carstens <i>et al.</i> , 2003; David, 2004
Animals	Play a digestive role.	Jeuniaux <i>et al.</i> , 1961; Lundblad <i>et al.</i> , 1974
Human	Involve in asthma and inflammatory conditions.	Elias <i>et al.</i> , 2005; Kawada <i>et al.</i> , 2007; Wills-Karp and Karp, 2004

1.3 Classification of Chitinases

Chitinases are divided into endo- and exochitinases (Cohen-Kupiec and Chet, 1998). Endochitinases cleave chitin randomly at internal sites, generating soluble chitooligo fragments, such as GlcNAc₂, GlcNAc₃ and GlcNAc₄ (Sahai and Manocha, 1993). On the other hand, exochitinases catalyze the progressive release of GlcNAc₂ via an action that starts at the non-reducing end of the chitin microfibril. *N*-acetylglucosaminidases (also known as chitobiases) catalyze the release of terminal, non-reducing GlcNAc residues from chitin, but in general they have highest affinity for the GlcNAc₂ the major product of chitin hydrolysis by chitinases and convert it into two GlcNAc as shown in Figure 1.4 (Horsch *et al.*, 1997; Suzuki *et al.*, 2002).

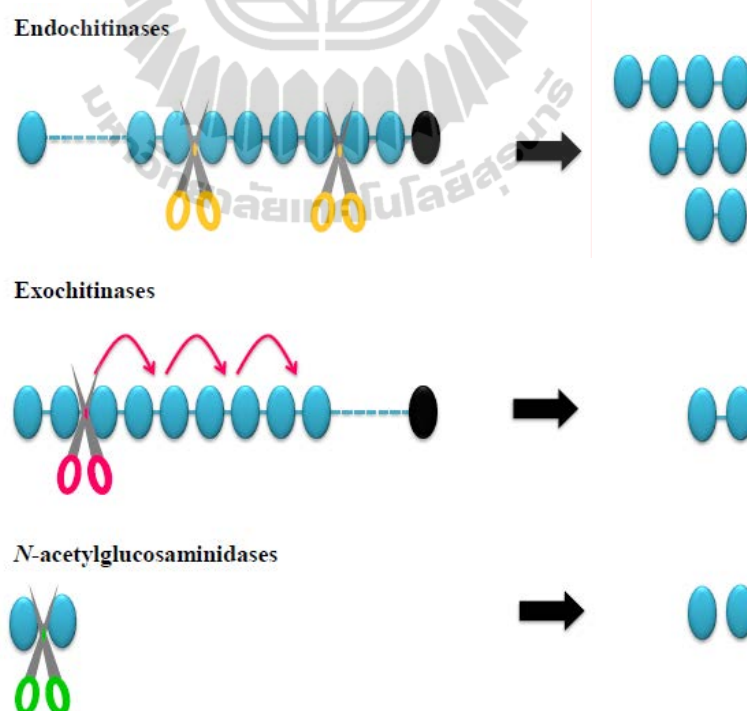


Figure 1.4 Schematic drawing of the cleaved patterns of chitinolytic enzymes. The non-reducing end is on the left and the reducing end on the right (modified from Seidl, 2008).

In the carbohydrate active enzymes (CAZy) database (<http://www.cazy.org/>), carbohydrate enzymes are classified based on the similarity of their amino acid sequence and their catalytic domain as glycosyl hydrolases (GHs), glycosyl transferases (GTs), polysaccharide lyases (PLs), and carbohydrate esterases (CEs). Chitinases are members of glycosyl hydrolases family 18 and family 19. Both families show little homology, differing in both structure and mechanism (Davids and Henrissat, 1995; Henrissat, 1991; Henrissat and Bairoch, 1993). Families 18 chitinases are mainly produced by bacteria, fungi, virus, plants and animals. Family 18 enzymes have substantial sequence divergence, whereas family 19 chitinases are almost exclusively found in plants, and have a high degree of sequence identity (Lu *et al.*, 2002). A chitinase from a Gram-positive bacterium *Streptomyces griseus* HUT 6037 was identified as the first family 19 chitinase (Ohno *et al.*, 1996).

The catalytic domain of family 18 chitinases consists of a $(\beta/\alpha)_8$ -triosephosphate isomerase (TIM) barrel with a deep substrate-binding cleft formed by the loop following the C-termini of the eight parallel β -strands. In contrast, the catalytic domain of family 19 chitinases does not possess a TIM-barrel structure, but is composed of two loops, each of which is rich in α -helical structure. The substrate binding cleft is positioned between the two loops as shown in Figure 1.5 (Aronson *et al.*, 2003; Hart *et al.*, 1995).

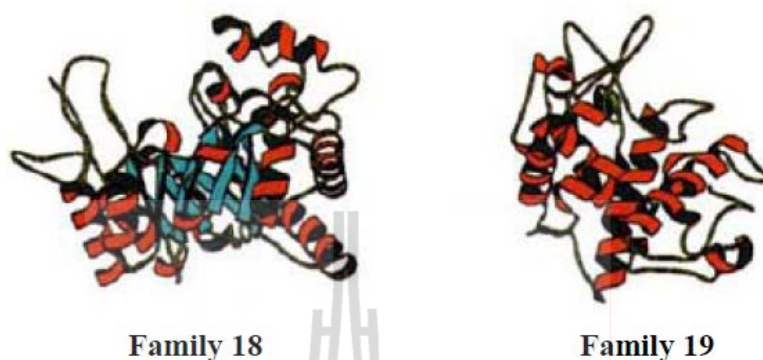


Figure 1.5 A ribbon representation of the main structural characteristics of the catalytic domains of the family 18 and 19 chitinases. β -strands are shown in cyan and α -helices in red (modified from Davies and Henrissat, 1995).

The mode of catalytic action of family 18 chitinases has been proposed to be the anchimeric stabilization or retaining mechanism (Brameld and Goddard, 1998). Catalysis by a retaining mechanism results in the preservation of the β -conformation (Aronson *et al.*, 2006; Brameld *et al.*, 1998; Suginta *et al.*, 2004; Tews *et al.*, 1997). On the other hand, the mode of action of family 19 chitinases employs the concerted single displacement mechanism, yielding an inversion of anomeric configuration with a predominant α -anomeric product as shown in Figure 1.6 (Brameld *et al.*, 1998).

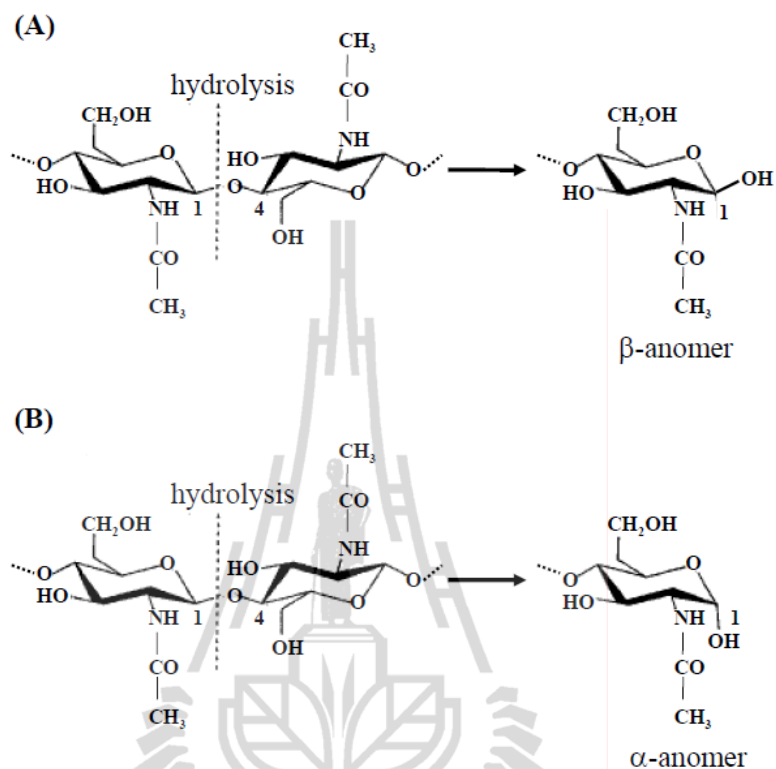


Figure 1.6 The two conformations of catalyzed chitin chains by chitinases (A) retention of β -conformation and (B) inversion of α -conformation (modified from Aronson *et al.*, 2006).

1.4 The Catalytic Mechanism of Chitinases

There are two major general mechanistic pathways that describe the acid hydrolysis catalyzed by glycosyl hydrolases namely, i) the retention of the stereochemistry of the anomeric oxygen at C1' relative to the initial configuration and ii) the inversion of the stereochemistry (Brameld and Goddard, 1998).

An example of retaining mechanism is hen egg white lysozyme. The mechanism is believed to proceed as follows. The β - (1, 4) glycosidic oxygen is first protonated (leading to an oxocarbenium ion intermediate), the stabilized by a second carboxylate

(either through covalent or electrostatic interactions). Nucleophilic attack by water yields the hydrolysis products, which necessarily retains the initial anomeric configuration. This is commonly referred to as the double-displacement mechanism of hydrolysis as shown in Figure 1.7(A).

Although the X-ray crystal structure of family 19 chitinase reveals a lysozyme-like fold suggesting a double-displacement mechanism, the hydrolysis products for two family 19 chitinases show inversion of anomeric configuration. This leads to the second commonly discussed hydrolysis mechanism, a concerted single-displacement reaction in which a bound water molecule acts as the nucleophile as shown in Figure 1.7(B).

Brameld and Goddard (1998) employed the molecular dynamics (MD) simulations to demonstrate the substrate binding and the possible resulting hydrolysis intermediates of chitinase A from *Serratia marcescens*. They found that the GlcNAc₆ substrate was forced to distort to boat sugar geometry at subsite -1 prior to protonation, which then led to spontaneous anomeric bond cleavage and subsequent formation of an oxazolinium ion. The X-ray diffraction analyses confirmed that the reaction mechanism of all the family 18 chitinases proceeds through the substrate-assisted catalytic mechanism as shown in Figure 1.7(C) (van Scheltinga *et al.*, 1995; Tews *et al.*, 1997).

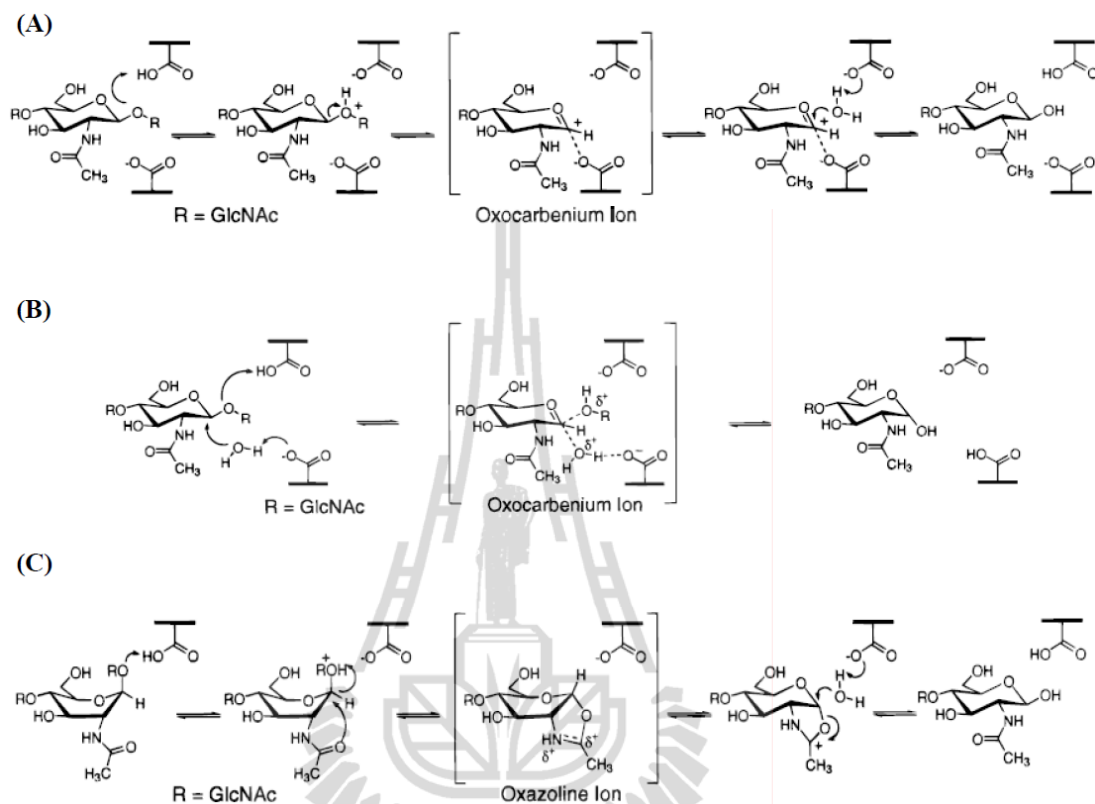


Figure 1.7 The catalytic mechanism of family 18 and 19 chitinases (A) double-displacement mechanism (B) single-displacement mechanism (C) anchimeric stabilization hydrolysis mechanism (modified from Brameld and Goddard, 1998).

1.5 Multiple Forms of Bacterial Family 18 Chitinases

Different bacteria secrete different forms of family 18 chitinases. *S. marcescens* is one of the most intensively studied chitinolytic bacterium. *S. marcescens* produces three types of chitinases: chitinase A (ChiA), chitinase B (ChiB), and chitinase C (ChiC1 and ChiC2) (Brurberg *et al.*, 1996; Suzuki *et al.*, 1998; 1999; 2002). Chitinase A1 (ChiA1), ChiC1 and chitinase D1 (ChiD1) are produced from *Bacillus circulans* (Alam *et al.*, 1996; Armand *et al.*, 1994; Jee *et al.*, 2002). *Streptomyces coelicolor* A3 (2) expressed ChiC (Kawase *et al.*, 2006). The Gram-negative marine bacterium *V.*

harveyi produces mainly ChiA (Suginta *et al.*, 2000; 2004; 2005) but *Alteromonas* sp. strain O-7 produces four different chitinases; ChiA, ChiB, ChiC and ChiD (Orikoshi *et al.*, 2003; Tsujibo *et al.*, 1993; 1994; 1995).

The distinct structure of ChiA consists of chitin-binding domain (ChBD) located at the *N*-terminus and a catalytic $(\beta/\alpha)_8$ TIM-barrel domain (CatD) with a small insertion domain inserted between the seventh and eighth β -strands of the catalytic $(\beta/\alpha)_8$ TIM-barrel domain at the *C*-terminus (Brurberg *et al.*, 2001). In contrast, ChiA1 from *B. circulans* comprises an *N*-terminal catalytic domain, two fibronectin type III-like domains (FnIIIDs) and the *C*-terminal ChBD (Watanabe *et al.*, 1990; 1994). On the other hand, the catalytic $(\beta/\alpha)_8$ TIM-barrel domain of ChiB is located at the *N*-terminus and the ChBD at *C*-terminus (Suzuki *et al.*, 1999). ChiC often occurs in two forms; the complete protein, sometimes called ChiC1 and a proteolytically truncated variant, called ChiC2. In ChiC1, the CatD is located at the *N*-terminus, FnIIID and the ChBD at *C*-terminus (Matsumoto *et al.*, 1999; Suzuki *et al.*, 1999) and ChiC2 is a derivative of ChiC1 generated by a removal of the FnIIID and the *C*-terminal ChBD (Suzuki *et al.*, 2002). Interestingly, ChiD1 from *B. circulans* also possesses an *N*-terminal ChBD that is similar to ChiA, but followed by FnIIID and a CatD at *C*-terminal as shown in Figure 1.8 (Ikegami *et al.*, 2000; Jee *et al.*, 2002).

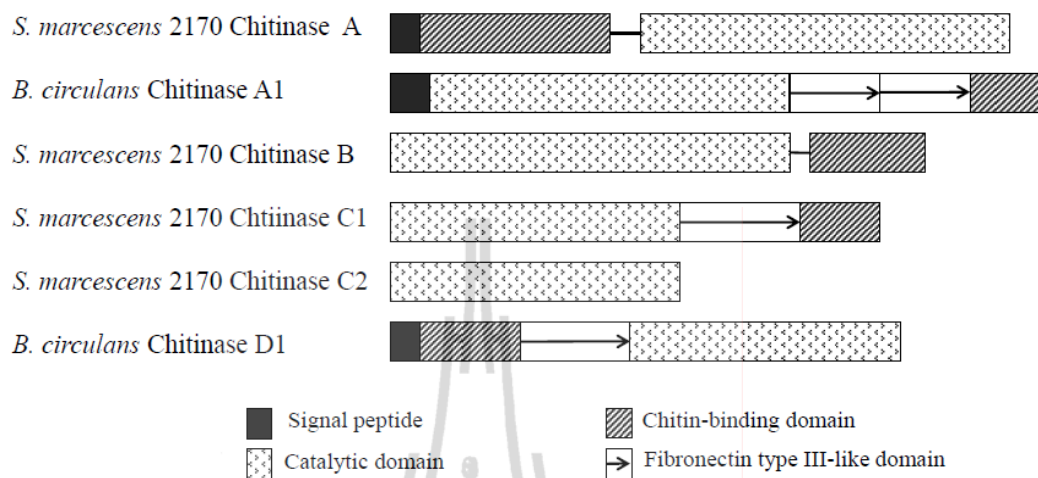


Figure 1.8 Modular architecture of chitinases A, A1, B, C1, C2 and D1 (modified from Brurberg *et al.*, 2000)

1.6 Structural Analysis of Bacterial Family 18 Chitinases

1.6.1 Structural Analysis of Chitinase A

The three-dimensional (3D) structure of bacterial chitinase A from *S. marcescens* was the first structure to be elucidated (Perrakis *et al.*, 1994). The crystal structure of this native enzyme was solved and refined to 2.3 Å resolutions. The overall structure of the *S. marcescens* ChiA consists of three domains: i) an N-terminal ChBD has a fold comprising mostly β -stands ii) a C-terminal catalytic domain has the TIM characteristic, which is referred as the β/α ₈-barrel fold comprising of eight β -strands tethered to eight α -helixes by loop and iii) a small insertion domain is a module inserted into the TIM barrel. Insertion domain comprises three α -helices and five β -strands. These strands make up all antiparallel β -strands, which are connected by β turns as shown in Figure 1.9.

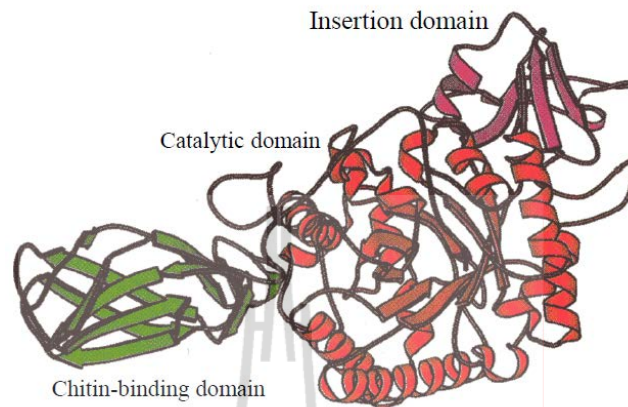


Figure 1.9 A structure of chitinase A from *S. marcescens* (Perrakis *et al.*, 1994).

Crystallographic studies of the complexes between *S. marcescens* chitinase A mutant E315L with GlcNAc₆ substrates demonstrated that the catalytic site of enzyme contained full occupancy of six substrate binding subsites extending from subsite -4 to +2. The enzyme was found to degrade a chitin chain from the reducing end. Trp275 and Phe396 are important in binding the substrate at the +1 and + 2 subsites and formed the opposite side of the cleft and stacked against the hydrophobic faces of the corresponding GlcNAcs. Although Tyr418 was found at the end of the cleft, the crystal structure clearly indicated that this residue did not interfere with the extension of the reducing end beyond the +2 site (Aronson *et al.*, 2003; Papanikolaou *et al.*, 2001).

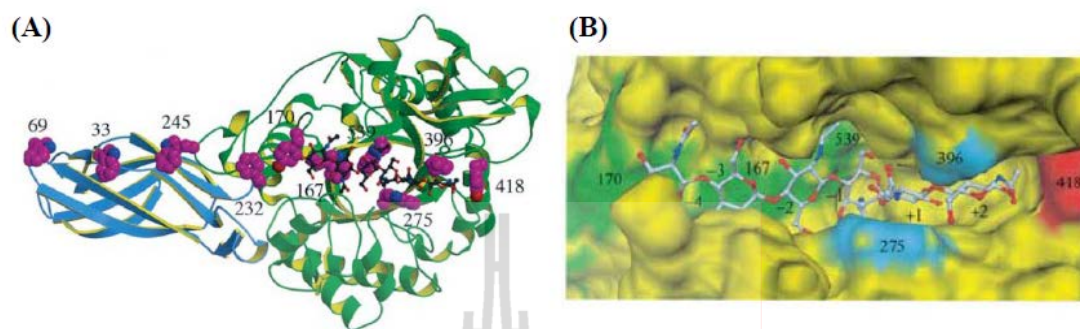


Figure 1.10 The 3D-structure of *S. marcescens* chitinase A mutant E315L with the GlcNAc₆. (A) The chitin-binding domain is shown in blue and the catalytic domain in green. Aromatic residues that line the substrate-binding cleft are shown in the space-filling mode. (B) Surface representation of the substrate-binding cleft. The aromatic residues that interact with the substrate are highlighted (Aronson *et al.*, 2003).

In addition, *S. marcescens* chitinase A has four exposed aromatic residues; Trp33, Trp69, Phe232 and Trp245 that play a vital role in the degradation of crystalline β -chitin, but not for the degradation of oligosaccharides. Phe232 was demonstrated to be important for guiding the chitin chain into the catalytic cleft. The subsequent hydrolysis leads to the release of the reducing-end disaccharide at positions +1 and +2, and then the enzyme moves symmetrically two GlcNAc residues towards the non-reducing end, allowing the chitin to be degraded processively as shown in Figure 1.11.

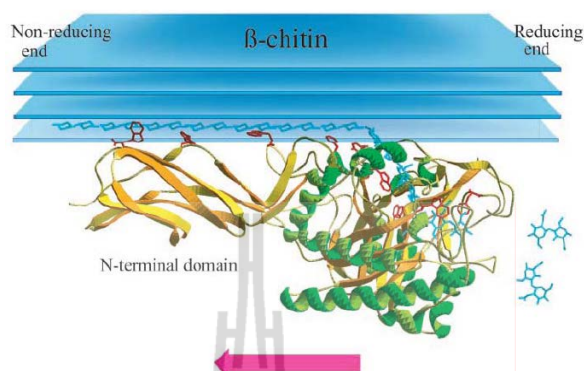


Figure 1.11 The model for crystalline β -chitin hydrolysis by chitinase A (Uchiyama *et al.*, 2001).

1.6.2 Structural Analysis of Chitinase B

The structure of chitinase B from *S. marcescens* was solved by multiple isomorphous replacements using anomalous scattering (MIRAS) and refined to 1.9 Å resolutions (van Aalten *et al.*, 2000). Chitinase B consists of a catalytic $(\beta/\alpha)_8$ -TIM barrel domain and a linker, plus a small C-terminal ChBD. The catalytic $(\beta/\alpha)_8$ -TIM barrel domain has a fold similar to that of chitinase A, including the existence of a tightly associated $(\beta/\alpha)_8$ -TIM barrel domain as shown in Figure 1.12 (van Aalten *et al.*, 2001).

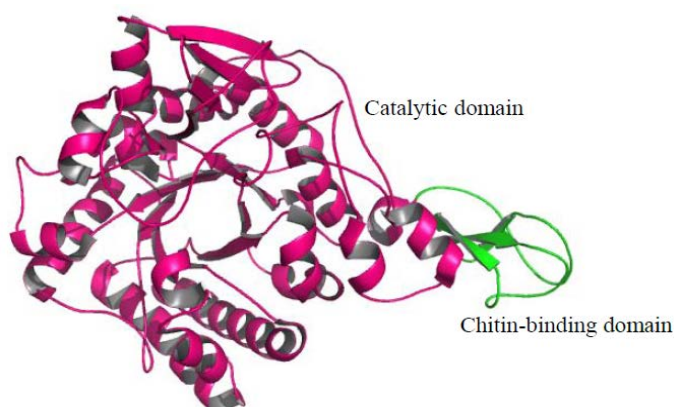


Figure 1.12 The structure of chitinase B from *S. marcescens*.

The active site of chitinase B has defined subsites from -3 to $+3$ and the substrate-binding cleft has a tunnel-like (van Aalten *et al.*, 2000). The crystal structure of chitinase B further suggests that the active site cleft is partially blocked at the -3 subsite meaning that chitinase B converts chitin primarily to dimers (Brurberg *et al.*, 1996; Suzuki *et al.*, 2002) with exo-activity and degrades a chitin chain from the non-reducing end (van Aalten *et al.*, 2000; 2001). Chitinase B has also four exposed aromatic residues Tyr240, Trp252, Tyr479 and Tyr481 that are linearly aligned toward the catalytic cleft and play important roles in crystalline chitin hydrolysis as described for chitinase A (Figure 1.13).

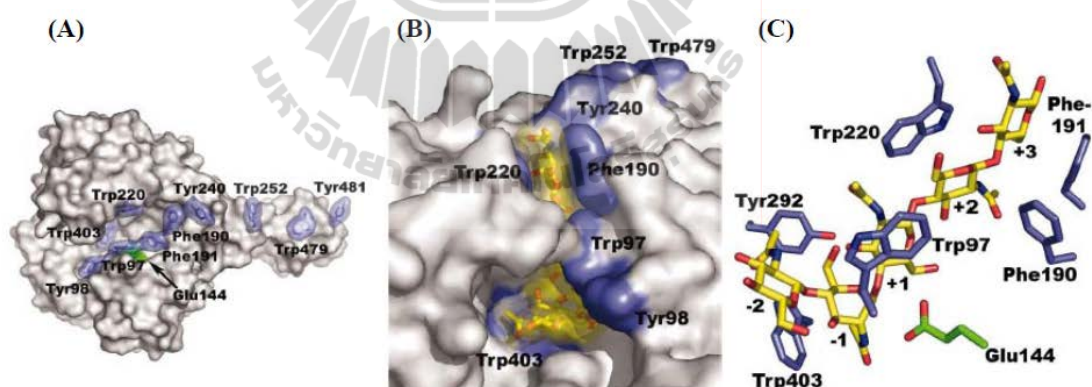


Figure 1.13 The surface structure of *S. marcescens* chitinase B (A) Surface representation showing aromatic side chains lining the substrate-binding cleft and the binding surface of the chitin-binding domain. (B) Surface representation of the E144Q mutant in complex with GlcNAc₅ bound to subsites -2 to $+3$. GlcNAc₅ is shown with a yellow van der Waals surface. The surface exposed aromatic residues are blue. (C) GlcNAc₅ and aromatic residues near the catalytic centre (Horn *et al.*, 2006).

1.6.3 Structural Analysis of Chitinase A1

The crystal structure of CatD of chitinase A1 from *B. circulans* was determined at atomic resolution of 1.13 Å (Matsumoto *et al.*, 1999). In CatD consist of three sub-domains including, an $(\alpha/\beta)_8$ -TIM barrel, and two β -domains, (β -domain 1 and β -domain 2), attached on top of the TIM barrel, providing a deep cleft for substrate binding as shown in Figure 1.14 (A and B). Like other family-18 chitinases, the catalytic cleavage of chitinase A1 is found almost at the bottom of the substrate-binding cleft.

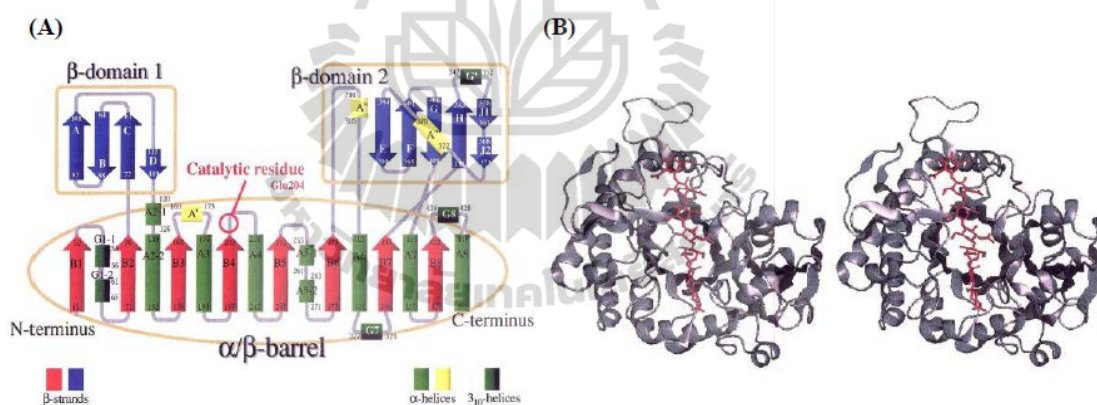


Figure 1.14 Chain-folding topology and structure of the CatD of chitinase A1 of *B. circulans*. (A) The CatD of chitinase. (B) Ribbon-drawing of the CatD of chitinase A1. The view is along the axis of the $(\alpha/\beta)_8$ -TIM barrel which forms the base of the molecule. Upon this base, two β -domains, namely the β -domain1 (on the left) and the β -domain 2 (on the right), are attached. The space between the two β -domains provides the substrate-binding cleft. This drawing is based on the crystal structure of the E204Q mutant enzyme complexed with the GlcNAc₇ substrate (red) (Matsumoto *et al.*, 1999).

The structure of the ChBD and FnIIID of *B. circulans* chitinase A1 was solved by NMR technique (Ikegami *et al.*, 2000; Jee *et al.*, 2002). The ChBD of this enzyme contains two-antiparallel β -sheets, one composed of three strands and the other of two strands as seen in Figure 1.15(A). The core region formed by the hydrophobic and aromatic residues makes the overall structure rigid and compact (Ikegami *et al.*, 2000). The FnIIIDs of chitinase A1 were the first fibronectin type III-like structure found in bacteria (Watanabe *et al.*, 1990). In general, bacterial FnIIIDs have been identified exclusively in glycosyl hydrolases (chitinases, cellulases and amylases) from soil bacteria (Little *et al.*, 1994). The FnIIIDs consist of a seven-stranded β -sandwiches fold and shows significant similarity to the Greek key β -sandwich fold as shown in Figure 1.15(B).

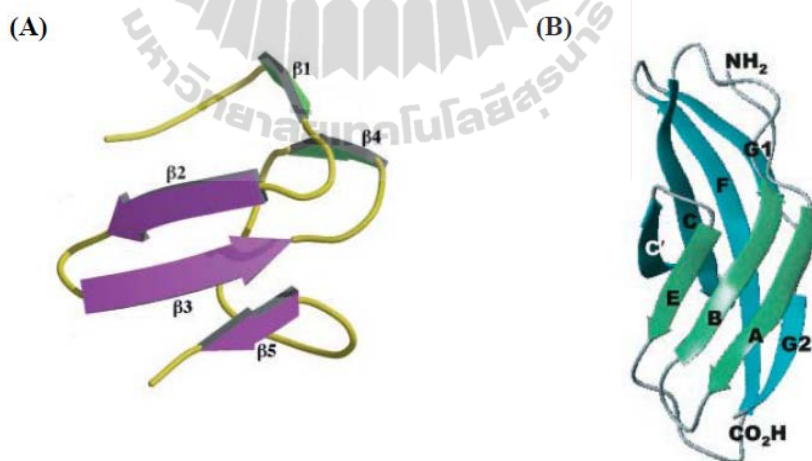


Figure 1.15 The solution structure of (A) ChBD and (B) FnIIID of chitinase A1 of *B. circulans* (Ikegami *et al.*, 2000; Jee *et al.*, 2002).

The structure of inactivated CatD of chitinase A1 complexed with GlcNAc₇ suggests that cleavage of the chitin chain occurs at the second linkage from the

reducing end and the presence of seven subsites -5 to $+2$ in the substrate-binding cleft was deduced from the complexed structure. At the exterior of the substrate-binding cleft, two exposed residues Trp122 and Trp134 thought to be important in guiding a chitin chain into the substrate-binding cleft during the crystalline chitin hydrolysis are shown in Figure 1.16(A) (Watanabe *et al.*, 2001). Tyr56 and Trp53 are only essential for crystalline-chitin hydrolysis, whereas Trp164 and Trp285 are very important for crystalline-chitin hydrolysis and also participate in hydrolysis of other substrates. Trp433 and Tyr279 are both essential for catalytic reaction as shown in Figure 1.16(B) (Watanabe *et al.*, 2003).

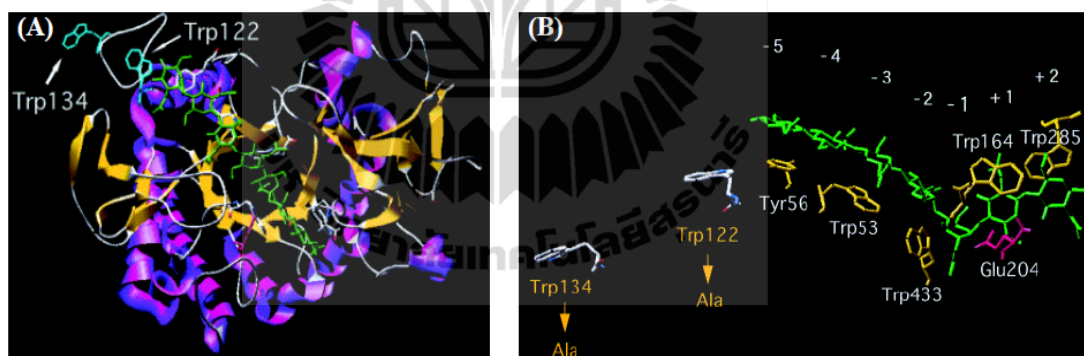


Figure 1.16 The catalytic domain of chitinase A1 from *B. circulans* complexed with GlcNAc₇. (A) Trp122 and Trp134 are shown with a ribbon-drawing of the structure of inactivated catalytic domain. (B) Trp122 and Trp134 are shown with the bound GlcNAc₇ and aromatic residues in the substrate-binding cleft (Watanabe *et al.*, 2001).

1.6.4 Structural Analysis of Chitinase C

The 3D-structure of chitinase C is not yet known, but its amino acids sequence shows that the CatD of chitinase C lacks the small insertion domain which makes up a

wall in the substrate binding grooves of chitinase A and B. In addition, chitinase C is predicted to be much more open and similar to the substrate binding cleft of endochitinase hevamine (van Scheltinga *et al.*, 1994).

1.7 Measurement of Chitinase Activities

Different methods are available for chitinase assays. Viscometric assay makes use of the rate of decrease in viscosity as a function of chitinase concentration (Jeuniaux, 1966). Insoluble compounds, such as colloidal chitin and glycol chitin are used in this assay procedure. Although this method is somewhat troublesome and time consuming, it provides an insight in the endo, exo characteristics of the studied enzymes. However, this method is not generally considered suitable for screening large number of samples.

Turbidmetric assay depends on the measurement of the rate of decrease in light scattering that accompanies depolymerisation of a suspension of a suspension of colloidal chitin. This method is suitable only for chitinases with relatively high activity (Jeuniaux, 1966).

Radioactive assay is highly sensitive but it has received much of environmental concern due to the generation of the hazardous radioactivity. The technique involves the radioactive counting of water-soluble oligosaccharides released from radio-labelled chitin (Cabib, 1988).

Fluorometric assay is highly sensitive and gives reproducible results. This assay employs fluorogenic substrates (Yang and Hamaguchi, 1980). The most widely used substrates for testing the chitinase activity are 4-methylumbelliferyl-*N*-acetyl-

chitoooligosaccharides (4-MU-GlcNAc₁₋₅) or methylumbelliferone (MUF). Enzyme activities are determined from the fluorescence units using a standard calibration curve of 4-MU or MUF and expressed as rates of 4-MU or MUF production (Fukamizo *et al.*, 2001; Hollis *et al.*, 1997; Tanaka *et al.*, 1999; 2001).

Dye-linked assay is based on the perceptibility of the non-hydrolyzed chitin by hydrochloric acid. A carboxymethyl-substituted soluble chitin covalently linked with Remazol brilliant Violet 5R can be used for detection of chitinases activity (Wirth and Wolf, 1990).

As an alternative, chitinase activity can be determined after polyacrylamide gel electrophoresis (PAGE) by incorporating glycol chitin into the gel. As glycol chitin exhibits high affinity toward Calcofluor white M2R, the lysis zones can be visualized by UV illumination as non-fluorescent dark bands in contrast to the fluorescent intact glycol chitin (Trudel and Asselin, 1989).

High-field nuclear magnetic resonance (NMR) spectroscopy can detect oligomers produced during the initial phase of chitin hydrolysis. This method indicates which enzyme of the chitinase complex initiates the hydrolysis (Vårum *et al.*, 1991). Rajamohanam *et al.* (1996) used this method to monitor the time course hydrolysis of chitin by the chitinase mixture produced by *Myrothecium verrucaria*.

Increase in the amount of reducing sugars as a result of the depolymerization of chitin has also been used as an assay for chitinases. Using this technique, dimethylaminobenzaldehyde (DMAB) (Boller and Mauch, 1988), 3,5-dinitrosalicylic acid (DNS) (Miller, 1959) or ferricyanide reagents (Imoto and Yagishita, 1971)

arrests the hydrolytic reaction, as well as helps to develop color, which can be monitored spectrophotometrically.

The degradation products obtained from the hydrolysis of colloidal chitin and soluble *N*-acetyl-chitooligosaccharides by chitinases can be carried out using chromatographic technique, such as thin layer chromatography (TLC), or high-performance liquid chromatography (HPLC) (Suginta *et al.*, 2005; Suzuki *et al.*, 2002). Recently, quantitative HPLC-mass spectrometry (HPLC-MS) has been developed as a direct and highly sensitive tool to investigate anomer selectivity and the binding behaviors of chitinases (Suginta *et al.*, 2009).

1.8 Studies of Chitinase A from *V. harveyi*

1.8.1 Expression of *V. harveyi* chitinase A

Based on genotypical and phenotypical features analyzed by Pedersen *et al.* (1998), *V. carchariae* has been re-classified as a heterotypic synonym of *V. harveyi*. *V. harveyi* (formerly *V. carchariae*) is a Gram-negative marine bacterium from the *Vibrionaceae* family. Suginta *et al.* (2000) previously reported the activity screening of fourteen species of *Vibrio* on agar plates containing swollen chitin. *V. harveyi* (formerly *V. carchariae*), *V. alginolyticus* 283 and *V. campbelli* showed high levels of chitinase expression. Later, chitinase A from *V. harveyi* was purified and found to be active as a monomer with M_r 63000-66000. Amino acid sequence analysis suggested that *V. harveyi* chitinase A is a member of family 18 of the glycosyl hydrolases (Henrissat *et al.*, 1991; Henrissat and Bairoch, 1993).

1.8.2 Function and characterization of chitinase A from *V. harveyi*

Native chitinase A degrades chitin to various lengths of small chitooligomeric fragments, suggesting that the enzyme acts as an endochitinase (Suginta *et al.*, 2004; 2005). The retention of the β over α anomer of all the products observed at initial time of the reaction is in agreement with the substrate-assisted mechanism employed by the enzyme. As suggested by molecular simulation and X-ray structure of family-18, the catalytic acid equivalent to Glu315 is presumed to donate a proton to the glycosidic oxygen, which leads to a distortion of the sugar molecule at the scissile position into a boat conformation. The resultant bond cleavage yields an oxazolinium intermediate and the retention of anomeric configuration in the products. The highest affinity of *V. harveyi* chitinases A for GlcNAc₆ (Suginta *et al.*, 2005) implied that the catalytic cleft of the enzyme comprises an array of most probably six binding subsites, comparable to that of CiX1 from *Coccidioides immitis* (Fukamizo *et al.*, 2001; Sasaki *et al.*, 2002) and chitinase A from *S. marcescens* (Aronson *et al.*, 2003; Perrakis *et al.*, 1994).

1.8.3 Mutational analysis of the active site residues

The effects of point mutations of the active-site residues Trp168, Tyr171, Trp275, Asp392, Trp397 and Trp570 were studied with *V. harveyi* chitinase A. The target residues for mutation, which extend over the substrate binding cleft of the TIM-barrel domain (Suginta *et al.*, 2007). Figure 1.17 displays superimposition of the active site of *V. harveyi* chitinase A on that of *S. marcescens* chitinase A E315L with the GlcNAc₆. Tyr171 is located at the edge of the binding cleft beyond subsite -4 (the non-reducing end), whereas Trp168, Trp570 and Trp275 stack against the pyranosyl

rings of GlcNAc units at subsites -3, -1 and +1, respectively. Trp397 is located near the GlcNAc unit at subsite +2 (the reducing end). The presence of Glu315 at the scissile bond between the GlcNAc residues at subsite -1 and +1 explains the catalytic role of this residue. Asp392 is situated further away from the cleavage site, but in close contact with the GlcNAc residues at subsites +1 and +2 (Suginta *et al.*, 2007).

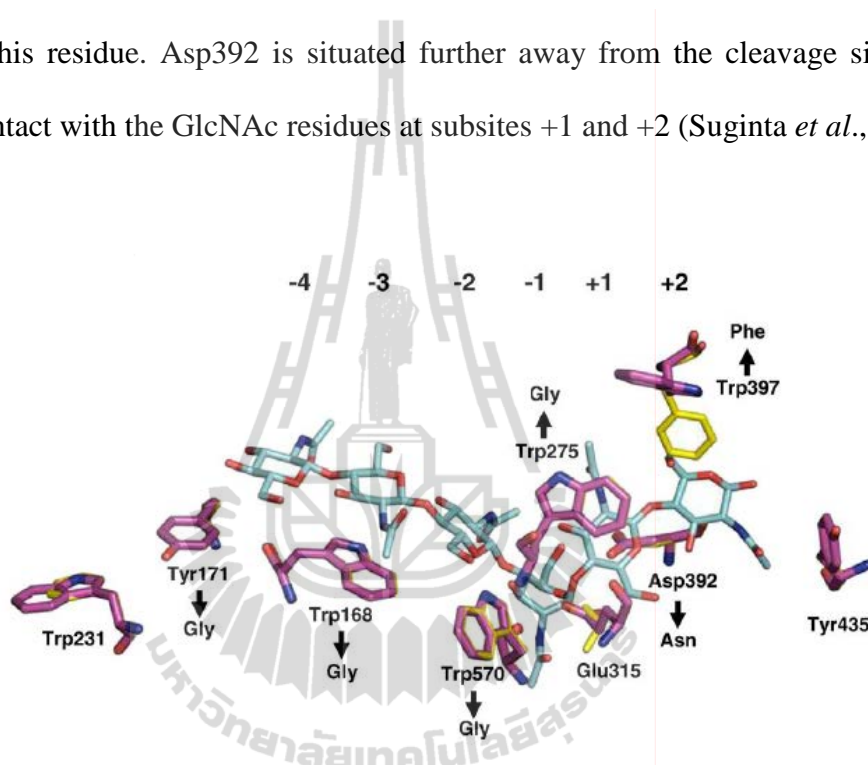


Figure 1.17 The stick model of the putative binding cleft of *V. harveyi* chitinase A was superimposed on that of *S. marcescens* chitinase A mutant E315L with the GlcNAc₆ (Suginta *et al.*, 2007).

Mutations of Trp168, Tyr171, Trp397 and Trp570 completely abolished the hydrolyzing activity against colloidal chitin, and greatly reduced the hydrolyzing activity against *p*NP-GlcNAc₂. The W570G mutant showed most severe effect on the hydrolyzing activity. In the modeled 3D-structure of the inactive mutant E315M complete with GlcNAc₆, revealed Trp570 was closest to the sugar ring at subsite -1, which is likely to be responsible for holding the GlcNAc₆ ring in place so that

cleavage of the glycosidic bond between subsites -1 and +1 can occur. On the other hand, W397F significantly enhanced the hydrolyzing activity towards the *p*NP-GlcNAc₂ but increased the activity towards colloidal chitin only slightly. The Asp392, Tyr171 and Trp275 mutants particularly reduced the K_m values, while W168G mutant did not considerably change the K_m value against the *p*NP substrate. The same mutants also greatly reduced the k_{cat} values. In contrast, the W397F mutant gave no significant changes in the K_m and k_{cat} of the enzyme with *p*NP-GlcNAc₂. These data suggested that Trp397 does not take part in the hydrolytic process of this substrate. Product analysis by thin layer chromatography that completely changed the degradation patterns of GlcNAc₄-GlcNAc₆ hydrolysis by the W275G and W397F mutants compared to the wild-type enzyme suggested that residues Trp275 and Trp397 are involved in defining the binding selectivity of the enzyme to soluble substrates (Suginta *et al.*, 2007).

1.8.4 Substrate binding modes and anomer selectivity

The binding behaviors of three chitin substrates to *V. harveyi* chitinase A was employed by quantitative HPLC-MS. The results showed that GlcNAc₆ preferred subsites -2 to +2 over substrates -3 to +2, whilst GlcNAc₅ only required subsites -2 to +2, while subsites -4 to +2 were not used at all by both substrates. The results suggested that binding of the chitooligosaccharides to the enzyme essentially occurred in compulsory fashion. On the other hand, the binding led to a full occupancy of the six binding sites by insoluble chitin, as shown in Figure 1.18.

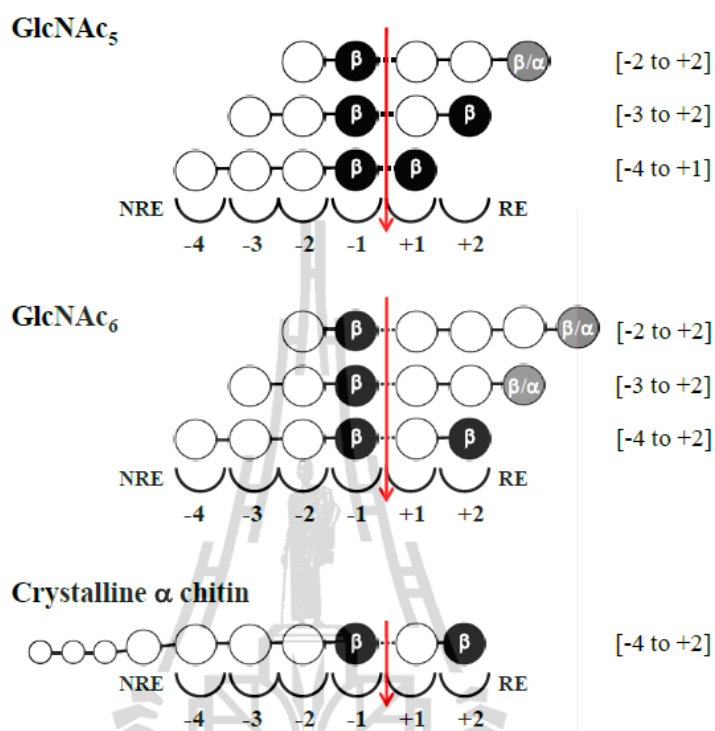


Figure 1.18 The possible models of chitin oligosaccharide bindings to the multiple binding subsites of *V. harveyi* chitinase A. GlcNAc unit with β configuration is shown in black circle, and α or β configuration is shown in gray circle (modified from Suginta *et al.*, 2009).

Substitutions of Trp275 to Gly and Trp397 to Phe significantly shifted the anomer selectivity of the enzyme toward β -anomeric substrate. The Trp275 residue is an important for substrate recognition at subsites -1 and +1. When Trp275 substituted to Gly appeared to weaken the binding strength of these subsites and at -1 subsite substrate might be α or β -anomeric configuration. However, W275G remain binding pattern same wild-type at subsite +2 GlcNAc is still β -anomer. Different situation were observed with mutant W397F was found to sever affect the anomer selectivity. Trp397 has specific with β -anomeric configuration of substrate and is a crucial binding

residue at subsite +2. After mutated Trp397 to Phe appeared weak substrate recognition at subsite +2, the substrates can move more freely and the substrates occurred in compulsory fashion. And in W397F mutant occurred α or β -anomic configuration at subsite +2.

1.8.5 Mutational analysis of the surface-exposed residues

The effects of the surface-exposed residues near chitin-binding domain on the binding and hydrolytic activities of *V. harveyi* chitinase A were studied (Pantoom *et al.*, 2008). The tertiary structure prediction of this enzyme has located the residues Ser33 and Trp70 at the end of ChBD and Trp231 and Tyr245 at the exterior of the catalytic cleft (Figure 1.19).

With respect to their binding activity towards crystalline α -chitin and colloidal chitin, chitin binding assays demonstrated a considerable decrease for the W70A and Y245W mutants and a notable increase for S33W and W231A. When the specific hydrolyzing activity was determined, mutant W231A displayed reduced hydrolytic activity, whilst Y245W showed enhanced activity. This suggested that an alteration in the hydrolytic activity was not correlated with a change in the ability of the enzyme to bind to chitin polymer. A mutation of Trp70 to Ala caused the most severe loss in both the binding and hydrolytic activities, which suggested that it is essential for crystalline chitin binding and hydrolysis. Mutations varied neither the specific hydrolyzing activity against *p*NP-GlcNAc₂, nor the catalytic efficiency against GlcNAc₆, implying that the mutated residues are not important in oligosaccharide hydrolysis (Pantoom *et al.*, 2008).

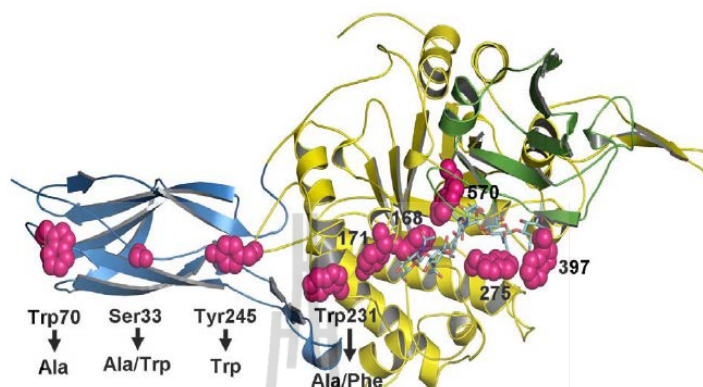


Figure 1.19 The representation of the 3D-structure of *V. harveyi* chitinase A was constructed based on the X-ray structure of *S. marcescens* chitinase A E315L mutant. The chitin-binding domain is shown in cyan, the catalytic domain in yellow and the insertion domain in green. The GlcNAc₆ is shown as a stick model with N atoms in blue and O atoms in red (Pantoom *et al.*, 2008).

1.8.6 Structural determination of *V. harveyi* chitinase A

Like other family 18 microbial enzymes (Hollis *et al.*, 2000; Perrakis *et al.*, 1994; Suzuki *et al.*, 1999), the ChBD has a β -strand rich fold formed by residues 22-138. This domain is connected to the core domain by a 21 amino-acid linker peptide (residues 139-159). The CatD (magenta) has a $(\alpha/\beta)_8$ -TIM barrel fold consisting of eight β -strands (B1-B8) tethered to eight α -helices (A1-A8) by loops and is made up of two parts, referred to as catalytic I (Cat I) (residues 160-460) and Cat II (residues 548-588). The catalytic residue (Glu315) is positioned in the loop of strand B4, which is part of a DxxDxDxE conserved motif. The $\alpha+\beta$ fold small insertion domain connects strand B7 of Cat I and helix A7 of Cat II and is made up of five anti-parallel β -strands flanked by short α -helices (residues 461-547). This small insertion domain

provides a signature for subfamily A chitinases (Suzuki *et al.*, 1999), although its function remains to be identified (Figure 1.20).

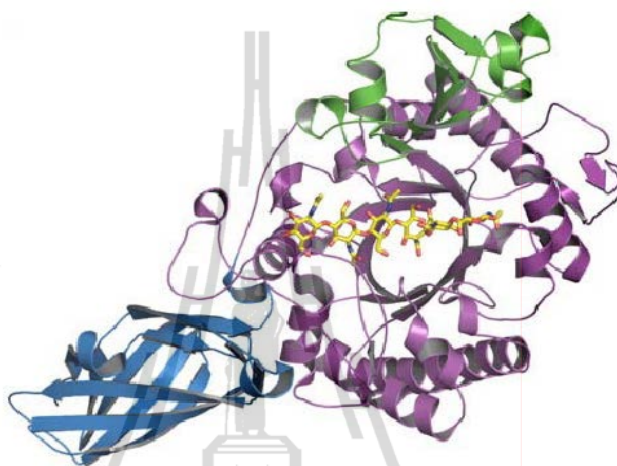


Figure 1.20 The structure of catalytically inactive mutant E315M complexed with GlcNAc₆ of *V. harveyi* chitinase A. Chitin-binding domain is in blue, the catalytic TIM-barrel domain in magenta, and the small insert domain in green (Songsiriritthigul *et al.*, 2008).

The crystal structures of *V. harveyi* chitinase A and its catalytically inactive mutant E315M in the absence or presence of chitooligosaccharides were solved by Suginta's group (Songsiriritthigul *et al.*, 2008) (Figure 1.21). The structure of the E315M+GlcNAc₆ complex reveals the substrate-binding cleft as a long deep groove, which contains six-binding subsites (-4), (-3), (-2), (-1), (+1), and (+2). This subsite topology defines subsite -4 at the non-reducing end (NRE), subsite +2 at the reducing end (RE) and the cleavage site between subsites -1 and +1. Similar subsites have been identified for *S. marcescens* chitinase A (Aronson *et al.*, 2003).

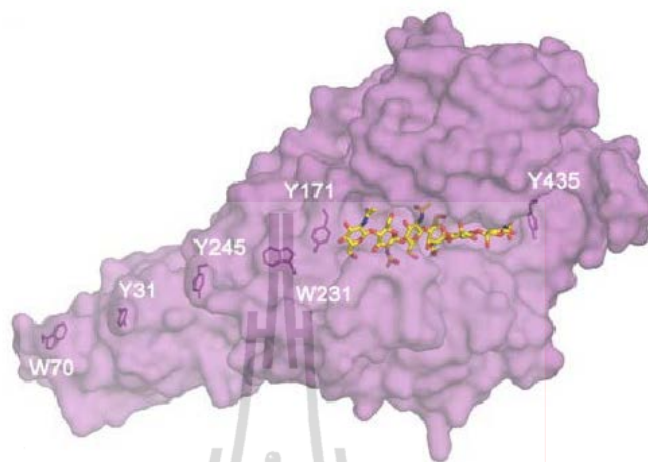


Figure 1.21 Surface representation of mutant E315M showing the positions of the regularly-spaced, surface-exposed hydrophobic residues. Tyr435 marks the reducing end of GlcNAc₆ and Tyr171 marks the non-reducing end. The linear track of hydrophobic residues extending away from the non-reducing end of GlcNAc₆ suggests the binding path for longer chain chitins (Songsiriritthigul *et al.*, 2008).

Tyr171 and Tyr435 are found at the edges of the catalytic cleft. Tyr171 marks the non-reducing end, whereas Trp435 marks the reducing end of both the GlcNAc₅ and GlcNAc₆. Tyr435 located at the end of the +2 site seems to provide a partial barrier that may favor the ending of both sugar chains. However, inspection of the electron density map of the reducing-end subsites displays adequate space for the incoming oligomer to move beyond the +2 site, allowing various glycosidic bonds to approach the cleavage site. This explains how *V. harveyi* chitinase A hydrolyses a polymeric substrate in an endo manner at the same time favoring smaller substrates, such as GlcNAc₆ (Figure 1.22).

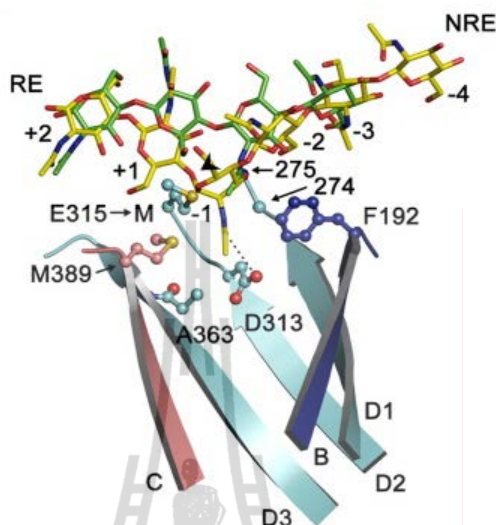


Figure 1.22 Structural comparisons of GlcNAc₅ and GlcNAc₆ in the catalytic cleft of mutant E315M. NRE and RE represent non-reducing end and reducing end, respectively (Songsiriritthigul *et al.*, 2008).

The availability of the structure of E315M mutant in the presence of GlcNAc₅ and GlcNAc₆ is a key solution to the catalytic mechanism of the *V. harveyi* chitinase A. The overlaid structures of GlcNAc₅ and GlcNAc₆ are shown in Figure 1.23. Considering the cluster of amino acid residues contributing to the binding of +2 and +1 GlcNAc, obvious differences of the interactions between GlcNAc₅ and GlcNAc₆ are seen at subsite -1. The -1 sugar in GlcNAc₆ makes contact with Tyr164, Asp313, Ala363, Met389, Tyr391, Asp392, Tyr461 and Arg463 via its boat conformation, whereas these residues did not interact with the chair conformation of -1 sugar in GlcNAc₅. Asp313 locates at the bottom of the catalytic cleft is found to be essential in stabilizing the boat form of -1 GlcNAc via hydrogen bonding. Therefore, the -1 to +1 glycosidic bond is in the position to be cleaved at the catalytic Glu315. The mutated residue E315M was found near the scissile bond joined between the -1GlcNAc and

+1GlcNAc of the bent conformation of GlcNAc₆, but was far away from the same bond in the straight conformation. This observation supports the catalytic role of Glu315 towards the bent conformation (Songsiriritthigul *et al.*, 2008).

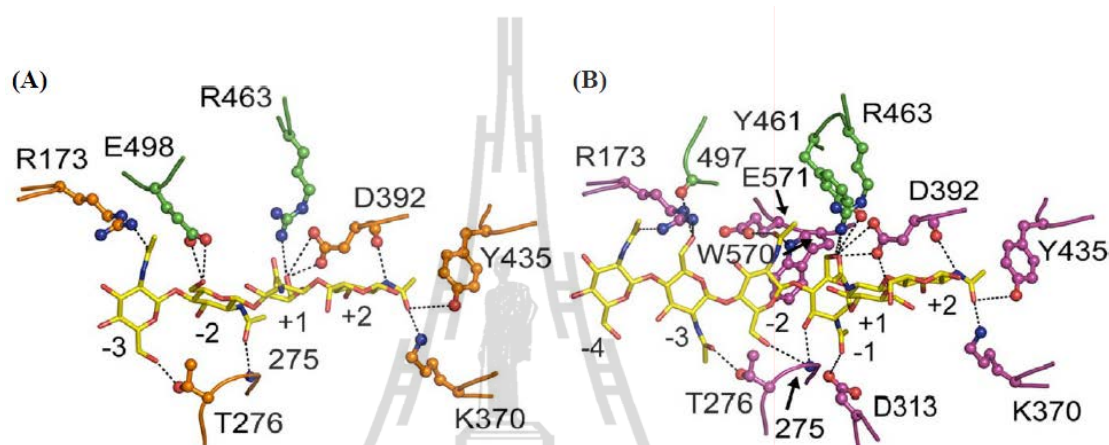


Figure 1.23 Specific interactions within the substrate-binding cleft of mutant E315M interactions of GlcNAc₅ and GlcNAc₆. (A) GlcNAc₅ and (B) GlcNAc₆, hydrogen bonds are shown as dashed lines. The binding residues are depicted as ball-and-stick with the sugar residues in a stick model. Carbon atoms of the binding residues in the catalytic domain are colored orange for GlcNAc₅ and magenta in GlcNAc₆. Green represents carbon in the small insertion domain and orange-yellow for sulfur. Sugar is colored yellow for carbon; blue for nitrogen; and red for oxygen (Songsiriritthigul *et al.*, 2008).

The structure data of E315M+GlcNAc₅ and E315M+GlcNAc₆ provide evidence that *V. harveyi* chitinase A presumably catalyzes the substrate hydrolysis following the “slide and bend” mechanism. The mechanism proposed by Songsiriritthigul *et al.* (2008) involves four steps: 1) the substrate recognition. The step is initiated through

the straight conformation of the incoming substrate; 2) the sliding, then bending. This process thermodynamically forces the substrate to adopt the bent conformation; 3) the bond cleavage. This process is proceeded via the bent conformation of -1 GlcNAc and the twist of the *scissile* bond; and 4) the release of the cleaved products from the subsites $+1$ and $+2$ as shown in Figure 1.24.

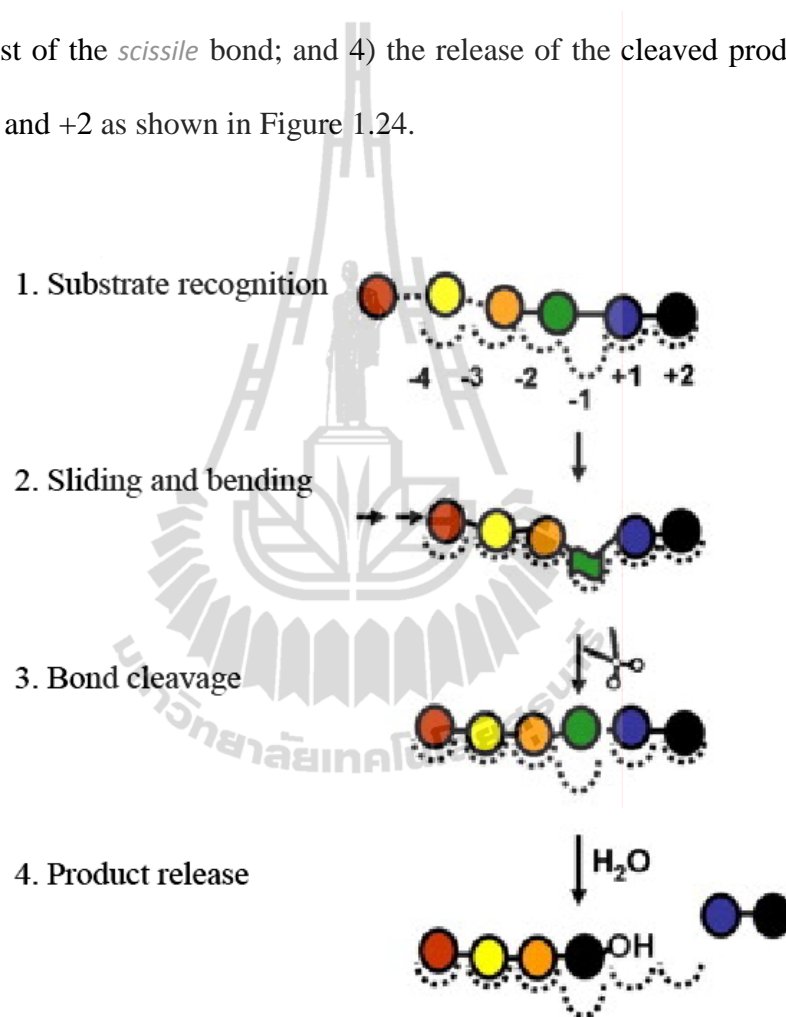


Figure 1.24 The schematic diagram highlighting the proposed catalytic mechanism of *V. harveyi* chitinase A (Songsiriritthigul *et al.*, 2008).

1.9 Research Objectives

The catalytic domain of *V. harveyi* chitinase A has a TIM-barrel fold and is characterized by the most prominent motif DxxDxDxE that spans through strand 4 of the TIM-barrel. This motif includes the Asp313 and Glu315 residues that are essential for catalytic activity. And at the edges of the catalytic cleft has the aromatic residue Tyr435, which seems to provide a partial barrier that may favor the ending of sugar chains. However, the functional roles of Asp313 and Tyr435 have not been demonstrated in *V. harveyi* chitinase A. Therefore, this study aims to clarify the possible roles of the two residues in chitin binding and hydrolysis. The objectives of this study are:

1. To mutate the residues Asp313 to Ala and Asn and Tyr435 to Ala and Trp by site-directed mutagenesis technique.
2. To express and purify the wild-type chitinase A and all the mutated proteins from *Escherichia coli* strain M15 by a single step of Ni-NTA agarose affinity chromatography.
3. To determine the effects of mutations on the binding and hydrolytic activities of the enzyme using appropriate biochemical techniques.

CHAPTER II

MATERIALS AND METHODS

2.1 Bacterial Strains and Vector

Bacteria *E. coli* strain XL1-Blue (Stratagene, La Jolla, CA, USA) was the host strain for the production of mutated DNA. *E. coli* type strain M15 (QIAGEN, Valencia, CA, USA) was used for routine cloning, subcloning and plasmid preparation and the pQE-60 expression vector harboring chitinase A DNA lacking the residues 598-850-amino acid fragment with a C-terminal (His)₆ sequence (Figure 2.1).

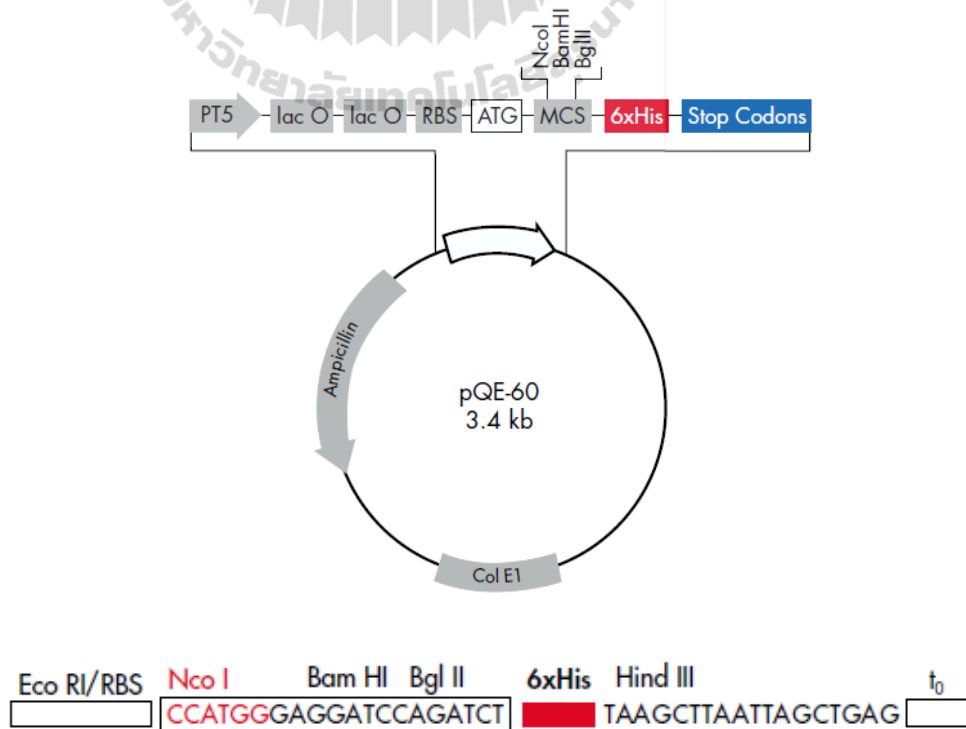


Figure 2.1 Mapping of pQE-60 vector.

2.2 Chemicals and Reagents

The Quick-Change Site-Directed Mutagenesis Kit including *Pfu* Turbo DNA polymerase was purchased from Stratagene. Chemicals and reagents used for protein expression, purification and characterization of *V. harveyi* chitinase A were of analytical grade. Acrylamide, aniline, ammonium sulphate, ammonium persulphate, bromophenol blue, bis-*N*, *N*'-methylenebisacrylamide, coomassie blue R250, coomassie blue G250, ethylenediamine tetra-acetic acid (EDTA), isopropyl- β -D-thiogalactoside (IPTG), 2- β -mercaptoethanol, magnesium chloride, glycerol, glycine, sodium azide, sodium dodecyl sulphate (SDS), Tris-(hydroxymethyl)-aminoethane, *N,N,N',N''*-tetramethylethylenediamine (TEMED), glycol chitosan and 4-methylumbelliferyl *N*-acetyl- β -D-*N,N'*-diacetylchitobioside (4-MU-GlcNAc₂) were purchased from Sigma-Aldrich (St. Louis, MO, USA).

Acetone, ammonium hydroxide, glacial acetic acid, hydrochloric acid, methanol, *n*-butanol, phosphoric acid, potassium chloride, potassium hydroxide, sodium acetate, sodium bicarbonate and 3, 5-dinitrosalicylic acid (DNS) were products of Carlo ERBA (Rodano, Milano, Italy).

Ampicillin, phenyl methylsulfonyl (PMSF), imidazole and hen egg white lysozyme were from USB Corporation (Cleveland, OH, USA).

Chitin from crab shells, chitooligosaccharides and *p*-nitrophenyl-di-*N*-acetylchitobioside (*p*NP-GlcNAc₂) were purchased from Seikagaku Corporation (Tokyo, Japan).

Nanosep membrane centrifugal filter (10 kDa molecular-weight cut off) was a product of PALL Life Science (Michigan, USA). Vivaspin-20 ultrafiltration membrane concentrators (10 kDa molecular-weight cut off) were obtained from

Vivascience AG (Hanover, Germany). Ni-nitrilotriacetic acid (Ni-NTA) agarose resin was a product of QIAGEN (QIAGEN, Germany). An aluminum sheet (Silica gel 60F₂₅₄ aluminium sheet, 20 x 20 cm) was purchased from Merck (Berlin, Germany).

2.3 Instrumentation

All instruments used were located at the Center for Scientific and Technology Equipment (F1 and F9), Suranaree University of Technology, Nakhon Ratchasima, Thailand. These instruments includes a Sonopuls Ultrasonic homogenizer with a 6 mm diameter probe (Sigma-Aldrich, St. Louis, MO, USA), a Mini-PROTEAN[®] 3 Cell (Bio-RAD, Hercules, CA, USA), a Genway UV-VIS spectrophotometer (Feisted, Dunmow, Essex, UK), a shaking incubator MRC/Israel (Bio-Active), a PCR thermocycler (Applied Biosystems, Norwalk, CA, USA), DNA electrophoresis apparatus (Cosmobio, Tokyo, Japan), a microtiter plate reader (Applied Biosystems, Foster City, CA, USA). A Thermomixer comfort (Eppendorf AG, Hamburg, Germany), a Microcentrifuge Denville 26OD (Denville Scientific, Metuchen, NJ, USA), and a Gemini EM microplate fluorometer (Sunnyvale, CA, USA)

2.4 General Methods

2.4.1 Site-directed mutagenesis

The program used for designed primers were obtained from the DNASTAR package (DNASTAR, Inc., Madison, WI, USA). The oligonucleotides used for recombinant chitinase A were synthesized by the Bio Service Unit (BSU) (Bangkok, Thailand) as shown in Table 2.1.

Table 2.1 Primers for site-directed mutagenesis.

Mutations	Primers ^a
D313A	Forward 5'-GACGGCGTAGATATT <u>GCG</u> TGGGAATTCCTGGTG-3' Reverse 5'-CACCAGGAAATTCCCAC <u>CGC</u> AATATCTACGCCGTC-3'
D313N	Forward 5'-GACGGCGTAGATATTA <u>AACT</u> GGGGAATTCCTGGTGGC-3' Reverse 5'-GCCACCAGGAAATTCCCAG <u>TTA</u> AATATCTACGCCGTC-3'
Y435A	Forward 5'-GACGGCGTAGATATT <u>GCC</u> ACTGCAGATAACGGTATC-3' Reverse 5'-GATACCGTTATCTGCAGT <u>GGC</u> TGCTGGACCTTTGTACG-3'
Y435W	Forward 5'-GATACCGTTATCTGCAGT <u>TCC</u> ATGCTGGACCTTTGTACG-3' Reverse 5'-CGTACAAAGGTCCAGCAT <u>GGA</u> CTGCAGATAACGGTATC-3'

^a Sequences underlined indicate mutated codons.

The mutation strategy using Quick-change® Site-Directed Mutagenesis Kit (Stratagene, La Jolla, CA, USA) is shown in Figure 2.2. Briefly, the targeted PCR products were digested with *Dpn* I endonuclease to eliminate methylated DNA of the non-mutated DNAs template. Repair of the nicked circular dsDNA products was performed by transformed into *E. coli* XL1-Blue competent cells (Stratagene), as described by Sambrook *et al.* (1989). About 2 µl of digestion was transformed into a 50 µl aliquot of the frozen competent cells and spread on Luria-Bertani (LB) agar plates containing 100 µg/ml ampicillin. Plasmid recombinant DNAs from the positive colonies were extracted with the Plasmid Miniprep kit (QIAGEN, Germany). The success of newly generated mutations was confirmed by automated DNA sequencing (BSU, Thailand).

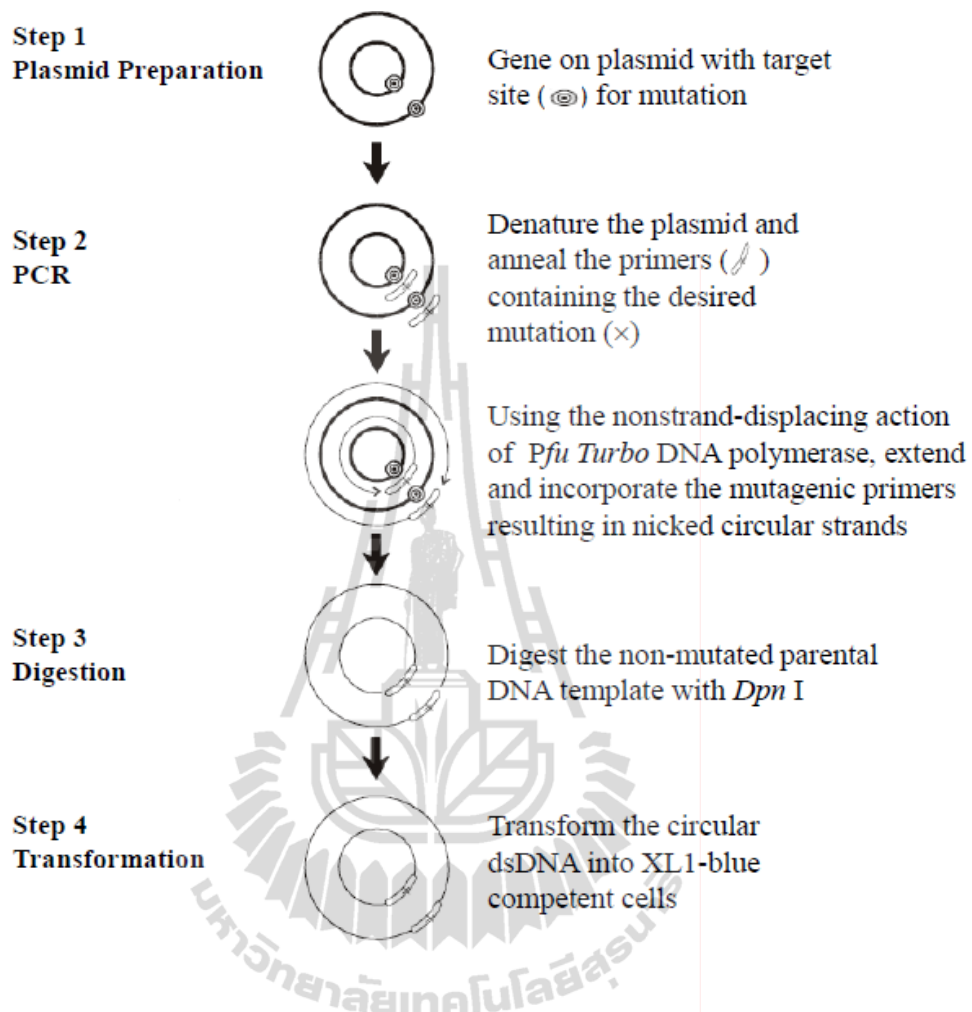


Figure 2.2 Schematic diagram of the Quikchange® Site-Directed Mutagenesis Kit (<http://wwwl.qiagen.com/literature/pqesequences/pqe60.pdf>).

The DNA fragment that encodes wild-type chitinase A (amino acid residues 22-597, without the 598-850 C-terminal fragment) was cloned into the pQE60 expression vector and highly expressed in *E. coli* M15 cells as the 576-amino acid fragment with a C-terminal (His)₆ sequence. About 100 ng of plasmid was transformed into a 50 μ l aliquot of competent cells and spread on LB agar plates containing 100 μ g/ml ampicillin.

2.4.2 Expression of recombinant chitinase A in *E. coli* M15

Chitinase A expression was carried out following Pantoom *et al.*, (2008). The ampicillin resistant colonies were picked and grown overnight at 37°C in 10 ml of LB medium containing 100 µg/ml ampicillin and the culture was shaken at 150 rpm. Freshly inoculated culture was diluted to a ratio of 1:100 with LB medium containing 100 µg/ml ampicillin, and further grown at 37°C until the OD₆₀₀ reached 0.5-0.6. The culture was cooled down to 25°C, and then IPTG was added to a final concentration of 0.5 mM and the culture shaken at 200 rpm at 25°C for an additional 18 hours. The IPTG induced cells were harvested by centrifugation at 4,500 rpm at 4°C for 20 min. The cell pellet was re-suspended in 15 ml lysis buffer (20 mM Tris-HCl, pH 8.0 containing 150 mM NaCl, 1 mM PMSF and 1 mg/ml lysozyme), and then incubated on ice for 30 min. The cell suspension was broken on ice by sonication with a Sonopuls Ultrasonic homogenizer with a 6 mm diameter probe (50% duty cycle, amplitude setting, 20%, total time 30 s, 10 cycles, Sigma-Aldrich). Unbroken cells were removed by centrifugation at 12,000 rpm at 4°C for 30 min.

2.4.3 Purification of recombinant chitinase A variants

The crude supernatant containing soluble chitinase A was purified by using Ni-NTA agarose affinity chromatography (QIAGEN). The Ni-NTA agarose column (1.0 x 10 cm.) was equilibrated with 100 ml of the equilibration buffer (20 mM Tris-HCl, pH 8.0, and 150 mM NaCl). After sample loading, the column was washed with 10 column volumes of the equilibration buffer containing 5 mM imidazole, followed by 5 column volumes of the equilibration buffer containing 20 mM imidazole. The column was eluted with 5 column volumes of the elution buffer (the equilibration

buffer containing 250 mM imidazole). Then, the eluted fraction was concentrated to 1 ml using Vivaspin-20 ultrafiltration membrane concentrator (M_r 10,000 cut-off, Vivascience AG). The collected chitinase solution was subjected to SDS-PAGE analysis and function characterization or stored at -30°C until use.

2.4.4 Determination of protein concentration by Bradford's method

Proteins concentrations were estimated by the method of Bradford (1976) with bovine serum albumin (BSA) as standard (0-10 μg). A properly diluted sample (100 μl) was mixed with 1 ml of dye reagent, and then mixed and incubated at room temperature for 5 min. The absorbance at A_{595} nm was measured in a Genway UV-VIS spectrophotometer.

2.4.5 Sodium Dodecyl Sulfate Polyacrylamide Gel Electrophoresis

SDS-PAGE was performed according to the method of Laemmli (Laemmli, 1970). Protein samples were mixed with sample buffer (150 mM Tris-HCl, pH 6.8, 5% 2-mercaptoethanol, 6% SDS, 30% glycerol and 0.03% bromophenol blue). The suspension was boiled for 5 min and a 10-15 μl aliquot was loaded onto 12% SDS-PAGE gel with a discontinuous Tris-glycine buffer system set in a Mini-PROTEAN[®] 3 cell (BioRAD), and then electrophoresed in Tris-glycine pH, 8.3, as a running buffer at a constant 120 V for 1 h from a cathodic (-) end to an anodic (+) end. After electrophoresis, the gel was stained with coomassie blue R250 for 30 min and then destained with a destaining solution (40% methanol and 7% acetic acid) until the background was clear. The sizes of protein bands were estimated by comparing with the low molecular weight protein marker (Amersham Bioscience) comprising

phosphorylase b (97 kDa), bovine serum albumin (66 kDa), ovalbumin (45 kDa), bovine carbonic anhydrase (30 kDa), trypsin inhibitor (20.1) and bovine α -lactalbumin (14.4 kDa).

2.4.6 TLC analysis of the hydrolytic products

Hydrolysis of chitooligosaccharides (GlcNAc₂-GlcNAc₆) by chitinase A and its mutants was carried out in a 20 μ l reaction mixture, containing 100 mM sodium acetate buffer, pH 5.5, 2.5 mM substrate and 200 ng purified enzyme. Chitooligosaccharides were hydrolyzed by incubating at various times from 2 min to 18 h at 37°C with shaking at 700 rpm. Then, the reaction was terminated by boiling for 5 min. For product analysis, each reaction mixture was applied 5 times (1 μ l each) to a silica TLC plate (7.0 x 10.0 cm), then chromatographed 3 times in a mobile phase containing n-butanol: methyl alcohol: 28% ammonia solution: distilled water (10:8:4:2) (v/v), followed by spraying with aniline-diphenylamine reagent and baking at 180°C for 5 min (Suginta *et al.*, 2007).

Hydrolytic products of chitinase A and its mutants against colloidal chitin at various time points were also determined. A reaction mixture (150 μ l) containing 20 mg of colloidal chitin suspended in 100 mM sodium acetate buffer, pH 5.5, was incubated with enzyme (80 μ g) at 37°C with shaking at 700 rpm for variable times. For glycol chitin, a 150 μ l reaction mixture, contained 100 mM sodium acetate buffer, pH 5.5, 1% (w/v) glycol chitin and 200 μ g enzymes. The degradation products were analyzed by TLC under the same condition as described for the chitooligosaccharides.

2.4.7 Determination of chitinase A activity

Chitinase activity was determined in a 96-well microtiter plate. A 100- μ l assay mixture contained enzyme sample (10 μ l), 100 μ M sodium acetate buffer, pH 5.5 and 100 mM *p*NP-GlcNAc₂ as substrate. The reaction mixture was incubated at 37°C for 15 min with constant agitating, and then the enzymatic reaction was terminated by the addition of 50 μ l 100 mM Na₂CO₃. The amount of *p*-nitrophenol (*p*NP) released was determined spectrophotometrically at A₄₀₅ nm in a microtiter plate reader (Applied Biosystems). The molar quantity of the liberated *p*NP was calculated from a calibration curve constructed with *p*NP standard varying from 0-30 nmol. One unit of chitinase activity was defined as the amount of enzyme which produces 1 μ mol of *p*NP per min at 37°C.

2.4.8 Determination of specific hydrolyzing activity

Specific hydrolyzing activity was determined in a microplate. A 100 μ l assay mixture contained enzyme sample (50 μ l), 100 mM sodium acetate buffer, pH 5.5 and 100 μ M *p*NP-GlcNAc₂. The reaction mixture was incubated at 37°C for 15 min with constant agitating, and then the enzymatic reaction was terminated by the addition of 50 μ l 100 mM Na₂CO₃. Quantification of the liberated was determined as described above.

For specific hydrolyzing activity using of *V. harveyi* chitinase A variants towards colloidal chitin, glycol chitin and crystalline chitin, a reaction mixture (650 μ l), containing 1% (w/v) substrate, 100 mM sodium acetate buffer, pH, 5.5, and 150 μ g wild type, D313N, Y435A/W or 250 μ g D313A was incubated at 37°C with shaking at 700 rpm for 15 min. The reaction was terminated by boiling at 100°C for 5 min,

and then centrifuged at 5,000 g for 1 min to precipitate the remaining chitin. A 100- μ l supernatant was subjected to reducing sugar assay using DNS reagent as described by Miller (1959). Release of the reducing sugar as detected by A_{540} nm was converted to molar concentrations using a standard calibration curve of GlcNAc₂ from 0-500 nmol.

Specific hydrolyzing activity was also determined using GlcNAc₃₋₆ substrates. A reaction mixture (200 μ l), containing 500 μ M chitooligosaccharides (GlcNAc₃₋₆), 100 mM sodium acetate buffer, pH, 5.5, and 50 μ g wild type, D313N, Y435A/W or 200 μ g D313A was incubated at 37°C with shaking at 700 rpm for 15 min. After reaction termination, the amounts of the reducing sugar released were determined described for insoluble chitin.

Specific hydrolyzing activity carried out with *N*-acetyl- β -D-*N,N'*-diacetylchitobioside (4-MU-GlcNAc₂) (Sigma-Aldrich, St. Louis, MO, USA) was determined in a black 96-well black microplate. A reaction mixture (100 μ l) containing 0.2 mM 4-MU-GlcNAc₂, 100 mM citrate/citric pH 5.5 containing 0.025% Triton X-100 and 150 μ g enzymes, was incubated at 28°C, and the amount of released 4-methylumbelliferone (4-MU) moiety was measured with excitation wavelength at 360 nm and emission wavelength at 450 nm using a Gemini EM Microplate Fluorometer (Sunnyvale, CA, USA). The amount of the 4-MU product was converted to molar concentration from the relative fluorescence units (RFUs) base on the standard curve of 4-MU of 0.625-10 nM. One unit of chitinase activity was defined as the amount of enzyme which produces 1 μ mol of 4-MU per min at 28°C.

2.4.9 Chitin binding assay and determination of equilibrium adsorption isotherm

Binding of three different polysaccharides (colloidal chitin, crystalline α -chitin and chitosan) to chitinase was performed at 0°C to minimize hydrolysis. A reaction mixture (500 μ l) comprised 1.0 μ mol enzyme, 1.0 mg polysaccharide, 20 mM Tris-HCl buffer, pH 8.0. The reaction was incubated for 30 min, and then terminated by centrifugation at 12000 rpm, 4°C for 10 min. The concentration of the enzyme remained in the supernatant (or free enzyme) was determined by Bradford's method. As a result, the concentration of the bound enzyme (E_b) was calculated from the difference between the initial protein concentration (E_t) and the free protein concentration (E_f) after binding. For adsorption isotherm experiments, the reaction mixture (also prepared as described above) containing concentrations of chitinase varied from 0 to 7.0 μ M was incubated with 1.0 mg of the tested polysaccharide for 30 min. After centrifugation, the concentration of the free enzyme in the supernatant was determined. A plot of $[E_b]$ vs $[E_f]$ was constructed and the equilibrium dissociation binding constant (K_d) was estimated using a non-linear regression function in the GraphPad Prism version 5.0 (GraphPad Software Inc., San Diego, CA).

2.4.10 Steady-state kinetics

Kinetics parameters of the chitinase variants were determined with chitooligosaccharides (GlcNAc₃-GlcNAc₆) or colloidal chitin as substrate. For GlcNAc₃ chitooligosaccharides, a reaction mixture (200 μ l), containing 0-500 μ M substrate, and 50 μ g enzyme in 100 mM sodium acetate buffer, pH 5.5, was incubated

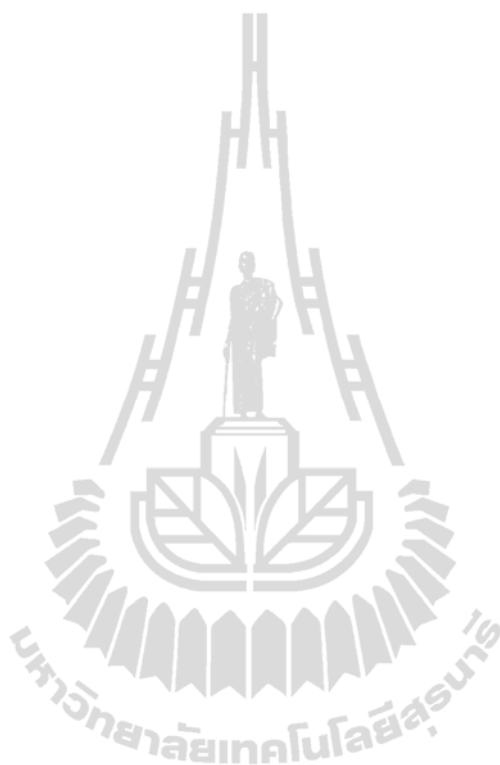
at 37°C with shaking at 700 rpm for 15 min. After cooling on ice 1 min, the entire reaction mixture was subjected to DNS assay as described earlier.

For colloidal chitin and glycol chitin, a reaction mixture (200 μ l), containing 0-10% (w/v) chitin, 150 μ g wild type, D313N, Y435A/W or 250 μ g D313A in 100 mM sodium acetate buffer, pH, 5.5 was incubated at 37°C with shaking at 700 rpm for 15 min. After boiling at 100°C for 5 min, the reaction was subjected to the reducing sugar assay. The kinetic values were evaluated from the reactions carried out in triplicate using a nonlinear regression function available in GraphPad Prism version 5.0 (GraphPad Software Inc., San Diego, CA).

2.4.11 Determination of the pH activity profiles of chitinase A with Asp313 mutation

Universal pH buffer was used to determine pH activity profiles of chitinase A and Asp313 mutants. The buffer contained 100 mM sodium citrate/citric acid and 200 mM sodium phosphate buffer and 0.025% Triton-100 pH 2.25 – 8.5. For the pH 8.5 - 12, the same buffer was prepared with additional pH adjustment with concentrated NaOH. Chitinase activity was determined at various pHs with 4-MU-GlcNAc₂, as substrate. A reaction mixture (55 μ l) was prepared in a black 96-well black microplate using a Gemini EM Microplate Fluorometer (Sunnyvale, CA, USA), the substrate 4MU-GlcNAc₂ was diluted from 0.2-250 μ M, and then the concentration of the wild type, D313N and D313A at 1.25 nM, 0.5 μ M and 1 μ M respectively. The reaction progression was monitored directly at the excitation wavelength of 360 nm and emission wavelength of 450 nm for 30 minutes. The progress curve was analyzed by

SoftMax Pro version 5 (SOFTmax PRO, Molecular Device, CA). The amount of the 4-MU product was quantified as described in Section 2.4.8.



CHAPTER III

RESULTS

3.1 Structure Analysis and Site Directed Mutation

Recently, four crystal structures of *V. harveyi* chitinase A with and without substrates were solved by the molecular replacement technique (Songsiriritthigul *et al.*, 2008). Structural analysis of the catalytically inactive mutant E315M complexed with GlcNAc₆ revealed the substrate-binding cleft as a long deep cleft comprising six-binding subsites (-4), (-3), (-2), (-1), (+1) and (+2). This subsite topology defines subsite -4 at the non-reducing end (NRE), subsite +2 at the reducing end (RE) and the cleavage site between -1 and +1 sites. Four surface-exposed residues, Ser31 and Trp70 at the ChBD and Trp231 and Tyr245 at the edge of the NRE of the substrate-binding site, were lined up in positions suitable for binding to a longer chain chitin. Site-directed mutagenesis of these residues suggested that Trp70 was the most crucial-binding residue for insoluble chitin (Pantoom *et al.*, 2008). As shown in Figure 3.1(A), Tyr171 marks the NRE, while- Tyr435 marks the RE of the GlcNAc₆ chain. Figure 3.1(B) represents the structural complex of E315M+GlcNAc₆, showing that the second glycosidic linkage is in the location to be cleaved by the catalytic residue Glu315. Subsequent cleavage will yield GlcNAc₂ as the end product (Suginta *et al.*, 2005; Songsiriritthigul *et al.*, 2008).

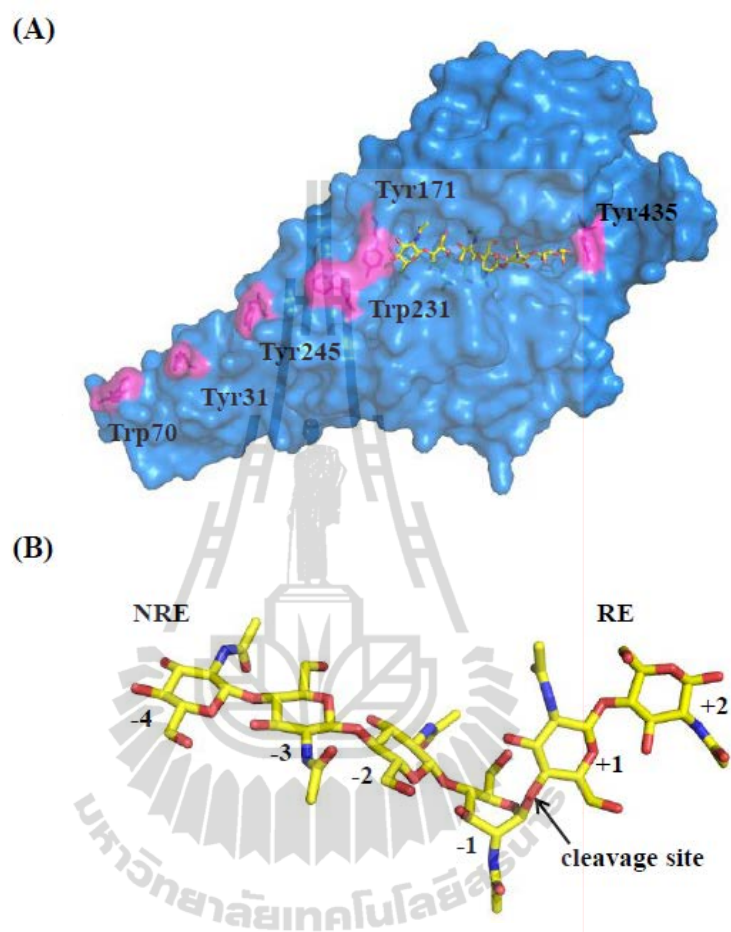


Figure 3.1 Surface representation of the 3D-structure of the *V. harveyi* chitinase A E315M mutant bound with GlcNAc₆. (A) The surface-exposed residues and the mutated residues are labeled and presented in magenta. (B) The GlcNAc₆ structure in the active site of the chitinase A E315M mutant. Carbon (yellow), oxygen (red) and nitrogen (blue) atoms are indicated at the reducing end sugar. NRE: the non-reducing end sugar; RE: the reducing end sugar.

The structural complex of E315M+GlcNAc₆ provides several key features as depicted in Figure 3.2. Firstly, Tyr171 at the edge of subsite -4 forms hydrophobic interactions and a hydrogen bond with the subsite -4 GlcNAc. Secondly, subsite -3

contains Trp168 that stacks against the hydrophobic face of the corresponding sugar, while Trp275 from the opposite side of the binding cleft stacks against the hydrophobic face of +1GlcNAc. In addition, the nitrogen atom of the Trp275 side chain forms two critical hydrogen bonds with the O3 and O6 hydroxyl groups of the -1 GlcNAc and -2 GlcNAc, respectively. Thirdly, Trp570 stacks against the pyranosyl ring of the GlcNAc unit at subsite +1. Fourthly, Glu315 is located at the scissile bond between -1 GlcNAc and +1 GlcNAc and it is meant to act as a proton donor. On the other hand, the carbonyl oxygen (O7) of the acetamido group of the -1 GlcNAc acts as a nucleophile in the substrate-assisted mechanism. Fifthly, Asp313 located at the bottom of the catalytic cleft could play an important role in stabilization of the transition state (oxazolinium ion) by maintaining the strained “boat”-conformation of the -1 subsite GlcNAc (Songsiriritthigul *et al.*, 2008). Lastly, Tyr435 located at the end of the RE of the sugar forms a hydrogen bond with the O7 of the +2 GlcNAc via its OH group.

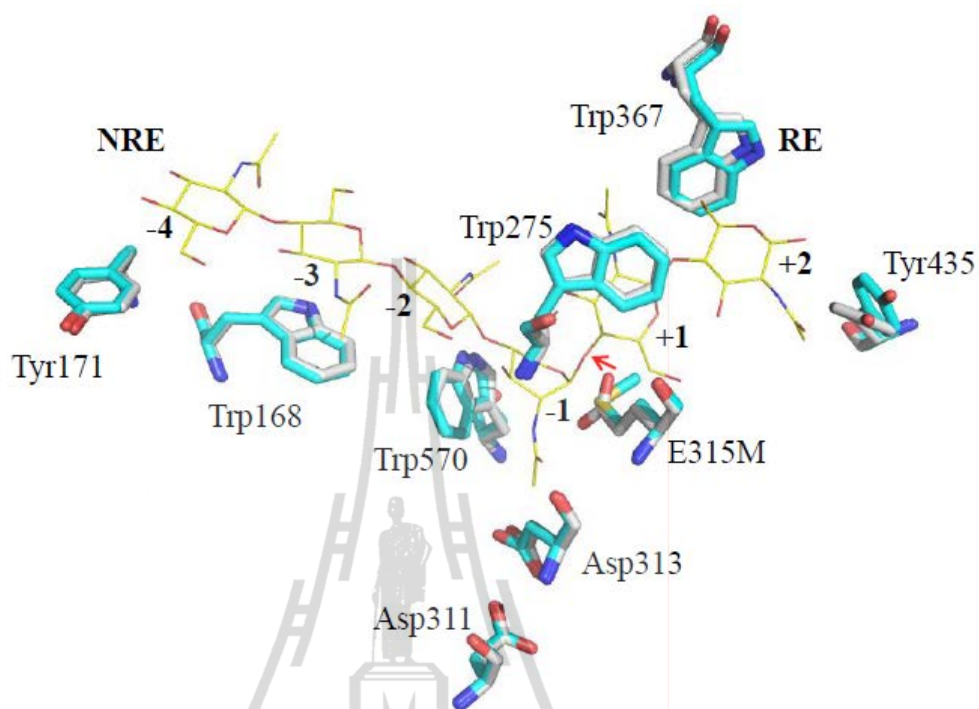


Figure 3.2 Superimposition of the binding residues in the active cleft of wild-type and E315M+GlcNAc₆ complex of *V. harveyi* chitinase A. The binding residues are depicted as stick models wild-type with carbons in gray and mutant E315M are stick in cyan. GlcNAc₆ are depicted as line models with carbons in yellow. Colors of other atoms are blue for nitrogen and red for oxygen. The cleavage site is indicated by an arrow.

3.2 Structural comparison of *V. harveyi* chitinase A and *S. marcescens* chitinase A

Figure 3.3 shows superimposition of the *V. harveyi* chitinase A inactive mutant E315M structure (pdb code 3B9A) with the *S. marcescens* chitinase A inactivate mutant E315Q structure (pdb code 1EHN). The overall structures of the two enzymes are very similar. As mentioned earlier, the surface-exposed aromatic residues from the ChBD are essential for the binding to insoluble chitin substrates. These residues include Ser31, Trp70, Tyr231 and Tyr245 in *V. harveyi* chitinase A (Pantoom *et al.*, 2008 and Songsiririthigul *et al.*, 2008) or Ser33, Trp69, Phe232 and Trp245 in *S. marcescens* chitinase A (Uchiyama *et al.*, 2001) (Figure 3.3(A)). The catalytic domain of both chitinases has a TIM-barrel fold and includes a conserved glutamate residue that acts as an acid at the first step of catalysis. The active site of both enzymes also shows that GlcNAc₆ units are embedded at subsites -4, -3, -2, -1, +2 and +2 and the scissile bond is placed between subsites -1 and +1. Many conserved residues are located in the catalytic domain, including Trp168, Tyr171, Trp275, Asp313, Glu315Met, Trp397, Tyr435 and Trp570 in *V. harveyi* chitinase A (Suginta *et al.*, 2005 and 2007), which are in equivalent positions with Trp167, Tyr170, Trp275, Asp313, E315Q, Phe396, Tyr418 and Trp570, respectively, in *S. marcescens* chitinase A (Papanikolau *et al.*, 2001 and Zakariassen *et al.*, 2009) (Figure 3.3(B)).

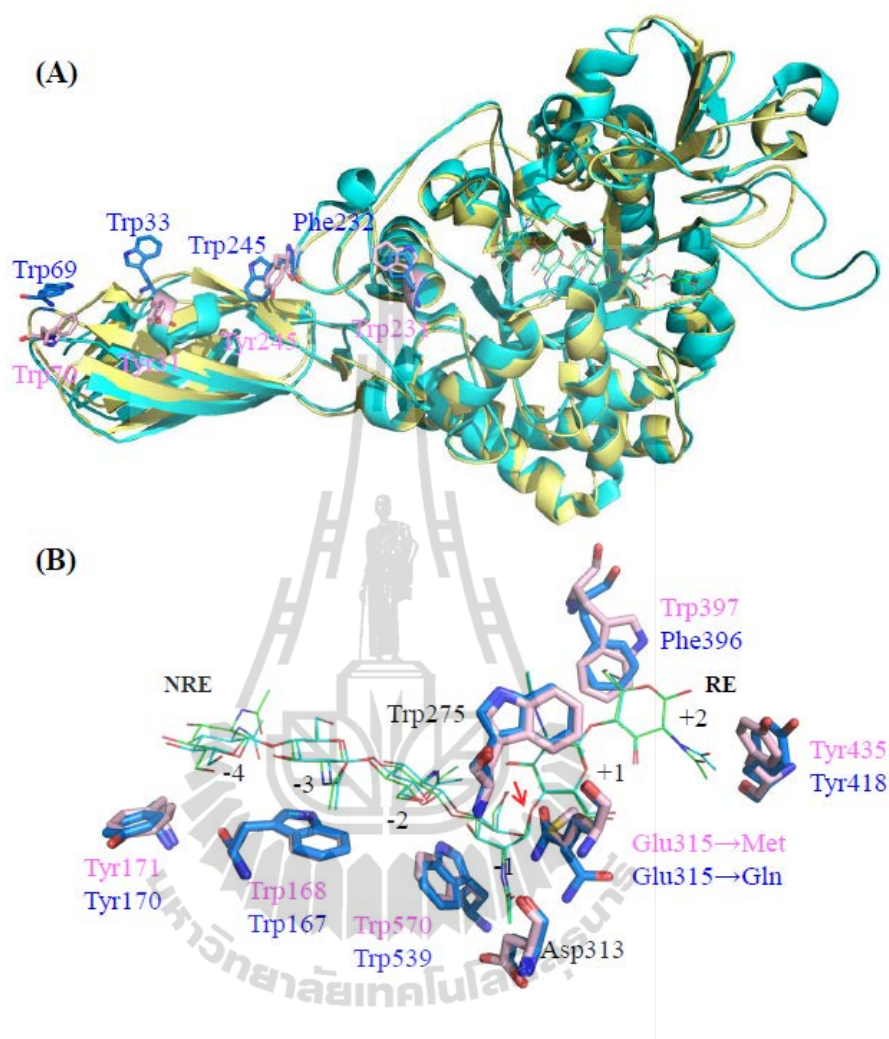


Figure 3.3 Superimposition of *V. harveyi* chitinase A and *S. marcescens* chitinase A structure. (A) A ribbon representation of *V. harveyi* chitinase A in cyan and *S. marcescens* chitinase A in yellow. The aromatic residues at the ChBD of *V. harveyi* chitinase A are depicted as stick models in pink and *S. marcescens* chitinase A in blue. (B) The binding residues of *V. harveyi* chitinase A mutant E315M-GlcNAc₆ complex are presented in green and *S. marcescens* chitinase A mutant E315Q-GlcNAc₆ complex in blue and GlcNAc₆ in cyan. The cleavage site is indicated by an arrow.

3.3 Structural comparison of *V. harveyi* chitinase A and *S. marcescens* chitinase B

Chitinase A and chitinase B are the key enzymes responsible for chitin degradation, but both enzymes are known to degrade chitin from opposite directions. Figure 3.4(A) shows superimposition of the *V. harveyi* chitinase A inactive mutant E315M structure (pdb code 3B9A) with the *S. marcescens* chitinase B inactivate mutant E144Q structure (pdb code 1E6N), which here an at RMSD of 2.041 Å for 241 Ca atoms. The catalytic domain of the two enzymes aligns with each other relatively well, whereas their ChBDs are oriented in opposite directions. In *V. harveyi* chitinase A, the surface-exposed residues Trp70, Trp31, Tyr24, and Trp231 situated outside the non-reducing end towards the ChBD, are equivalent with Tyr481, Trp479, Trp252 and Tyr240, respectively, of *S. marcescens* chitinase B. Figure 3.4(B) represents the occupation GlcNAc₆ in the substrate binding groove of *V. harveyi* chitinase A in comparison with GlcNAc₅ in *S. marcescens* chitinase B. It is clear that the orientation of the two substrates follows the subsite architecture of the individual enzyme whereby the NRE of GlcNAc₆ in *V. harveyi* chitinase A starts at position -4 and the RE ends at position -2. In *S. marcescens* chitinase A, the NRE of GlcNAc₅ resides at subsite -2 and the RE at subsite +3. Considering the substrate binding residues, Trp397 (+2 site) and Trp570 (-1 site) of *V. harveyi* chitinase A are in equivalent positions with Trp220 and Trp403 of *S. marcescens* chitinase B, whereas Glu315, Asp313, Tyr435 of the *Vibrio* chitinase A are in identical locations with Glu144, Asp142 and Leu126 of the *Serratia* chitinase B respectively.

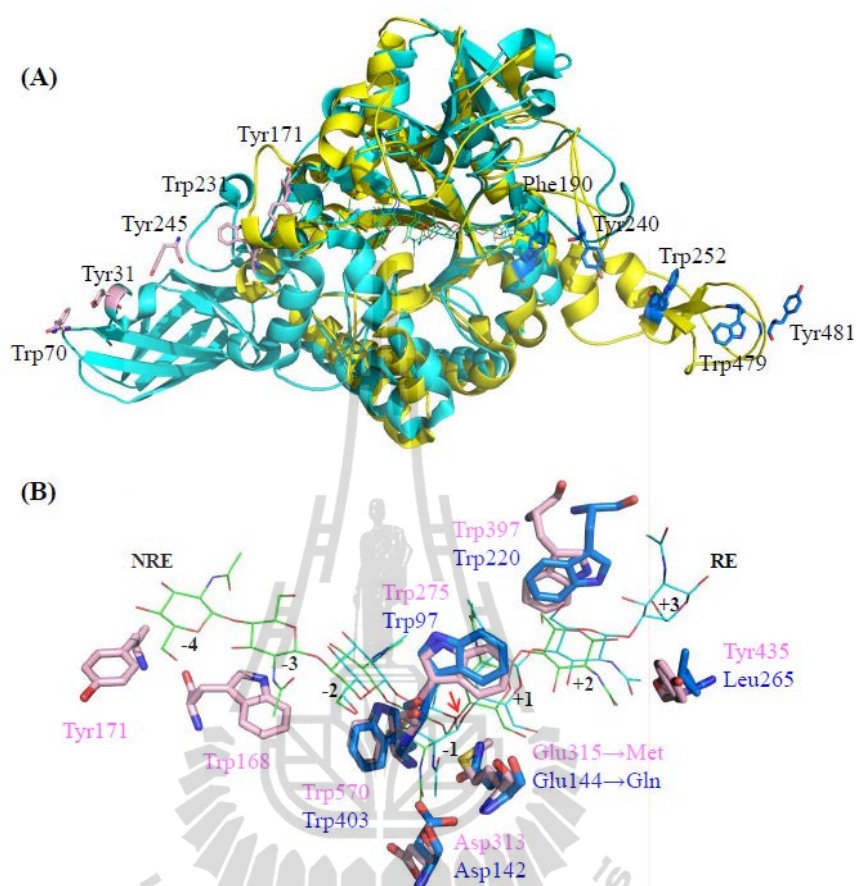


Figure 3.4 Superimposition of *V. harveyi* chitinase A and *S. marcescens* chitinase B structure. (A) A ribbon representation of superposition of *V. harveyi* chitinase A in cyan and *S. marcescens* chitinase B in yellow. The aromatic at the chitin-binding domain *V. harveyi* chitinase A are depicted as stick models in pink and *S. marcescens* chitinase A in blue. (B) The binding residues of *V. harveyi* chitinase A mutant E315M- GlcNAc₆ complex in pink and GlcNAc₆ in green and *S. marcescens* chitinase B mutant E315Q-GlcNAc₅ complex in blue and GlcNAc₅ in cyan. The cleavage site is indicated by an arrow.

3.4 Structural comparison of *V. harveyi* chitinase A and *B. circulans* chitinase A1

As shown in Figure 3.5, the catalytic domain of chitinase A1 from *B. circulans* wild-type (pdb code 1ITX) is well superimposed on that of the chitinase A from *V. harveyi* inactive mutant E315M structure (pdb code 3B9A). The crystal structure of an inactivated CatDChiA1 complexed with GlcNAc₇ suggests that cleavage of the chitin chain occurs at the second linkage from the reducing end and the presence of seven subsites, numbered -5 to +2, and in the substrate binding cleft was deduced from the complex structure (Watanabe *et al.*, 2003). The conserved residues located in the catalytic domain include Tyr56, Trp53, Trp433, Asp202, Glu204, Trp164, Trp285 and Phe312 in *B. circulans* chitinase A1 (Watanabe *et al.*, 2003). Considering the substrate binding residues, Trp397 (+2 sites) and Trp570 (-1 site) of *V. harveyi* chitinase A are in equivalent positions with Trp285 and Trp433 of *B. circulans* chitinase A1, whereas Glu315, Asp313, Tyr435 of the *Vibrio* chitinase A align with Glu204, Asp202 and Phe312 of the *B. circulans* chitinase A1.

In addition, the outside of the substrate-binding cleft, two tryptophan residues (Trp122 and Trp134) are aligned on the extension of the oligomer chain bound to the cleft. These two aromatic residues have been shown to be essential for hydrolysis of crystalline chitin and play an important role in guiding a chitin chain into the substrate-binding cleft during crystalline-chitin hydrolysis (Watanabe *et al.*, 2001).

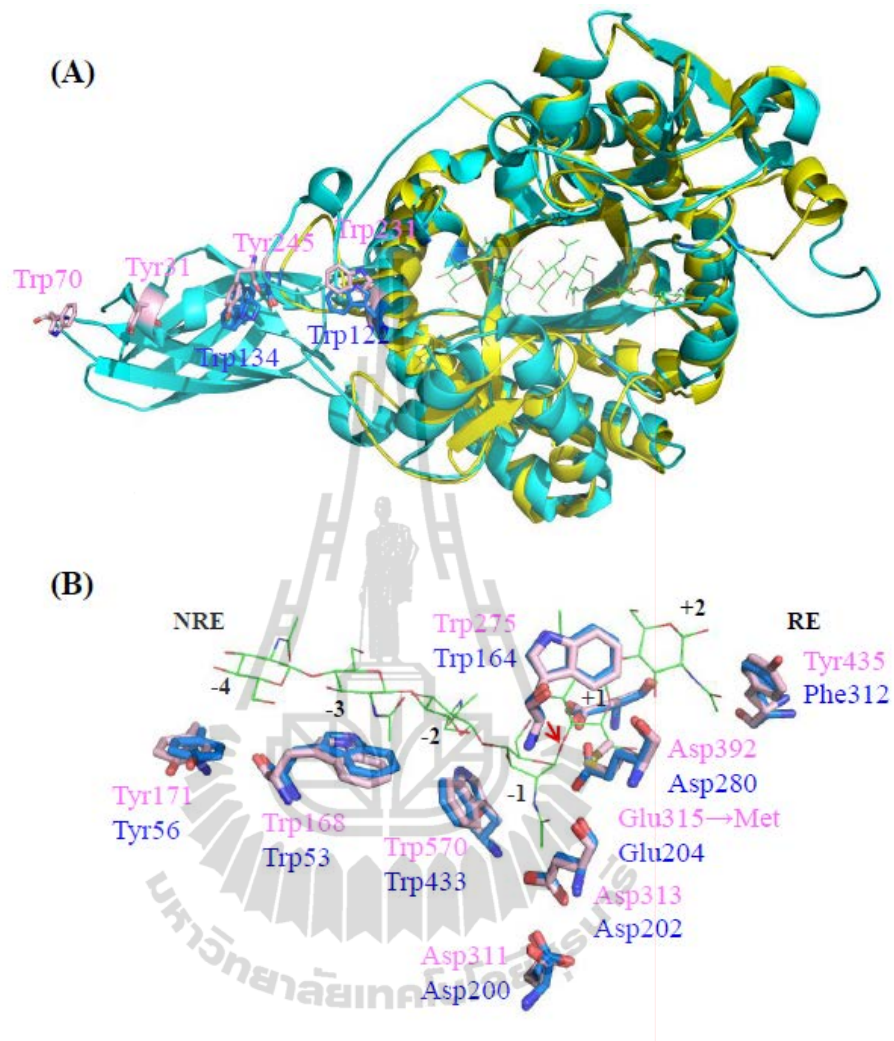


Figure 3.5 Superimposition of *V. harveyi* chitinase A and *B. circulans* chitinase A1 structure. (A) A ribbon representation of *V. harveyi* chitinase A (in cyan) and *B. circulans* chitinase A1 (in yellow). The aromatic residues at the ChBD *V. harveyi* chitinase A are depicted as stick models with carbons in pink and *B. circulans* chitinase A1 with carbons in blue. (B) The binding residues of *V. harveyi* chitinase A mutant E315M- GlcNAc₆ complex with carbons in pink and GlcNAc₆ in green and *B. circulans* chitinase A1 with carbons in blue. The cleavage site is indicated by an arrow.

3.5 Expression and purification of the recombinant chitinase A and its Asp313 and Tyr435 mutants

The location of the residue Asp313 suggests that this residue is most likely involved in the stabilization of the oxazolinium intermediate, while Tyr435 may aid the termination process of the sugar chain from moving beyond subsite +2. To demonstrate the roles of Asp313 and Tyr435, these residues were mutated. Asp313 was substituted by Ala and Asn and Tyr435 to Ala and Trp. The four mutants are designated D313A, D313N, Y435A and Y435W.

After confirming the correct mutation of the target bases by automatic DNA sequencing, the recombinant proteins were highly expressed in *E. coli* M15 host cells. The six histidine residues tagged at the *C*-terminus allowed the proteins to be readily purified by Ni-NTA agarose affinity chromatography. Figure 3.6 demonstrates expression following purification patterns of *V. harveyi* chitinase A at 63 kDa migration. After crude protein was incubated with Ni-NTA agarose, washed with 5 mM and by 20 mM imidazole (lanes 4-6), the purified chitinase A was eluted with 250 mM imidazole (lane 7).

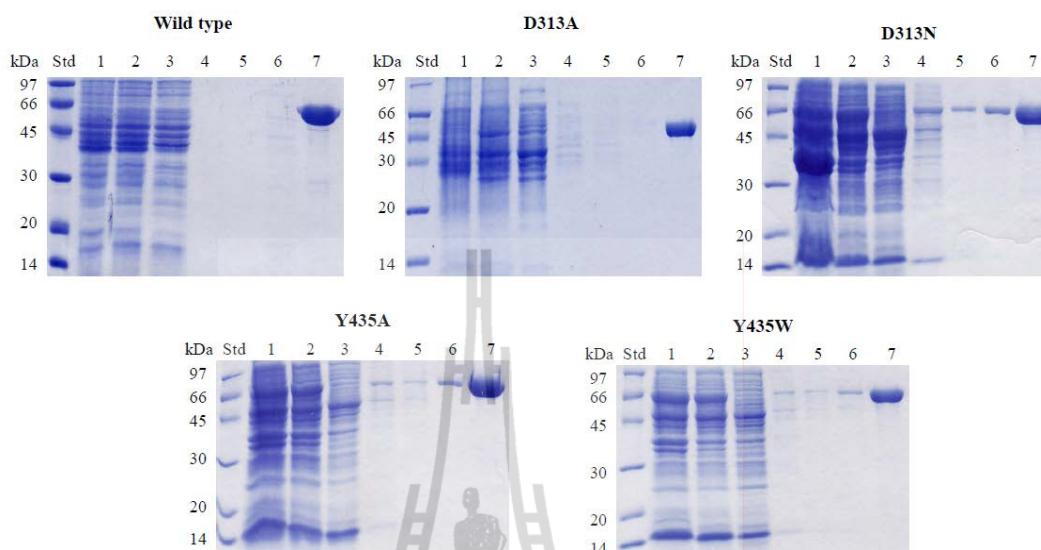


Figure 3.6 Purification of the recombinant chitinase A and mutants using Ni-NTA agarose affinity chromatography. Lanes: Std, low molecular weight protein marker; 1, cells induced with 0.5 mM IPTG; 2, crude supernatant; 3, flow through; 4, the first wash with 5 mM imidazole; 5, the second wash with 5 mM imidazole; 6, 20 mM imidazole wash fraction; 7, the eluted fraction with 250 mM imidazole;

After a single-step purification using Ni-NTA agarose affinity chromatography, the yield of the purified proteins was estimated to be approx. 20 to 25 mg/ml per litre of bacterial culture. As analyzed by SDS-PAGE, all the mutated proteins displayed a single band of molecular weight of ~63 kDa (Figure 3.7), which is identical to the molecular weight of the wild-type enzyme.

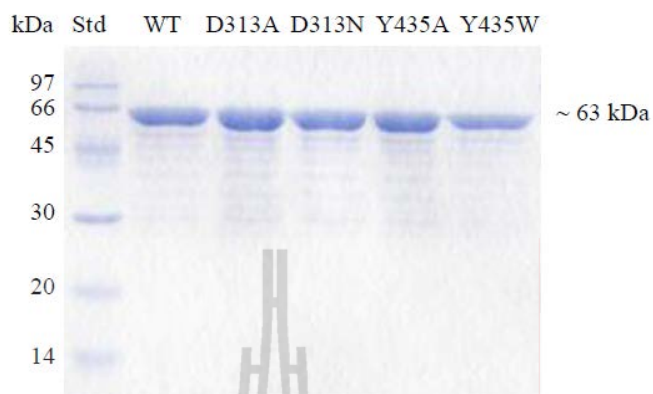
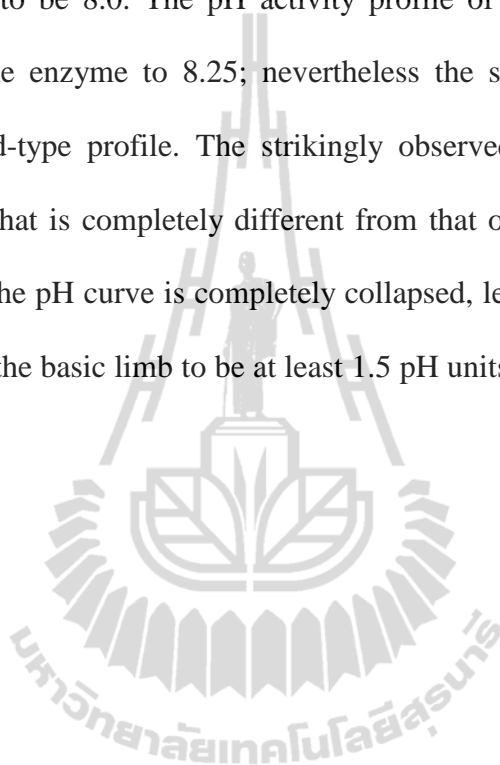


Figure 3.7 SDS-PAGE analysis of purified chitinase A and its mutants. The amount of protein applied to each lane was 5 μ g.

3.6 Effects of Asp313 mutations on pH activity profiles

The chitinase activity of wild-type and two variants D313A and D313N were assayed at a wide pH range using fluorogenic 4-MU-GlcNAc₂ substrate. The fluorescence of the liberated 4-MU, representing the progress of the reaction was monitored continuously for 30 min with the excitation wavelength of 360 nm and emission wavelength of 450 nm. For wild-type and mutant D313N, the enzyme activity was measured from pH 2.25 to 8.5, while mutant D313A was monitored from pH 2.25 to 12 using concentration of 4-MU-GlcNAc₂ from 1 μ M to 250 μ M. As shown in Figure 3.8(A), The K_m values of wild-type and mutant D313A and D313N were decreased at pH 4.5 to 7.75 and increased at pH >8 or <4. In the case of mutant D313A, the K_m values were increased at pH >8.5. The k_{cat} versus pH plot of mutant D313N was significantly decreased over the entire range of pHs, but still displayed the same bell-shape as that of the wild-type enzyme. In Figure 3.8(C) the plot of the k_{cat} / K_m versus pH for wild-type and mutant D313N also displays the bell-shaped

curves. It can be clearly seen from the pH activity profiles obtained from the k_{cat} / K_m that the pH optimum of the wild-type enzymes is at pH 6.0, giving the $\text{p}K_a$ of the nucleophilic group on the acidic limb to be 3.5 and the $\text{p}K_a$ of the proton donor group on the basic limb to be 8.0. The pH activity profile of mutant D313A shifted the optimum pH of the enzyme to 8.25; nevertheless the shape of the curve remains similar to the wild-type profile. The strikingly observed result is the pH activity profile of D313A that is completely different from that of the wild-type. Especially, the acidic limb of the pH curve is completely collapsed, leaving the $\text{p}K_a$ of the proton donating group on the basic limb to be at least 1.5 pH units (9.25) greater than the $\text{p}K_a$ of the wild-type.



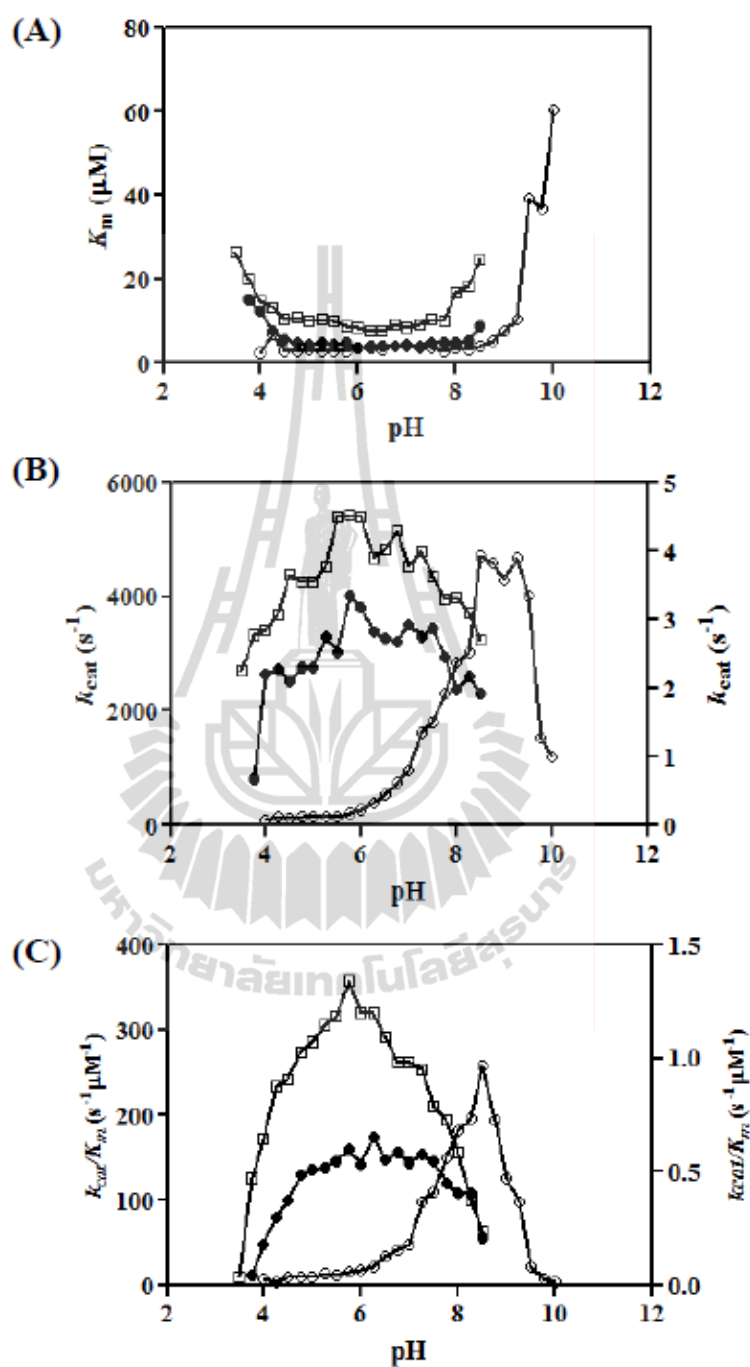


Figure 3.8 Effects of mutations on the pH activity profiles of *V. harveyi* chitinase A.

(A) The K_m value versus pH. (B) The k_{cat} value versus pH (C) The k_{cat}/K_m versus pH.

The wild type activity is shown as \square and its activity unit represent to right y-axis.

For D313A and D313N, the kinetic parameters are shown as \circ , and \bullet , respectively,

and their kinetic values are plotted in the left y-axis.

3.7 Effects of Mutations on the Specific Hydrolyzing Activities of Chitinase A and Mutants

The specific hydrolyzing activity was assayed based on the use of the natural substrates (GlcNAc₃₋₆, chitin derivatives) and artificial substrates (*p*NP-GlcNAc₂) (Table 3.1). Mutation of Asp313 severely impaired the activity of all substrates. Mutant D313A dramatically decreased the chitinase activity (ca. 0.08-fold of the wild-type activity) on all the tested substrates. Mutant D313N also showed significant activity reduction, although to lesser extent than the D313A mutant (ca. 0.2-fold of the wild-type activity). Regarding the Tyr435 mutations, increases in the specific activity were observed with mutant Y435A with the highest activity detected with crystalline chitin hydrolysis (ca. 1.2-fold of the wild-type activity). In contrast, mutant Y435W displayed considerable decreases in the specific activity with all the tested substrates.

Table 3.1 Specific hydrolyzing activity of chitinase A and its mutants

Substrates	Specific hydrolyzing activity				
	Wild-type	D313A	D313N	Y435A	Y435W
4MU-(GlcNAc) ₂ ^a	28.2 ± 1.2 (1) ^e	2.5 ± 0.02 (0.08)	5.8 ± 0.06 (0.2)	31.4 ± 1.6 (1.1)	22.3 ± 1.3 (0.8)
pNP-(GlcNAc) ₂ ^b	39.2 ± 2.4 (1)	3.3 ± 0.6 (0.08)	7.6 ± 0.8 (0.2)	40.9 ± 3.4 (1.1)	37.8 ± 2.2 (0.9)
GlcNAc ₃ ^c	13.5 ± 0.4 (1)	0.3 ± 0.04 (0.02)	0.6 ± 0.02 (0.04)	14.8 ± 0.8 (1.1)	9.6 ± 0.7 (0.7)
GlcNAc ₄ ^c	14.1 ± 0.5 (1)	n.d. ^d	0.4 ± 0.03 (0.03)	16.1 ± 0.3 (1.1)	12.4 ± 0.8 (0.9)
GlcNAc ₅ ^c	17.8 ± 0.6 (1)	n.d.	0.3 ± 0.01 (0.02)	20.8 ± 1.1 (1.2)	13.9 ± 0.6 (0.8)
GlcNAc ₆ ^c	35.2 ± 1.6 (1)	n.d.	n.d.	36.2 ± 1.4 (1)	32.2 ± 1.2 (0.9)
colloidal chitin ^c	23.6 ± 0.5 (1)	n.d.	n.d.	26.1 ± 0.8 (1.1)	22.4 ± 0.3 (0.9)
glycol chitin ^c	12.8 ± 0.2 (1)	n.d.	n.d.	14.4 ± 0.3 (1.1)	11.4 ± 0.4 (0.9)
crystalline chitin ^c	3.2 ± 0.01 (1)	n.d.	n.d.	3.8 ± 0.03 (1.2)	2.5 ± 0.06 (0.8)

^a (μmol 4MU/min/μg)

^b (μmol pNP/min/μg)

^c (μmol GlcNAc₂/min/μg)

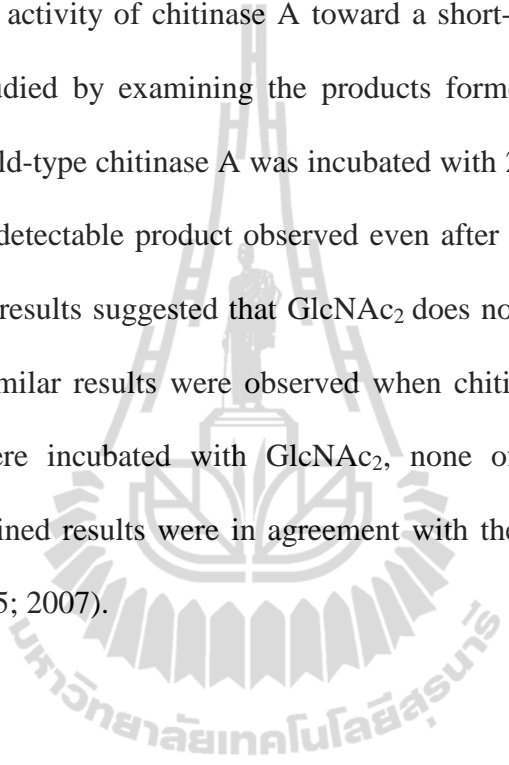
^d Non-detectable activity

^e Relative specific hydrolyzing activity (fold) are shown in parentheses.

3.8 TLC Analysis of the Hydrolytic Products of Chitinase A and Mutants

3.8.1 TLC analysis of GlcNAc₂ hydrolysis

The hydrolytic activity of chitinase A toward a short-chain chitiologosaccharide (GlcNAc₂) was studied by examining the products formed at various time points. When 200 ng of wild-type chitinase A was incubated with 2.5 mM GlcNAc₂, the TLC results showed no detectable product observed even after 18 h of incubation (Figure 3.9). The obtained results suggested that GlcNAc₂ does not at all act as the substrate of this enzyme. Similar results were observed when chitinase A mutants D313A/N and Y435A/W were incubated with GlcNAc₂, none of the mutants hydrolyzed GlcNAc₂. The obtained results were in agreement with the previously observed data (Suginta *et al.*, 2005; 2007).



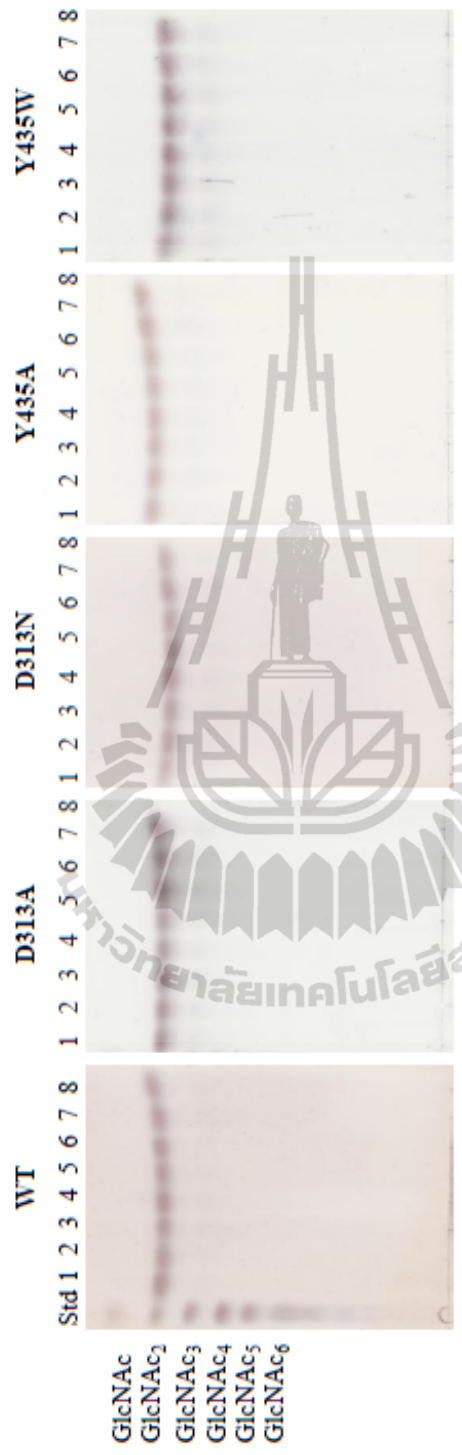


Figure 3.9 Time course of GlcNAc₂ hydrolyzed by chitinase A mutants as analyzed by TLC.

Lanes Std, a standard mixture of GlcNAc₂–GlcNAc₆, 1–7 the reaction products at 2, 5, 10, 15, 30, 60 min and 18 h, respectively; 8, substrate blank.

3.7.2 TLC analysis of GlcNAc₃ hydrolysis

With GlcNAc₃ substrate, no product was seen at incubation times between 0-60 min. Only pale spots corresponding to GlcNAc and GlcNAc₂ were detected at 18 h incubation, indicating that GlcNAc₃ was poorly hydrolyzed by the wild-type enzyme, as shown in Figure 3.10. Apparently, both mutants D313A and D313N did not utilize GlcNAc₃ at all. In the case of mutants Y435A and Y435W, both mutants cleaved GlcNAc₃ to GlcNAc₂ at incubation time of 18 h, giving GlcNAc and GlcNAc₂ as the end product. More intense spots corresponding to GlcNAc and GlcNAc₂ products were seen as a result of GlcNAc₃ hydrolysis by mutants Y435A than that of wild-type indicating that this mutant had a greater efficiency in the utilization of GlcNAc₃ than the non-mutated enzyme.



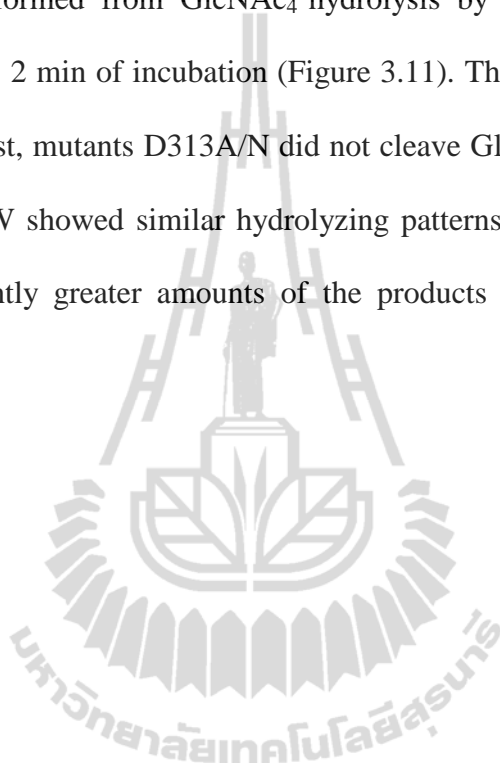


Figure 3.10 Time course of GlcNAc₃ hydrolyzed by chitinase A mutants as analyzed by TLC.

Lanes Std, a standard mixture of GlcNAc₂–GlcNAc₆; 1–7 the reaction products at 2, 5, 10, 15, 30, 60 min and 18 h, respectively; 8, substrate blank.

3.7.3 TLC analysis of GlcNAc₄ hydrolysis

With the GlcNAc₄ substrate, the wild-type enzyme mainly recognized the middle glycosidic bond of the tetrameric chain, releasing only GlcNAc₂ product. The GlcNAc₂ product formed from GlcNAc₄ hydrolysis by wild-type chitinase A was detected as early as 2 min of incubation (Figure 3.11). The hydrolysis was completed at 18 hs. In contrast, mutants D313A/N did not cleave GlcNAc₄ at all, while mutants Y435A and Y435W showed similar hydrolyzing patterns for GlcNAc₄ hydrolysis as wild-type but slightly greater amounts of the products were detected with mutant Y435W.



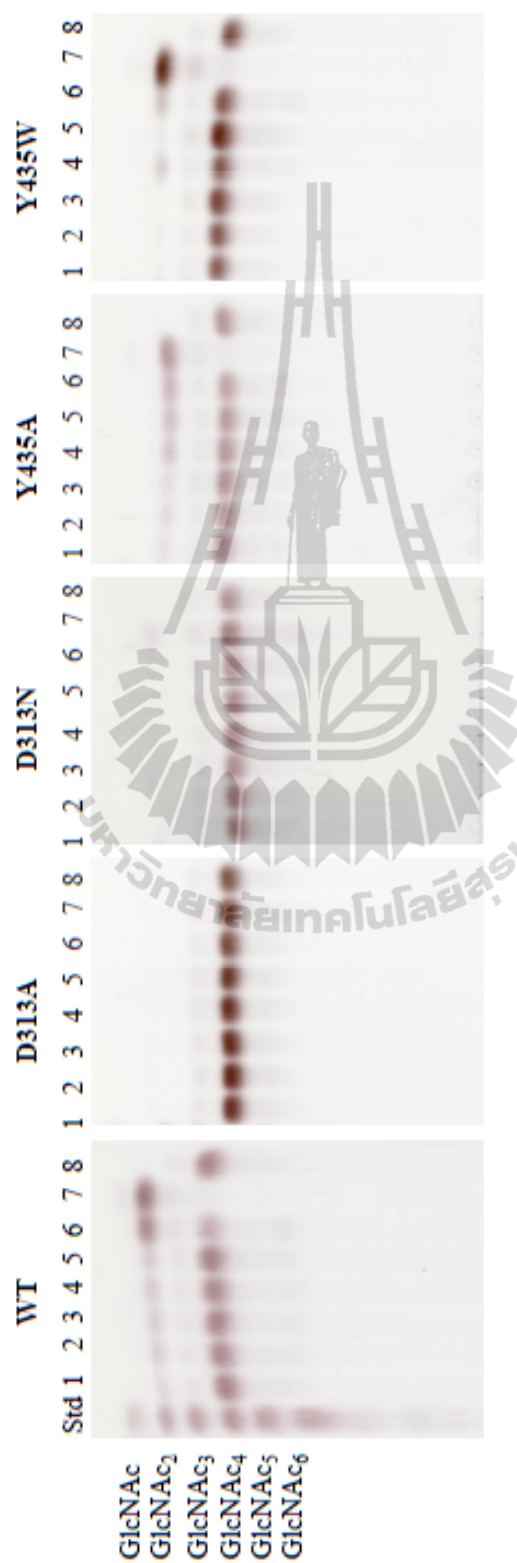


Figure 3.11 Time course of GlcNAc₄ hydrolyzed by chitinase A mutants as analyzed by TLC.

Lanes Std, a standard mixture of GlcNAc₂–GlcNAc₆, 1-7 the reaction products at 2, 5, 10, 15, 30, 60 min and 18 h, respectively. 8, substrate blank.

3.7.4 TLC analysis of GlcNAc₅ hydrolysis

The hydrolytic activity of chitinase A wild-type was investigated with GlcNAc₅ substrate. The enzyme mainly hydrolyzed GlcNAc₅ to GlcNAc₃ and GlcNAc₂. However, at 18 h of incubation GlcNAc was subsequently produced (Figure 3.12). D313A did not hydrolyze GlcNAc₅ at all, while mutant D313N could hydrolyze the pentameric substrate only when the reaction was continued as long as 18 h. Y435A hydrolyzed GlcNAc₅ releasing GlcNAc₃ to GlcNAc₂ within 2 min and the reaction was completed at 18 h of incubation, yielding GlcNAc₃, GlcNAc₂ and GlcNAc as the end products, On the other hand, Y435W hydrolyzed GlcNAc₅ releasing only GlcNAc₃ and GlcNAc₂ after 30 min of the reaction. The hydrolytic activity of Y435W was lower than wild-type and mutant Y435A.





Figure 3.12 Time course of GlcNAc₅ hydrolyzed by chitinase A mutants as analyzed by TLC.

Lanes Std, a standard mixture of GlcNAc₂–GlcNAc₆, 1-7 the reaction products at 2, 5, 10, 15, 30, 60 min and 18 h, respectively; 8, substrate blank.

3.8.5 TLC analysis of GlcNAc₆ hydrolysis

Figure 3.9 shows products formed by hydrolysis of GlcNAc₆ with wild-type chitinase A and mutants at different times of reaction. The hydrolysis of wild-type chitinase A initially yielded GlcNAc₄, GlcNAc₃ and GlcNAc₂ (Figure 3.13). After 10 min of incubation the reaction was completed, giving GlcNAc₃ and GlcNAc₂ as the final products. The results obtained from TLC suggested the cleavage of the GlcNAc₆ chain occurred at the second and the middle bonds. GlcNAc₄ + GlcNAc₂ were the outcome of the second bond cleavage, whereas GlcNAc₃ was the outcome of the middle bond degradation. Asp313 mutants did not at all hydrolyze GlcNAc₆. Mutation of Tyr435 to Ala led to the hydrolysis of GlcNAc₆ much more efficiently than the wild-type. More GlcNAc₂ and GlcNAc₃ products were visible in the mutant Y435A reaction than in the wild-type reaction, whereas mutant Y345W hydrolyzed GlcNAc₆ releasing pale spots of GlcNAc₂ and GlcNAc₃. The hydrolysis by mutant Y435A was completed at 5 min of incubation, while the hydrolysis by Y435W was completed at 60 min of incubation.



Figure 3.13 Time course of GlcNAc₆ hydrolyzed by chitinase A mutants as analyzed by TLC.

Lanes Std, a standard mixture of GlcNAc₂–GlcNAc₆, 1–7 the reaction products at 2, 5, 10, 15, 30, 60 min and 18 h, respectively, 8, substrate blank.

3.8.6 TLC analysis of colloidal chitin hydrolysis

The hydrolytic activity of wild-type chitinase A against colloidal chitin was also studied at various incubation times. The TLC results showed that wild-type chitinase hydrolyzed chitin to GlcNAc₂ within 2 min of incubation. GlcNAc was also observed only when the reaction proceeded up to 18 h. Mutation of D313A hydrolyzed colloidal chitin releasing a very small amount of GlcNAc₂ only at 18 h incubation, as shown in Figure 3.14. Mutant D313N clearly showed slightly higher actions than D313A by hydrolyzing chitin to GlcNAc₂ after 5 min of reaction, while D313A only released a very small amount of GlcNAc₂ at 18 h of incubation. Mutant Y435A showed highest efficiency by degrading chitin to GlcNAc₂ as the major product and trace amount, of GlcNAc₃. After 60 min, GlcNAc₂ and GlcNAc were produced as the major end products, with some GlcNAc₃ also being present in the reaction. The hydrolytic patterns of Y435A/W were similar to that of wild-type chitinase A.



Figure 3.14 Time course of colloidal chitin hydrolyzed by chitinase A mutants as analyzed by TLC. Lanes Std, a standard mixture of GlcNAc₂-GlcNAc₆ 1-7 the reaction products at 2, 5, 10, 15, 30, 60 min and 18 h, respectively; 8, substrate blank.

3.8.7 TLC analysis of glycol chitin hydrolysis

TLC analysis of wild-type chitinase A against glycol chitin is shown in Figure 3.15. The TLC results showed that mutant D313A completely abolished the activity against glycol chitin, while mutant D313N could degrade glycol chitin to GlcNAc₂ slightly better than D313A when the reaction was incubated as long as 60 min. Mutations of Y435A/W showed slightly higher activity in glycol chitin degradation than the wild-type. For glycol chitin hydrolysis, only GlcNAc₂ was the only detectable product for all the enzyme variants.

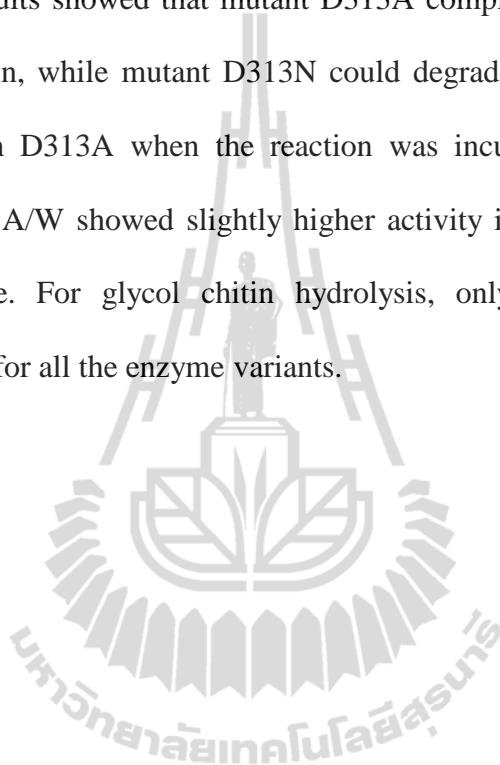




Figure 3.15 Time course of glycol chitin hydrolyzed by chitinase A mutants as analyzed by TLC.

Lanes Std, a standard mixture of GlcNAc₂–GlcNAc₆, 1–7 the reaction products at 2, 5, 10, 15, 30, 60 min and 18 h, respectively; 8, substrate blank.

3.9 Steady-state Kinetics of Chitinase A and Mutants

3.9.1 Hydrolytic activity of *p*NP-GlcNAc₂

The effects of mutations on kinetic parameters of *p*NP-GlcNAc₂ hydrolysis are shown in Figure 3.16 and Table 3.2. The K_m values of both mutants D313A and D313N are $110.9 \pm 23.3 \mu\text{M}$ and $67.6 \pm 18.5 \mu\text{M}$, respectively. These values are significantly higher than the wild-type K_m value ($57.9 \pm 7.2 \mu\text{M}$). Mutants Y435A and Y435W showed slightly reduced K_m values of $48.9 \pm 5.9 \mu\text{M}$ and $52.2 \pm 5.8 \mu\text{M}$, respectively, comparing with the wild-type's value. The k_{cat} values of mutants D313A, D313N and Y435W (0.01 s^{-1} , 0.02 s^{-1} and 0.06 s^{-1} , respectively) were 0.07, 0.05 and 0.15 fold, respectively less than the wild-type chitinase A (0.14 s^{-1}), whereas the k_{cat} value of Y435A (0.15 s^{-1}) was higher than the wild-type value. The k_{cat}/K_m values of the mutants D313A, D313N and Y435W were approx. 0.04, 0.1 and 0.5-fold ($0.9 \times 10^{-4} \text{ s}^{-1} \mu\text{M}^{-1}$, $2.9 \times 10^{-4} \text{ s}^{-1} \mu\text{M}^{-1}$ and $1.2 \times 10^{-3} \text{ s}^{-1} \mu\text{M}^{-1}$, respectively) of the wild-type k_{cat}/K_m ($2.4 \times 10^{-3} \text{ s}^{-1} \mu\text{M}^{-1}$). On the other hand, the k_{cat}/K_m values of Y435A ($3.1 \times 10^{-3} \text{ s}^{-1} \mu\text{M}^{-1}$) was approx. 1.3 fold higher than the wild-type's k_{cat}/K_m value.

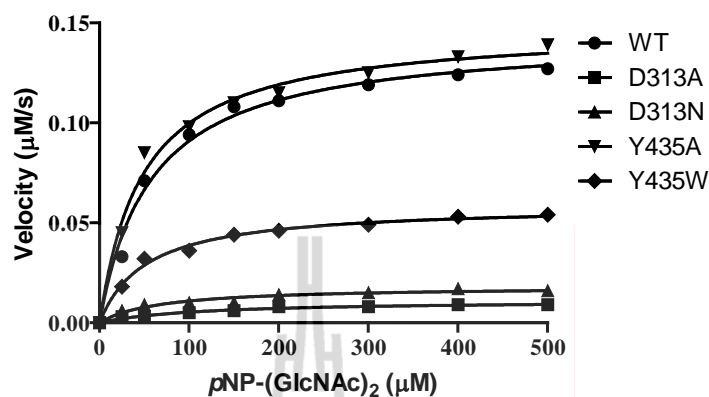


Figure 3.16 The Michaelis-Menten plot of *pNP-GlcNAc*₂. The kinetic assay was carried out using 0–500 μM of *pNP-GlcNAc*₂ as the substrate. After 15 minutes of incubation at 37°C, the amounts of the reaction products were determined by detection of pNP released at A_{405} nm.

Table 3.2 Kinetic parameters of *pNP-GlcNAc*₂ hydrolysis

Chitinase A variant	V_{\max} ($\mu\text{mol}/\text{min}$)	K_m (μM)	k_{cat} (s^{-1})	k_{cat} / K_m ($\text{s}^{-1} \mu\text{M}^{-1}$)
Wild-type	0.14 ± 0.004	58 ± 7	0.14	2.4×10^{-3} (1)*
D313A	0.01 ± 0.001	111 ± 23	0.01	0.9×10^{-4} (0.04)
D313N	0.02 ± 0.001	68 ± 19	0.02	2.9×10^{-4} (0.1)
Y435A	0.15 ± 0.004	49 ± 6	0.15	3.1×10^{-3} (1.3)
Y435W	0.06 ± 0.001	52 ± 6	0.06	1.2×10^{-3} (0.5)

* Relative catalytic efficiencies are shown in parentheses.

3.9.2 Steady-state kinetics of GlcNAc₃ hydrolysis

The effect of the mutations on the hydrolysis of natural substrate short-chain GlcNAc₃ was determined as shown in Figure 3.17 and Table 3.3. Mutations of D313A and D313N showed 0.8 and 0.9-fold increases in the K_m values of $276 \pm 63 \mu\text{M}$ and $223 \pm 46 \mu\text{M}$, respectively, compared to the value for wild-type enzyme ($163 \pm 37 \mu\text{M}$). On the other hand, mutants Y435A and Y435W did not show a visible change in the K_m value ($161 \pm 20 \mu\text{M}$ and $169 \pm 41 \mu\text{M}$, respectively) against the GlcNAc₃ substrate. The k_{cat} values of mutants D313A, D313N and Y435W (0.08 s^{-1} , 0.09 s^{-1} and 0.09 s^{-1} , respectively) were less than the wild-type chitinase A (0.1 s^{-1}); whereas the k_{cat} value of Y435A (0.13 s^{-1}) was higher than the wild-type value. The overall catalytic efficiency (k_{cat}/K_m) was calculated for the hydrolysis of GlcNAc₃. The k_{cat}/K_m values of mutants D313A, D313N and Y435W ($2.8 \times 10^{-4} \text{ s}^{-1} \mu\text{M}^{-1}$, $4 \times 10^{-4} \text{ s}^{-1} \mu\text{M}^{-1}$ and $5.4 \times 10^{-4} \text{ s}^{-1} \mu\text{M}^{-1}$, respectively) were approx. 0.5, 0.7 and 0.8-fold, respectively which were considerably lower than the value of the wild-type ($6.1 \times 10^{-4} \text{ s}^{-1} \mu\text{M}^{-1}$). The k_{cat}/K_m of mutant Y435A ($8.1 \times 10^{-4} \text{ s}^{-1} \mu\text{M}^{-1}$) was approx. 1.3-fold higher than the wild-type value.

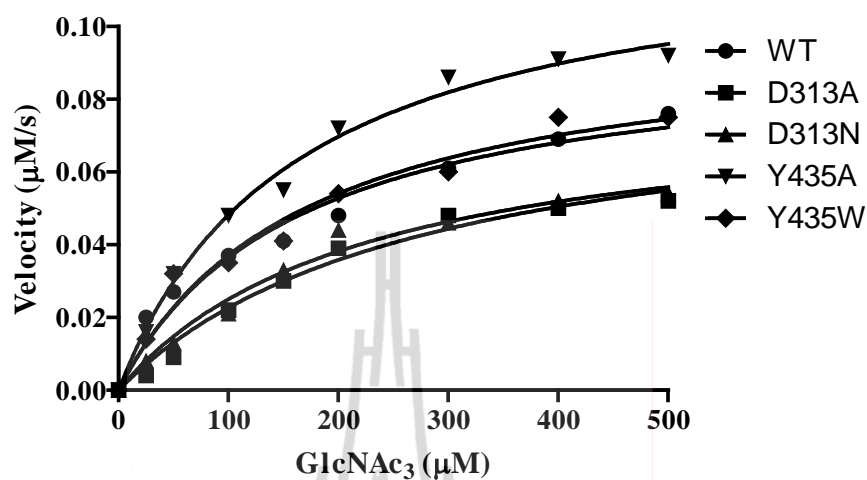


Figure 3.17 The Michaelis-Menten plot of GlcNAc₃. The kinetic assay was carried out using 0–500 μM of GlcNAc₃ as the substrate. After 15 minutes of incubation at 37°C, the amounts of the reaction products were determined by DNS method using a standard curve of GlcNAc₂.

Table 3.3 Kinetic parameters of GlcNAc₃ hydrolysis

Chitinase A	V_{\max}	K_m	k_{cat}	k_{cat} / K_m
variant	(μmol/min)	(μM)	(s⁻¹)	(s⁻¹ μM⁻¹)
Wild-type	0.1 ± 0.008	163 ± 37	0.1	6.1 × 10 ⁻⁴ (1)*
D313A	0.08 ± 0.009	276 ± 63	0.08	2.8 × 10 ⁻⁴ (0.5)
D313N	0.09 ± 0.002	223 ± 46	0.09	4.0 × 10 ⁻⁴ (0.7)
Y435A	0.13 ± 0.006	161 ± 20	0.13	8.1 × 10 ⁻⁴ (1.3)
Y435W	0.1 ± 0.009	169 ± 41	0.09	5.4 × 10 ⁻⁴ (0.8)

*Relative catalytic efficiencies are shown in parentheses.

3.9.3 Steady-state kinetics of GlcNAc₄ hydrolysis

Kinetic analysis using GlcNAc₄ as substrate was performed and the results are shown in Figure 3.18 and in Table 3.4. With GlcNAc₄ substrate, the K_m values of mutants D313A ($321 \pm 10 \mu\text{M}$), D313N ($256 \pm 20 \mu\text{M}$) and Y435W ($227 \pm 37 \mu\text{M}$) were higher than the wild-type K_m ($208 \pm 26 \mu\text{M}$). The k_{cat} values of mutants D313A, D313N and Y435W (0.07 s^{-1} , 0.09 s^{-1} and 0.13 s^{-1} , respectively) were less than the wild-type chitinase A (0.19 s^{-1}), whereas the k_{cat} value of Y435A (0.21 s^{-1}) was higher than the wild-type value. The mutants that caused a large decrease in the enzyme's catalytic efficiency (k_{cat}/K_m) were D313A, and D313N. Their values ($2.2 \times 10^{-4} \text{ s}^{-1} \mu\text{M}^{-1}$, $3.5 \times 10^{-4} \text{ s}^{-1} \mu\text{M}^{-1}$ and $5.8 \times 10^{-4} \text{ s}^{-1} \mu\text{M}^{-1}$, respectively) were approx. 0.2, 0.4 and 0.6-fold, respectively of the wild-type value ($9.1 \times 10^{-4} \text{ s}^{-1} \mu\text{M}^{-1}$). The mutant Y435A showed an increase in the k_{cat}/K_m value with 1.1-fold ($10 \times 10^{-4} \text{ s}^{-1} \mu\text{M}^{-1}$) of the wild-type value.

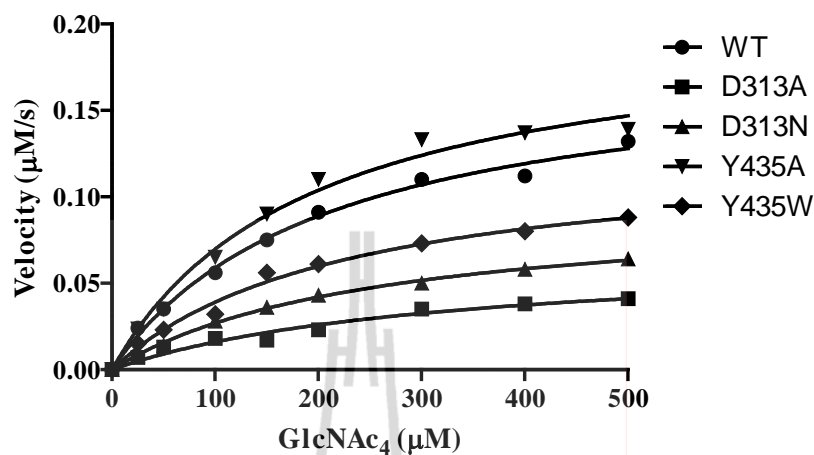


Figure 3.18 The Michaelis-Menten plot of GlcNAc₄. The kinetic assay was carried out using 0–500 μM of GlcNAc₄ as the substrate. After 15 minutes of incubation at 37°C, the amounts of the reaction products were determined by DNS method using a standard curve of GlcNAc₂.

Table 3.4 Kinetic parameters of GlcNAc₄ hydrolysis

Chitinase A variant	V_{\max} (μmol/min)	K_m (μM)	k_{cat} (s ⁻¹)	k_{cat} / K_m (s ⁻¹ μM ⁻¹)
Wild-type	0.18 ± 0.009	208 ± 26	0.19	9.1 × 10 ⁻⁴ (1)*
D313A	0.07 ± 0.001	321 ± 10	0.07	2.2 × 10 ⁻⁴ (0.2)
D313N	0.1 ± 0.003	256 ± 20	0.09	3.5 × 10 ⁻⁴ (0.4)
Y435A	0.2 ± 0.01	191 ± 30.2	0.21	10 × 10 ⁻⁴ (1.1)
Y435W	0.13 ± 0.009	227 ± 37	0.13	5.7 × 10 ⁻⁴ (0.6)

* Relative catalytic efficiencies are shown in parentheses.

3.9.4 Steady-state kinetics of GlcNAc₅ hydrolysis

The kinetic parameters of the hydrolytic activity of chitinase A and mutants were further determined with GlcNAc₅. As presented in Figure 3.19 and Table 3.5, the K_m values of D313A ($291 \pm 51 \mu\text{M}$), D313N ($252 \pm 54 \mu\text{M}$) and Y435W ($191 \pm 36 \mu\text{M}$) were higher than the wild-type K_m ($198 \pm 35 \mu\text{M}$). In contrast, mutant Y435A showed less K_m values ($168.0 \pm 33.2 \mu\text{M}$) than the wild-type chitinase A. The k_{cat} values of mutants D313A, D313N and Y435W (0.08 s^{-1} , 0.1 s^{-1} and 0.15 s^{-1} , respectively) were less than the wild-type chitinase A (0.16 s^{-1}), whereas the k_{cat} value of Y435A (0.17 s^{-1}) was higher than the wild-type value. The k_{cat}/K_m value of mutants D313A, D313N and Y435W ($2.7 \times 10^{-4} \text{ s}^{-1} \mu\text{M}^{-1}$, $3.9 \times 10^{-4} \text{ s}^{-1} \mu\text{M}^{-1}$ and $7.8 \times 10^{-4} \text{ s}^{-1} \mu\text{M}^{-1}$, respectively) were approx. 0.3, 0.5 and 1.2-fold, respectively the k_{cat}/K_m of the wild-type value. The mutant Y435A was approx. 0.9-fold ($10 \times 10^{-4} \text{ s}^{-1} \mu\text{M}^{-1}$) increased in the k_{cat}/K_m value.

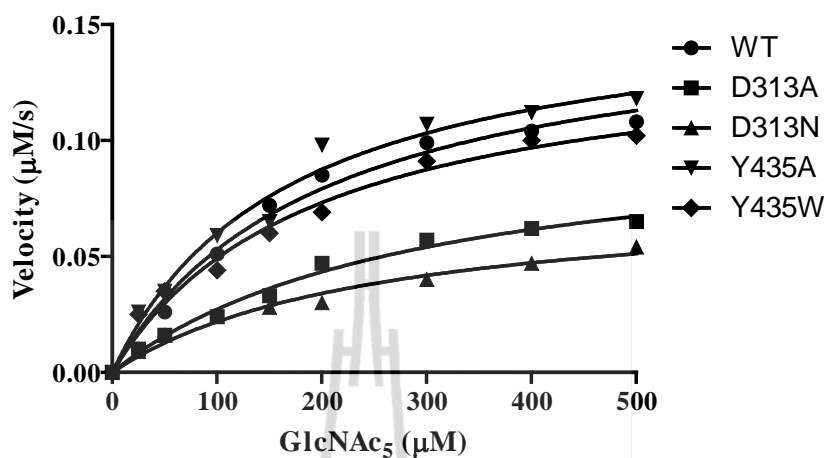


Figure 3.19 The Michaelis-Menten plot of GlcNAc₅ hydrolysis. The kinetic assay was carried out using 0–500 μM of GlcNAc₅ as the substrate. After 15 minutes of incubation at 37°C, the amounts of the reaction products were determined by DNS method using a standard curve of GlcNAc₂.

Table 3.5 Kinetic parameters of GlcNAc₅ hydrolysis

Chitinase A variant	V_{\max} (μmol/min)	K_m (μM)	k_{cat} (s ⁻¹)	k_{cat} / K_m (s ⁻¹ μM ⁻¹)
Wild-type	0.16 ± 0.01	198 ± 35	0.16	8.1 x 10 ⁻⁴ (1)*
D313A	0.1 ± 0.009	291 ± 51	0.08	2.7 x 10 ⁻⁴ (0.3)
D313N	0.1 ± 0.008	252 ± 54	0.1	3.9 x 10 ⁻⁴ (0.5)
Y435A	0.16 ± 0.01	168 ± 33	0.17	10 x 10 ⁻⁴ (1.2)
Y435W	0.14 ± 0.01	191 ± 36	0.15	7.8 x 10 ⁻⁴ (0.9)

*Relative catalytic efficiencies are shown in parentheses.

3.9.5 Steady-state kinetics of GlcNAc₆ hydrolysis

The Michaelis-Menten plot of GlcNAc₆ is shown in Figure 3.20. The kinetic parameters of the hydrolytic activity of chitinase A and mutants with GlcNAc₆ is presented in Table 3.6, the K_m values of mutants D313A ($275 \pm 42 \mu\text{M}$), D313N ($247 \pm 84 \mu\text{M}$) and Y435W ($174 \pm 34 \mu\text{M}$) were higher than the wild-type K_m ($168 \pm 25 \mu\text{M}$), while mutant Y435A gave lower K_m ($157 \pm 35 \mu\text{M}$) than wild-type's K_m . The k_{cat} values of mutants D313A, D313N and Y435W (0.12 s^{-1} , 0.14 s^{-1} and 1.45 s^{-1} , respectively) were less than the wild-type k_{cat} (1.65 s^{-1}), whereas the k_{cat} value of Y435A (1.66 s^{-1}) was higher than the wild-type value. The overall catalytic efficiency (k_{cat}/K_m) that was calculated for the hydrolysis of GlcNAc₆ was reduced for D313A ($4.4 \times 10^{-4} \text{ s}^{-1} \mu\text{M}^{-1}$), D313N ($5.7 \times 10^{-4} \text{ s}^{-1} \mu\text{M}^{-1}$) and Y435W ($8.3 \times 10^{-3} \text{ s}^{-1} \mu\text{M}^{-1}$) were approx. 0.04, 0.06 and 0.8, respectively, that of the wild-type. However, the value of mutant Y435A was approx. 1.02-fold ($10 \times 10^{-3} \text{ s}^{-1} \mu\text{M}^{-1}$) slightly increased from the value observed for the wild-type enzyme ($9.8 \times 10^{-3} \text{ s}^{-1} \mu\text{M}^{-1}$).

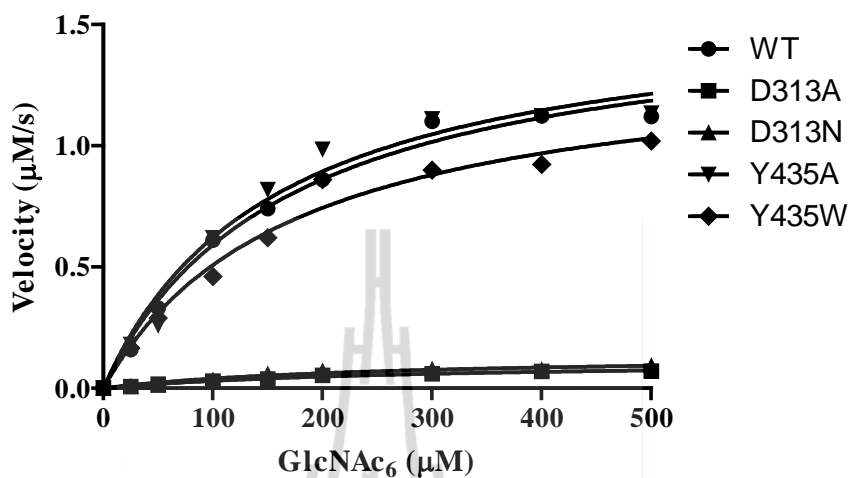


Figure 3.20 The Michaelis-Menten plot of GlcNAc₆ hydrolysis. The kinetic experiment was carried out using 0–500 μM of GlcNAc₆ as the substrate. After 15 minutes of incubation at 37°C, the amounts of the reaction products were determined by DNS method using a standard curve of GlcNAc₂.

Table 3.6 Kinetic parameters of GlcNAc₆ hydrolysis

Chitinase A variant	V_{max} (μmol/min)	K_m (μM)	k_{cat} (s ⁻¹)	k_{cat} / K_m (s ⁻¹ μM ⁻¹)
Wild-type	1.6 ± 0.1	168 ± 25	1.65	9.8 × 10 ⁻³ (1)*
D313A	0.1 ± 0.08	275 ± 42	0.12	4.4 × 10 ⁻⁴ (0.04)
D313N	0.1 ± 0.02	247 ± 84	0.14	5.7 × 10 ⁻⁴ (0.06)
Y435A	1.6 ± 0.1	157 ± 35	1.66	10 × 10 ⁻³ (1.02)
Y435W	1.4 ± 0.1	174 ± 34	1.45	8.3 × 10 ⁻³ (0.8)

*Relative catalytic efficiencies are shown in parentheses.

3.9.6 Steady-state kinetics of colloidal chitin hydrolysis

The kinetic analyses using water-insoluble substrate colloidal chitin was carried out. The Michaelis-Menten plot of colloidal chitin concentrations versus initial velocity is shown in Figure 3.21. The K_m of mutants D313A ($3.0 \pm 0.6 \text{ mg ml}^{-1}$), D313N ($2.0 \pm 0.5 \text{ mg ml}^{-1}$) and Y435W ($1.7 \pm 0.2 \text{ mg ml}^{-1}$), indicating an increase in the affinity of the enzyme for the substrate as the K_m values were higher than that of the wild-type enzyme ($1.5 \pm 0.2 \text{ mg ml}^{-1}$). However, the K_m value for the Y435A was slightly decreased ($1.4 \pm 0.2 \text{ mg ml}^{-1}$). Most of mutants had lower k_{cat} value except for the Y435A (1.8 s^{-1}) enzyme. The k_{cat} values of the mutants D313A (0.12 s^{-1}), D313N (0.14 s^{-1}) and Y435W (1.4 s^{-1}) were lower than the wild-type value (1.5 s^{-1}). The k_{cat}/K_m ratio of the mutants D313A, D313N and Y435W were approx. 0.04, 0.07 and 0.9-fold, respectively ($0.04 \text{ s}^{-1} \text{ mg ml}^{-1}$, $0.07 \text{ s}^{-1} \text{ mg ml}^{-1}$ and $0.9 \text{ s}^{-1} \text{ mg ml}^{-1}$, respectively) were lower than the wild-type value ($1 \text{ s}^{-1} \text{ mg ml}^{-1}$). For the Y435A, its k_{cat}/K_m was approx. 1.3-fold ($1.3 \text{ s}^{-1} \text{ mg ml}^{-1}$) was increased from the wild-type value.

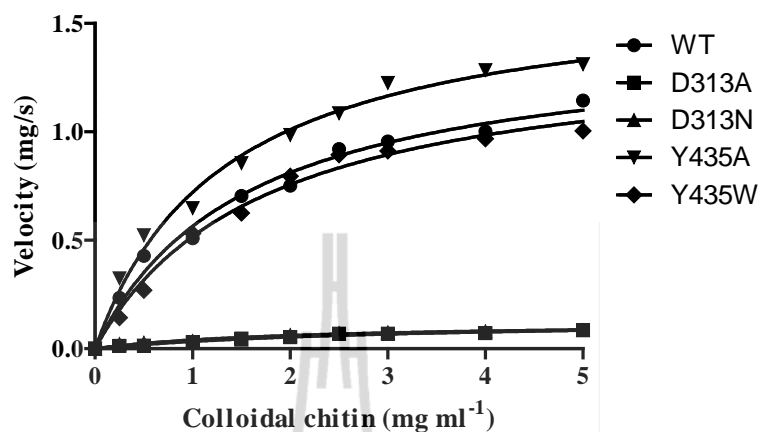


Figure 3.21 The Michaelis-Menten plot of colloidal chitin. The kinetic assay was carried out using 0–5 mg/ml of colloidal chitin as the substrate. After 15 minutes of incubation at 37°C, the amounts of the reaction products were determined by DNS method a standard curve of GlcNAc₂.

Table 3.7 Kinetic parameters of colloidal chitin hydrolysis

Chitinase A variant	V_{\max} (mg/s)	K_m (mg ml ⁻¹)	k_{cat} (s ⁻¹)	k_{cat} / K_m (s ⁻¹ /mg ml ⁻¹)
Wild-type	1.5 ± 0.08	1.5 ± 0.2	1.5	1 (1)*
D313A	0.1 ± 0.01	3.0 ± 0.6	0.1	0.04 (0.04)
D313N	0.1 ± 0.01	2.0 ± 0.5	0.1	0.07 (0.07)
Y435A	1.7 ± 0.08	1.4 ± 0.2	1.7	1.3 (1.3)
Y435W	1.4 ± 0.08	1.7 ± 0.2	1.4	0.9 (0.9)

* Relative catalytic efficiencies are shown in parentheses.

3.9.6 Steady-state kinetics of glycol chitin hydrolysis

The kinetic analyses using soluble-water substrate glycol chitin was carried out. The Michaelis-Menten plot of glycol chitin concentration versus product velocity is shown in Figure 3.22. The K_m value of mutants D313A ($3.6 \pm 0.6 \text{ mg ml}^{-1}$), D313N ($3.2 \pm 0.7 \text{ mg ml}^{-1}$) and Y435W ($2.3 \pm 0.6 \text{ mg ml}^{-1}$), increased the affinity of the enzyme for the substrate as the K_m values were higher than that of the wild-type enzyme ($2.2 \pm 0.4 \text{ mg ml}^{-1}$). However, the K_m value for the Y435A was slightly decreased ($1.8 \pm 0.3 \text{ mg ml}^{-1}$). Most of mutants had lower k_{cat} value except for the Y435A (0.28 s^{-1}). The k_{cat} values of mutant D313A (0.1 s^{-1}), D313N (0.12 s^{-1}) and Y435W (0.21 s^{-1}) were lower than that of wild-type (0.26 s^{-1}). The k_{cat}/K_m ratio of the mutants D313A, D313N and Y435W were approx. 0.2, 0.3 and 0.8-fold, respectively ($0.02 \text{ s}^{-1} \text{ mg ml}^{-1}$, $0.03 \text{ s}^{-1} \text{ mg ml}^{-1}$ and $0.09 \text{ s}^{-1} \text{ mg ml}^{-1}$, respectively) lower than the wild-type value ($0.12 \text{ s}^{-1} \text{ mg ml}^{-1}$), whereas for the Y435A was approx. 1.3-fold ($0.15 \text{ s}^{-1} \text{ mg ml}^{-1}$) slightly increased from the wild-type value.

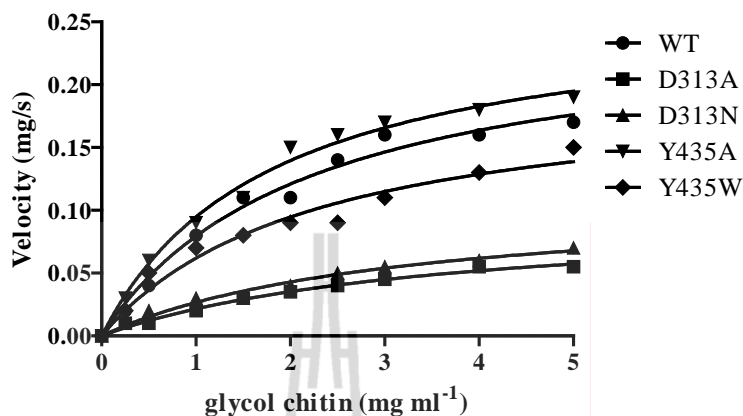


Figure 3.22 The Michaelis-Menten plot of glycol chitin hydrolysis. The assay was carried out using 0–5 mg/ml of glycol chitin as the substrate. After 15 minutes of incubation at 37°C, the amounts of the reaction products were determined by DNS method using a standard curve of GlcNAc₂.

Table 3.8 Kinetic parameters of glycol chitin hydrolysis

Chitinase A variant	V_{\max} (mg/s)	K_m (mg ml ⁻¹)	k_{cat} (s ⁻¹)	k_{cat} / K_m (s ⁻¹ / mg ml ⁻¹)
Wild-type	0.25 ± 0.02	2.2 ± 0.4	0.2	0.12 (1)*
D313A	0.1 ± 0.01	3.6 ± 0.6	0.1	0.02 (0.2)
D313N	0.1 ± 0.01	3.2 ± 0.7	0.1	0.03 (0.3)
Y435A	0.26 ± 0.01	1.8 ± 0.3	0.2	0.15 (1.3)
Y435W	0.2 ± 0.02	2.3 ± 0.6	0.2	0.09 (0.8)

* Relative catalytic efficiencies are shown in parentheses.

3.10 Effects of Mutations on the Chitin Binding Activity

The binding activity towards crystalline chitin, colloidal chitin and chitosan were compared at a single time point of 30 min at 0°C. As shown in Figure 3.23, all the chitinase variants showed highest binding activity towards colloidal chitin, followed by crystalline chitosan and crystalline chitin. When compared among the enzymes, the binding efficiency follows the order: Y435A > wild-type > Y435W > D313N > D313A. The D313 mutation showed most effect on colloidal chitin and least effect on crystalline chitin.

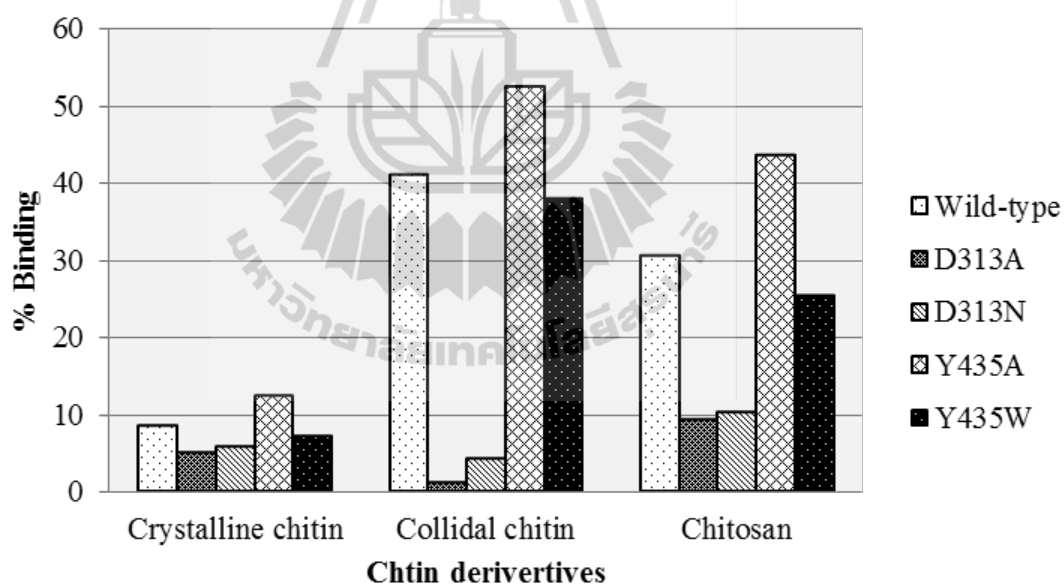


Figure 3.23 Binding of chitinase A and mutants to insoluble chitin.

Table 3.9 shows the maximum binding capacity (B_{\max}) and equilibrium constant (K_d) of the chitinase A variants, which were obtained from the equilibrium binding isotherm experiments in Figure 3.24. For crystalline chitin, chitinase A wild-type shows the B_{\max} of 6 $\mu\text{mol/g}$ and the K_d of 2.2 μM . The binding curves of the mutants D313A, D313N and Y435W represented a decrease in chitin affinity (3.1, 3.9 and 5.6 $\mu\text{mol/g}$, respectively) and the largest increase in K_d values were observed for 2.3, 1.9 and 1.4-fold, respectively (5.1, 4.2 and 3.1 μM , respectively). On the other hand, the bound enzyme of mutant Y435A was slightly increased shows a B_{\max} of 6.2 $\mu\text{mol/g}$ and a K_d was 0.8-fold (1.8 μM) less than the wild-type value. These estimated K_d values gave a indication of the enzyme's binding strength in the following order Y435A > wild-type > Y435W > D313N > D313A. This data are in absolute accordance with the binding activities determined by the chitin binding assay.

Table 3.9 Binding of crystalline chitin by chitinase A wild-type and mutants.

Chitinase A variant	B_{\max} ($\mu\text{mol/g}$)	K_d (μM)
Wild-type	6.0 ± 0.5	2.2 ± 0.5 (1)*
D313A	3.1 ± 0.3	5.1 ± 0.8 (2.3)
D313N	3.9 ± 0.3	4.2 ± 0.6 (1.9)
Y435A	6.2 ± 0.5	1.8 ± 0.4 (0.8)
Y435W	5.6 ± 0.6	3.1 ± 0.7 (1.4)

* Values in brackets represent relative activity compared to that of wild-type (fold).

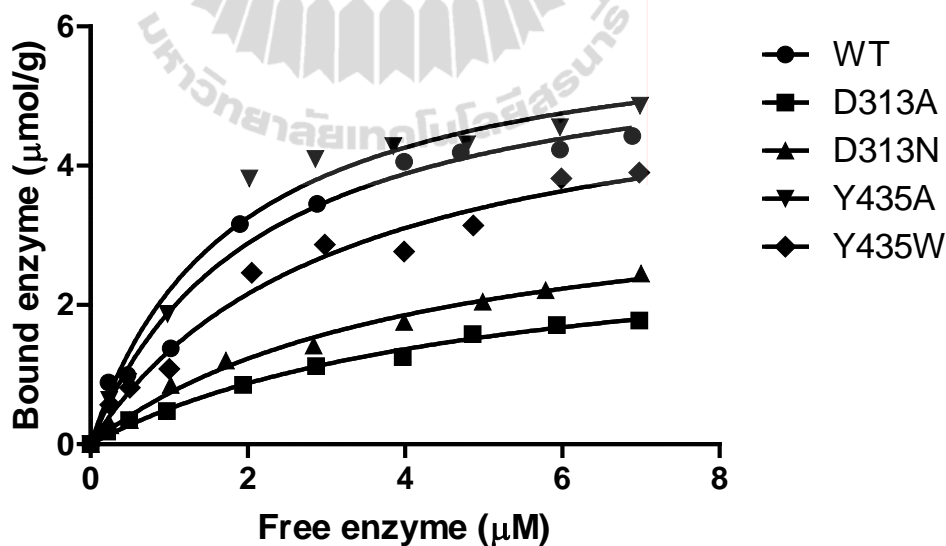


Figure 3.24 Equilibrium adsorption isotherms of wild-type and mutant chitinases to crystalline chitin.

Table 3.10 shows the binding capacitive (B_{\max}) and equilibrium constant (K_d) of colloidal chitin. The wild-type shows a B_{\max} of 5.1 $\mu\text{mol/g}$ and a K_d of 0.7 μM . The binding curves of the mutants D313A, D313N and Y435W indicated a decrease in chitin affinity, with B_{\max} of 1.2, 2.2 and 5 $\mu\text{mol/g}$, respectively and increase in K_d (1.8, 1.6 and 0.9 μM , respectively) by 2.5, 2.2 and 1.3-fold, respectively from the wild type's K_d . On the other hand, the bound enzyme of mutant Y435A was slightly increased with a B_{\max} of 5.5 $\mu\text{mol/g}$ and a K_d (0.5 μM) that was 0.7-fold that of the wild-type value. Therefore, the enzyme's binding strength is in the same order as already seen for crystalline chitin.

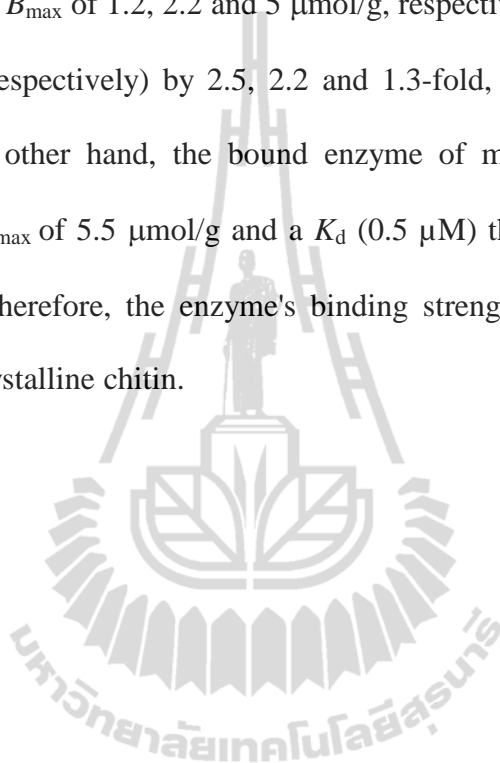


Table 3.10 Binding of colloidal chitin by chitinase A wild-type and mutants.

Chitinase A variant	B_{\max} ($\mu\text{mol/g}$)	K_d (μM)
Wild-type	5.1 ± 0.2	0.7 ± 0.2 (1)*
D313A	1.2 ± 0.1	1.8 ± 0.3 (2.5)
D313N	2.2 ± 0.3	1.6 ± 0.3 (2.2)
Y435A	5.5 ± 0.1	0.5 ± 0.1 (0.7)
Y435W	5.0 ± 0.2	0.9 ± 0.1 (1.3)

* Values in brackets represent relative activity compared to that of wild-type (fold).

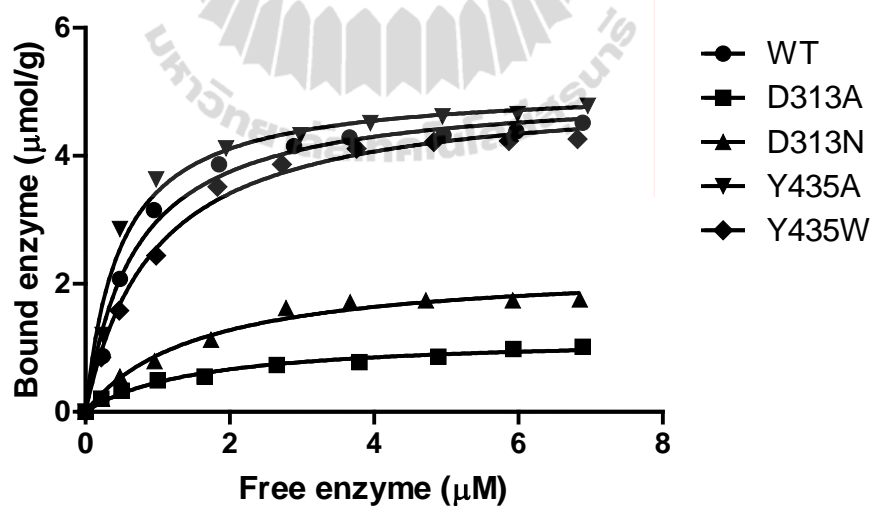


Figure 3.25 Equilibrium adsorption isotherms of wild-type and mutant chitinases A to colloidal chitin.

Table 3.11 shows the binding capacitive (B_{\max}) and equilibrium dissociation constant (K_d) of of chitosan. Chitinase A wild-type shows a B_{\max} of 5.6 $\mu\text{mol/g}$ and a K_d of 2.2 μM . The binding curves of the mutants D313A, D313N and Y435W show decreases in chitin affinity (3.1, 3.7 and 5.1 $\mu\text{mol/g}$, respectively). Their observed K_d (3.8, 3.2 and 2.3 μM , respectively) were 2, 1.9 and 1.2-fold, respectively of the wild-type K_d . On the other hand, the bound enzyme of mutant Y435A shows a B_{\max} of 5.1 $\mu\text{mol/g}$ and a K_d (1.5 μM) was 0.7-fold of the wild-type value. Again the binding strength towards this substrate follows the order Y435A > wild-type > Y435W > D313N > D313A.

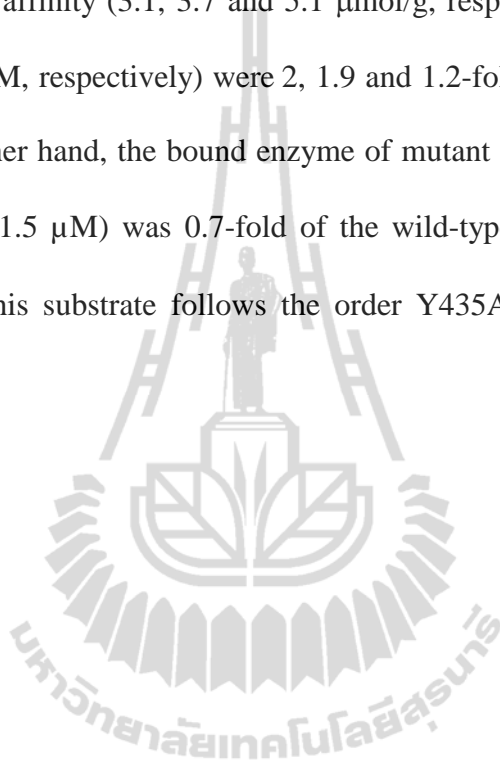


Table 3.11 Binding of chitosan by chitinase A wild-type and mutants.

Chitinase A variant	B_{\max} ($\mu\text{mol/g}$)	K_d (μM)
Wild-type	5.6 ± 0.3	1.9 ± 0.3 (1)*
D313A	3.1 ± 0.4	3.8 ± 0.1 (2)
D313N	3.7 ± 0.7	3.2 ± 0.4 (1.7)
Y435A	6.1 ± 0.3	1.5 ± 0.3 (0.7)
Y435W	5.1 ± 0.4	2.3 ± 0.4 (1.2)

* Values in brackets represent relative activity compared to that of wild-type (fold).

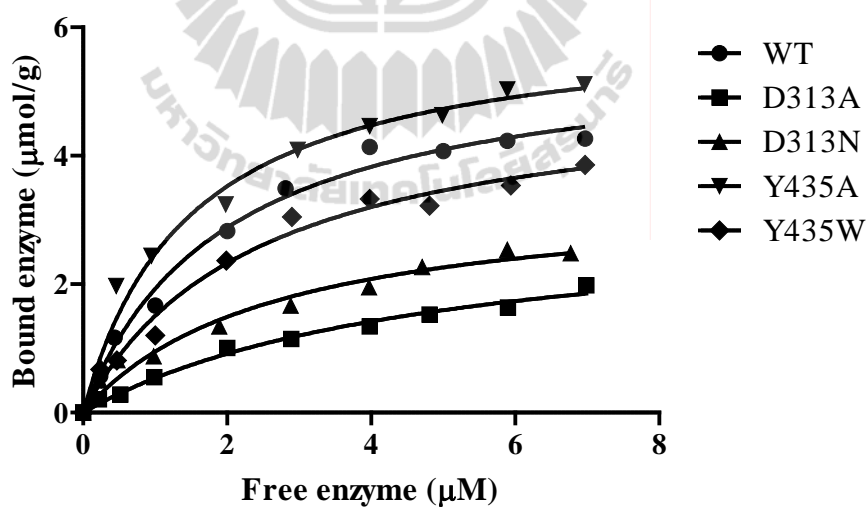


Figure 3.26 Equilibrium adsorption isotherms of wild-type and mutant chitinase A to chitosan.

CHAPTER IV

DISCUSSION

4.1 Site-directed mutagenesis of DxxDxDxE motif of family 18 chitinases

Previously, the roles of the last two acidic residues in the conserved DxxDxDxE motif of family-18 chitinases from from *S. marcescens* (Papanikolau *et al.*, 2001), *B. circulans* W1-12 and *Alteromonas* sp. (Tsujiibo *et al.*, 1996) and *V. harveyi* (Songsiriritthigul *et al.*, 2008; Suginta *et al.*, 2007) were investigated as shown in Table 4.1. The important roles of such residues have been studied by site-directed mutagenesis and further kinetic characterization (Watanabe *et al.*, 1993, 1994; Papanikolau *et al.*, 2001; Suginta *et al.*, 2000; 2004; 2005; 2007; 2009). All studies confirmed that the Glu residue is most critical for catalysis. Although the Asp residue does not play a direct role as a nucleophile as described for general acid-base catalysis of many glycosyl hydrolases, its role has been verified to be as almost equally essential as the Glu one.

Table 4.1 Site-directed mutagenesis on DxxDxDxE motif of family 18 chitinases

Sources	Asp		Asp		Glu		Reference		
	D→E	D→N	D→A	D→E	D→N	E→D	E→Q	E→M	
Chitinase A (<i>S. marcescens</i>)	-	-	Inactive D313A	-	-	-	Inactive E315Q	-	Papanikolaou <i>et al.</i> , 2001
Chitinase A (<i>V. harveyi</i>)	-	-	-	-	-	-	Inactive E315Q	Inactive E315M	Suginta <i>et al.</i> , 2005
Chitinase A (<i>V. harveyi</i>)	-	-	Inactive D313A	-	Low D313N	-	-	-	This work
Chitinase A1 (<i>B. circulans</i>)	Same WT D200E	Low D200N	-	Low D202E	Low D202N	Inactive E204D	Inactive E204Q	-	Watanabe <i>et al.</i> , 1993; 1994
Chitinase B (<i>S. marcescens</i>)	-	-	-	-	Inactive D142N	-	Inactive E144Q	-	Vaaje-Kolstad <i>et al.</i> , 2004
Chitinase (<i>A. cavatae</i>)	-	-	-	Low D313E	Moderate D313N	Inactive E315D	Inactive E315Q	-	Lin <i>et al.</i> , 1999

4.2 Influence of the Asp313 Mutants on the pH Activity Profile

The pH dependence of the K_m value reflects the involvement of acid-base groups that are essential to initial substrate binding event that precede catalysis. As agreed completely with the K_m versus pH of wild-type shown in Figure 3.8A, substrate binding affinity decreased (K_m increased) with increasing pH between the apparent pK_a values of ($pK_{a1}=4.0$ and $pK_{a2}=8.0$). These pK_a is a reflection of deprotonated form of Asp313 and protonated form of Glu315. The explanation is these different deprotonation states of the two residues are strictly by the enzyme to adopt a conformation capable of binding substrate.

On the other hand, effect of pH on k_{cat} mainly reflects acid-base group involvement in the catalytic steps of substrate to product conversion; that is, these ionization steps occur in the enzyme-substrate complex. The value of k_{cat} for this enzyme increases with increasing pH and displays an apparent pK_{a1} of 4.0 and reached the maximum value at optimum pH (pH 6.0), then decrease at further increasing pH with an apparent pK_{a2} of 8.0 (Figure 3.8(B)). The data confirmed the catalytic function of the ionization of the deprotonated state of the nucleophilic group (most likely Asp313) and the protonated state of the catalytic group (Glu315).

Regarding a plot of k_{cat}/K_m as a function of pH is said to reflect essential ionizing group of the enzyme that play a role in both substrate binding and catalytic processes (Figure 3.8(C)) (Palmer, 1985). The pH profile of k_{cat}/K_m for this enzyme is a bell-shaped curve. This plot represents the cumulative effects of two titratable groups that influence the catalytic efficiency of the enzyme in opposite ways.

Structural studies have shown that residue aspartate 313 makes an important contribution to distortion of the -1 sugar, in particular distortion of the *N*-acetyl group (Figure 3.2). Hydrogen bonds provided by an Asn can to a large extent replace the hydrogen bonds made by Asp, which may explain why the D313N mutant retains considerable activity, whereas the D313A mutant does not. The Asp313 replacement by alanine in other family 18 chitinases puts the *N*-acetyl group in a conformation which is not favorable for nucleophilic attack on the anomeric carbon (Aronson *et al.*, 2006; Bokma *et al.*, 2002; Papanikolau *et al.*, 2001).

The kinetic properties of the Asp313A/N mutants were analyzed by determining K_m and k_{cat} and k_{cat}/K_m at various pH values (Figure 3.8). The D313N mutation decreased significantly the enzyme activity, while retained the similar pH activity profile. The pH profile of the values of k_{cat} closely resembles the profile observed for k_{cat}/K_m , and has a similar optimum between wild-type and mutant D313N. The basic limb of the profile presumably reflects ionization of the acid/base moiety as indicated by the earlier studies of Williams *et al.* (2002), with the *Streptomyces plicatus N*-acetyl- β -hexosaminidase (*SpHex*) D313A/N variant. On the other hand, the D313A mutant has greatly decreased catalytic activity and displays changes in the pH profiles. One of the remarkable properties of D313A mutant is highly alkaline. This is probably D313A mutant acting as a base. Catalysis is independent of pH until value about 8.0. Activity is then lost as acid is deprotonated.

4.3 Reaction Patterns of the Chitinase A and Its Mutants

The reaction products of chitinase A from *V. harveyi* and its mutants D313A/N and Y435A/W were examined using colloidal chitin and several chitooligosaccharides as the substrates. The results obtained from TLC showed that wild-type chitinase A and mutants Y435A and Y435W degraded chitin to GlcNAc₂ as the major end products, indicating that the enzymes recognized mainly the second bond in chitin chain. When GlcNAc₆ was used as the substrate, GlcNAc₂, GlcNAc₃ and GlcNAc₄ were produced in the initial phase of the reactions. The obtained results indicate that a random attack, which is a characteristic of an endo-acting enzyme. This agrees with the previous observation by Suginta et al. (Suginta *et al.*, 2004, 2005; 2009). The mutation of Tyr435 to Ala and Trp did not seem to alter the pattern of substrate hydrolysis. No observations of the hydrolytic products were made with mutants D313A and D313N.

Uchiyama *et al.* (2001) reported that chitooligosaccharides randomly enter the catalytic cleft of *S. marcescens* chitinase A. It is presumed that binding of the incoming sugar chain may begin at variable sites to allow various glycosidic bonds to be accessible to the cleavage site located between sites -1 to +1. For GlcNAc₅ hydrolysis by wild-type enzyme initially produced GlcNAc₂ and GlcNAc₃, assuming that GlcNAc₅ occupied subsite -3 to +2 in the substrate-binding cleft. However, Suginta *et al.* (2009) employed HPLC-MS to demonstrate only four units of GlcNAc₆ and GlcNAc₅ bind to subsites -2 to +2, leaving the reducing-end GlcNAc unbound at the exterior of the substrate binding cleft. With the GlcNAc₆ substrate, the structural data reported by Songsiriritthigul *et al.* (2008) showed that GlcNAc₆ bind to subsites

-4 to +2 in a similar manner as it was observed with the *S. marcescens* chitinase A (Figure 3.3) (Aronson *et al.*, 2003).

4.4 The Effects of Mutations on the Specific Hydrolyzing Activity

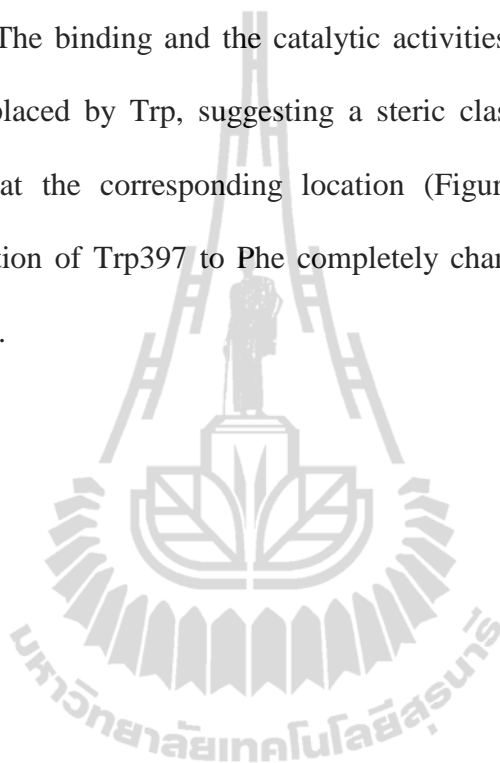
Mutations of Asp313 at subsite -1 to Ala/Asn were generated to address the important roles of this residue. The mutants D313A and D313N were found to affect the kinetic properties involving the catalytic center by slightly increasing the K_m values, but dramatically decreasing the k_{cat} and the k_{cat}/K_m values toward *p*NP-GlcNAc₂ and 4MU-GlcNAc₂. Similar effects were also reported with ChiA from *S. marcescens*, where mutation of Asp313 to Ala drastically reduced the hydrolytic activity of their enzymes toward *p*NP-GlcNAc₂, with about 1,000-fold reduction of the k_{cat}/K_m value (Papanikolau *et al.*, 2001). In the case of soluble chitooligosaccharides, mutants D313A and D313N led to an increase in the K_m value and a decrease in the k_{cat}/K_m value. Both mutants D313A and D313N had reduced the k_{cat}/K_m values by toward colloidal chitin 0.04 and 0.8-fold, respectively. This observation suggested a unique role of Asp313 in the catalytic mechanism. Since Asp313 is located close to Glu315, the mutation of Asp313 may affect the physicochemical characteristics of this most critical Glu residue. Difference was seen with mutant Y435A, since a decrease in the K_m values and increase in the k_{cat}/K_m values toward all substrates were detected.

4.5 The effects of mutations on chitin binding activity

Chitin binding assays demonstrate modifications in the binding activity of all the mutants to various extents. The most severe effect was observed with D313A. A single time-point study displayed diminished binding activity of D313A and D313N but retained activity of Y435A and W435W mutants to insoluble chitin polysaccharides. Point mutation of Asp313 to Ala drastically impaired the ability of the enzyme to bind and to hydrolyze all the tested substrates. The Asn substitution of Asp313 showed decreases in both binding and hydrolytic activity. This could be explained as an effect of spontaneous deamination of the primary NH_2 on the amide group of Asn. This phenomenon was already observed in *Clostridium symbiosum* glutamate dehydrogenase (GDH) where mutation of Asp165 to Asn displayed a residual GDH activity of 2% of the wild-type activity (Paradisi *et al.*, 2005). As mentioned earlier, Asp is located at the bottom of the substrate binding cleft next to the catalytic residue Glu315 and its $\beta\text{-COOH}$ is in the vicinity to form a H-bond with the carbonyl O of the acetamido group of the oxazolinium ion intermediate at subsite -1. Unlike previously observed in *S. marcescens* chitinase A and *S. marcescens* chitinase B (van Aalten *et al.*, 2001 and Papanikolaou *et al.*, 2001), our structural data revealed only one conformation of the Asp313. As a result, we could not rule out the role of Asp313 in assisting the catalytic process by lowering the pK_a of Glu315 via a proton donation as suggested for *S. marcescens* chitinase B. However, it more likely plays a possible role in stabilizing the developing oxazolinium ion intermediate.

The Ala substitution (mutant Y435A) yielded significant increases in the binding affinity (decreased K_d) and the hydrolytic activity (increased k_{cat}/K_m and specific

hydrolyzing activity) toward chitin substrates (Figure 4.1(B)). Tyr435 is located at the end of the reducing end of the substrate binding cleft. This residue appears to partially block the substrates to access the enzyme's active site rather than to take part in substrate binding. The binding and the catalytic activities were decreased when Tyr side chain was replaced by Trp, suggesting a steric clash of the newly-introduced bulky side chain at the corresponding location (Figure 4.1C). From previously reported that mutation of Trp397 to Phe completely changed the binding affinity at the RE subsite (+2).



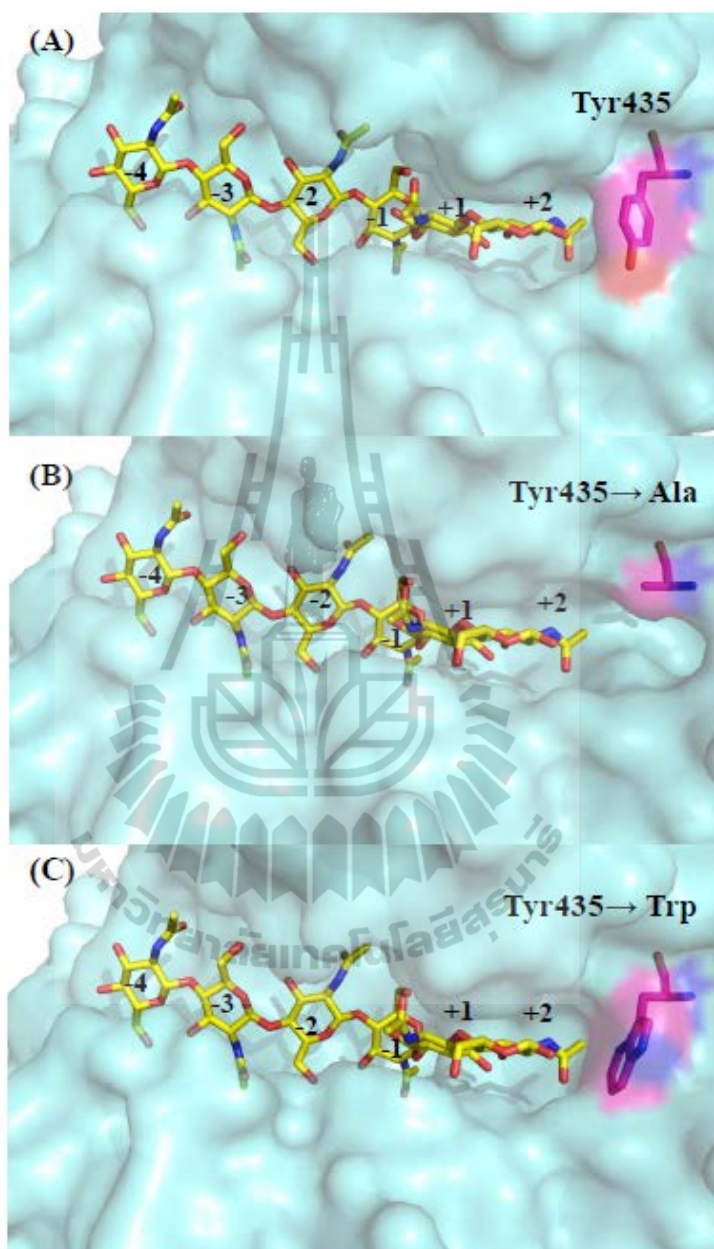
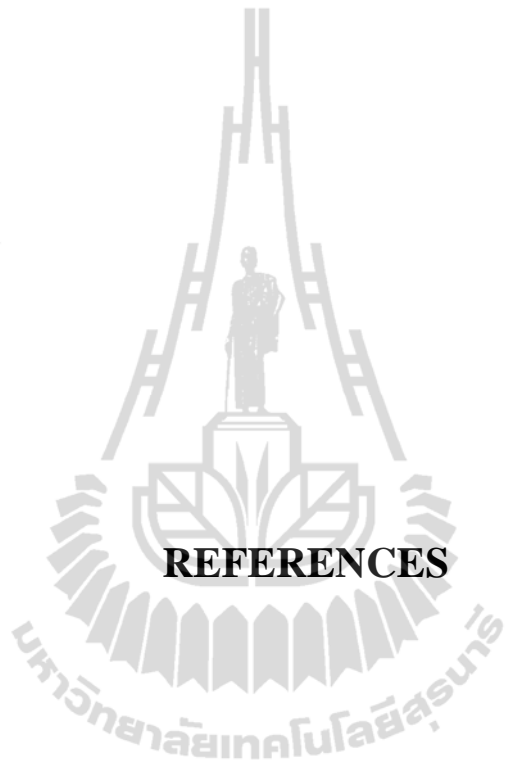


Figure 4.1 A surface representation of the binding cleft of *V. harveyi* chitinase A mutant E315M+GlcNAc₆. N atoms are shown in blue, O atoms in red. C atoms are in pink for binding site residues and in yellow for GlcNAc₆. (A) Wild-type, (B) Mutant Y435A and (C) Mutant Y435W.

CHAPTER V

CONCLUSION

This research describes mutational, following kinetic studies of *V. harveyi* chitinase A and its mutants D313A/N and Y435A/W. Point mutations were generated by PCR technique and the recombinant enzymes were expressed and purified by a single step Ni-NTA affinity chromatography. The final yield obtained after purification were about 20-25 mg per liter of culture. The pH activity profiles indicated that the wild-type enzyme had the optimum pH of 6.0 and the two pK_a values of the two ionizing groups were estimated to be 4.0 and 8.0. Mutations of Asp313 and Asp313A severely affected the k_{cat} and the k_{cat}/K_m over the entire range of pH but not significantly changed the K_m values. The dramatic effects of D313A/N on the activity of *V. harveyi* chitinase A were further observed on the specific activity, kinetic and TLC assays Regarding Tyr435 mutations, increases in the both catalytic and the binding activities were observed with mutant Y435A with all the biochemical assays, leading to a conclusion that the alanine substitution partially removed the steric clash around the reducing subsites. Mutation of Tyr435 to Trp consistently supported the steric clash idea as the Trp substitution of this residue showed considerable decreases in the enzymatic and binding properties of the enzymes.



REFERENCES

REFERENCES

- Alam, M. M., Mizutani, T., Isono, M., Nikaidou, N. and Watanabe, T. (1996). Three chitinase genes (chiA, chiC and chiD) comprise the chitinase system of *Bacillus circulans* WL-12. **J. Ferment. Bioeng.** 82: 28-36.
- Armand, S., Tomita, H., Heyraud, A., Gey, C., Watanabe, T. and Henrissat, B. (1994). Stereochemical course of the hydrolysis reaction catalyzed by chitinases A1 and D1 from *Bacillus circulans* WL-12. **FEBS Lett.** 343: 177-180.
- Aronson Jr, N. N., Halloran, B. A., Alexeyev, M. F., Zhou, X. E., Wang, Y., Meehan, E. J. and Chen, L. (2006). Mutation of a conserved tryptophan in the chitin-binding cleft of *Serratia marcescens* chitinase A enhances transglycosylation. **Biosci. Biotechnol. Biochem.** 70: 243-51.
- Aronson Jr. N.N., Halloran, B.A., Alexyev, M.F., Amable, L., Madura, J.D., Pasupulati, L., Worth, C. and van Roey, P. (2003). Family 18 chitinase-oligosaccharide substrate interaction: subsite preference and anomer selectivity of *Serratia marcescens* chitinase A, **Biochem. J.** 376: 87-95.
- Blake, C.C.F., D.F. Koenig, G.A. Mair, A.C.T. North, D.C. Phillips, and V.R. Sarma (1965). Structure of hen egg-white lysozyme. **Nature.** 206: 757-761.
- Bradford, M. M. (1976). A rapid and sensitive method for the quantitation of microgram quantities of protein utilizing the principle of protein-dye binding. **Anal. Biochem.** 72: 248-254.

- Brameld, K.A., William, D., Imperiali, B. and Goddard, W.A. III. (1998). Substrate assistance in the mechanism of family 18 chitinases: theoretical studies of potential intermediates and inhibitors. **J. Mol. Biol.** 280: 913-923.
- Brurberg, M. B., Nes, I. F. and Eijsink, V. G. H. (1996). Comparative studies of chitinases A and B from *Serratia marcescens*. **Microbiol.** 142: 1581-1589.
- Cohen-Kupiec, R. and Chet, I. (1998). The molecular biology of chitin digestion. **Curr. Opin. Biotechnol.** 9: 270-277.
- Cottrell, M. T., Moore, J. A. and Kirchman, D. L. (1999). Chitinases from Uncultured Marine Microorganisms. **Appl. Environ. Microbiol.** 65: 2553-2557.
- David, G. and Henrissat, B. (1995). Structures and mechanisms of glycosyl hydrolases. **Structure.** 3: 853-859.
- Dixon, B. (1995). Using fungal dressings to heal wounds. **Biotechnol.** 13: 120-121.
- Elias, J. A., Homer, R. J., Hamid, Q. and Lee, C. G. (2005). Chitinases and chitinase-like proteins in T_H2 inflammation and asthma. **J. Allergy. Clin. Immunol.** 116: 497-500.
- Flach, J., Pilet, P. E. and Jolles, P. (1992). What's new in chitinase research?. **Experimentia.** 48: 701-706.
- Fukamizo, T., Sasaki, C., Schelp, E., Bortone, K. and Robertus, J. D. (2001). Kinetic properties of chitinase-1 from the fungal pathogen *Coccidioides immitis*. **Biochemistry.** 40: 2448-2454.
- Gooday, G. W., Zhu, W. Y. and O'Donnell, R. W. (1992). What are the roles of chitinases in the growing fungus?. **FEMS Microbiol. Lett.** 100: 387-392.

- Gooday, G.W. (1990). Physiology of microbial degradation of chitin and chitosan. **Biodegradation**. 1: 177–190.
- Gooday, G.W. (1999). Aggressive and defensive roles of chitinases. **EXS**. 87: 157-169.
- Hart, P. J., Pfluger, H. D., Monzingo, A. F., Hollis, T. and Robertus, J. D. (1995). The refined crystal structure of an endochitinase from *Hordeum vulgare* L. seeds at 1.8 Å resolution. **J. Mol. Biol.** 248: 402-413.
- Henrissat, B. (1991). A classification of glycosyl hydrolases based on amino acid sequence similarity. **Biochem. J.** 280: 309-316.
- Henrissat, B. and Bairoch, A. (1993). New families in the classification of glycosyl hydrolases based on amino acid sequence similarities. **Biochem. J.** 293: 781-788.
- Horn, J. S., Sikorski, P., Cederkvist, B. J., Vaaje-Kolstad, G., Sørli, M., Synstad, B., Vriend, G., Vårum, M., K. and Eijsink, G. H. V. (2006). Costs and benefits of processivity in enzymatic degradation of recalcitrant polysaccharides. **PNAS**. 103: 18089-18094.
- Horsch, M., Mayer, C., Sennhauser, U. and Rast, D. M. (1997). β -N-acetylhexosaminidase: a target for the design of antifungal agents. **Pharmacology and Therapeutics**. 76: 187-218.
- Ikegami, T., Okada, T., Hashimoto, M., Seino, S., Watanabe, T. and Shirakawa, M. (2000). Solution structure of the chitin-binding domain of *Bacillus circulans* WL-12 chitinase A1. **J. Biol. Chem.** 275: 13654-13661.

- Jach, G., Gornhardt, B., Mundy, J., Logemann, J., Pinsdorf, E., Leah, R., Schell J. and Maas, C. (1995). Enhanced quantitative resistance against fungal disease by combinatorial expression of different barley antifungal proteins in transgenic tobacco. **Plant J.** 8: 97-109.
- Jee, J. G., Ikegami, T., Hashimoto, M., Kawabata, T., Ikeguchi, M., Watanabe, T. and Shirakawa, M. (2002). Solution structure of the fibronectin type III domain of *Bacillus circulans* WL-12 chitinase A1. **J. Biol. Chem.** 277: 1388-1397.
- Jeuniaux, C. (1961). Chitinase: An Addition to the List of Hydrolases in the Digestive Tract of Vertebrates. **Nature.** 192: 135-136.
- Jeuniaux, C. (1966). Chitinases. In: E.F. Neufeld and V. Ginsburg, Editors, **Methods in Enzymology.** 8: 644-650.
- Kadowaki, S., Saakiawan, I., Watanabe, J., Yamamoto, K., Bunno, M., Ichihara, Y. and Kumagi, H. (1997). Transglycosylation activity of *b*-N-acetylhexosaminidase from *Penicillium oxalicum* and its application to synthesis of a drug carrier. **J. Ferment. Bioeng.** 83: 341-345.
- Kawada, M., Hachiya, Y., Arihiro, A. and Mizoguchi, E. (2007). Role of mammalian chitinases in inflammatory conditions. **J. Med.** 56: 21-7.
- Kawase, T., Yokokawa, S., Saito, A., Fujii, T., Nikaidou, N., Miyashita, K. and Watanabe, T. (2006). Comparison of enzymatic and antifungal properties family 18 and 19 chitinases from *Streptomyces coelicolor* A3(2). **Biosci. Biotechnol. Biochem.** 70: 988-998.
- Kozloff, E. (1990). Invertebrates. Saunder College Publishing, New York.

- Laemmli, U. K. (1970). Cleavage of structural proteins during the assembly of the head of bacteriophage T4. **Nature**. 227: 680-685.
- Lower, S.E. (1984). Polymers from the sea chitin and chitosan I. **Manufacturing Chemis.** 55: 73-75.
- Lu, Y., Zen, K. C., Muthukrishnan, S. and Kramer, K. J. (2002). Site-directed mutagenesis and functional analysis of active site acidic amino acid residues Asp142, Asp144 and Glu146 in *Manduca sexta* (tobacco hornworm) chitinase. **Insect Biochem. Mol. Biol.** 11: 1369-138.
- Matsumoto, T., Nonaka, T., Hashimoyo, M., Watanabe, T. and Mitsui, Y. (1999). Three dimensional structure of the catalytic domain of chitinase A1 from *Bacillus circulans* WL-12 at a very high resolution. **Proc. Japan. Acad.** 75: 269-274.
- Miller, G. L. (1959). Use of dinitrosalicylic acid reagent for determination of reducing sugar. **Anal. Chem.** 31: 426-429.
- Mitsutomi, M., Hata, T. and Kuwahara, T. (1995). Purification and characterization of novel chitinases from *Streptomyces griseus* HUT, 6037. **Ferment. Bioeng.** 80: 153-158.
- Muzzarelli, R. A. A. (1977). Chitin. **Pergamon**. Oxford.
- Muzzarelli, R. A., Mattioli-Balmonte, M., Pugnaroni, A. and Biagini, G. (1999). Biochemistry, histology and clinical uses of chitins and chitosans in wound healing. **EXS.** 87: 251-264.
- Ohno, T., Armand, S., Hata, T., Nikaidou, N., Henrissat, B., Mitsutomi, M. and Watanabe, T. (1996). A modular family19 chitinase found in the prokaryotic organism *Streptomyces griseus* HUT 6037. **J. Bacteriol.** 17: 5065-5070.

- Orikoshi, H., Baba, N., Nakayama, S., Kashu, H., Miyamoto, K., Yasuda, M., Inamori, Y. and Tsujibo, H. (2003). Molecular analysis of the gene encoding a novel cold-adapted chitinase (ChiB) from *Alteromonas* sp. Strain O-7. **J. Bacteriol.** 185: 1135-1159.
- Pantoom, S., Songsiriritthigul, C. and Suginta, W. (2008). The effects of the surface-exposed residues on the binding and hydrolytic activities of *Vibrio carchariae* chitinase A. **BMC Biochem.** 9: 2.
- Papanikolau, Y., Prag, G., Tavlas, G., Vorgias, C. E., Oppenheim, A. B. and Patratos, K. (2001). High resolution structural analysis of mutant chitinase A complexes with substrates provide new insight into the mechanism of catalysis. **Biochemistry.** 40: 11338-11343.
- Patil, S. R., Ghormade, V. and Deshpande, M. V. (2000). Chitinolytic enzymes: an exploration. **Enzyme Microb. Technol.** 26: 473-483.
- Pedersen, K., Verdonck, L. and Austin, B. (1998). Taxonomic evidence that *Vibrio carchariae* is a junior synonym of *Vibrio harveyi*. **Int. J. Syst. Bacteriol.** 48: 749-758.
- Perrakis, A., Tews, I., Dauter, Z., Oppenheim, A. B., Chet, I., Wilson, K. S. and Vorgia, C. E. (1994). Crystal structure of a bacterial chitinase at 2.3 Å resolutions. **Structure.** 15: 1169-1180.
- Peter, M. G., Kegel, G. and Keller, R. (1986). Structural studies on sclerotized insect cuticle, in: *Chitin in Nature and Technology* (eds. Muzarelli R.A.A., Jeuniaux C., Gooday G.W.). **Plenum Press**, New York.

- Prashanth, K. V. and Tharanathan, R. N. (2007). Chitin/chitosan: modifications and their unlimited application potential-an overview. **Trends Food Sci. Technol.** 18: 117-131.
- Roberts, G. A. F. (1992). Chitin Chemistry. **The Macmillan Press Ltd.**; London.
- Roberts, W. K. and Selitrennikoff, C. P. (1988) . Plant and bacterial chitinases differ in antifungal activity, **J. Gen. Microbiol.** 134: 169–176.
- Sahai, A. S. and Manocha, M. S. (1993). Chitinases of fungi and plants: their involvement in morphogenesis and host-parasite interaction. **FEMS Microbiol. Rev.**4: 317-338.
- Sambrook, J., Fritsch, E.F. and Maniatis, T., Hrsg. (1989). Molecular Cloning - A Laboratory Manual, 2nd Edition. **Cold Spring Harbour Laboratory Press**, New York.
- Sasaki, C., Yokoyama, A., Itoh, Y., Hashimoto, M., Watanabe, T. and Fukamizo, T. (2002). Comparative study of the reaction mechanism of family 1 chitinases from plants and microbes. **J. Biochem.** 131: 557-564.
- Seidl, V. (2008). Chitinases of filamentous fungi: a large group of diverse proteins with multiple physiological functions. **Fungal Biol.** 22: 36-42.
- Shahidi, F., Arachchi, J. H. V. and You-Jin, J. (1999). Food applications of chitin and chitosans. **Trends Food Sci. Technol.** 10: 37-51.
- Skaugrud, O. and Sargent, G. (1990). Chitin and chitosan: Crustacean biopolymers with potential. **International By-products Conference.** 61-72.

- Songsiriritthigul, C., Pantoom, S., Aguda, A. H., Robinson, R. C. and Suginta, W. (2008). Crystal structures of *Vibrio harveyi* chitinase A complexed with chitooligosaccharides: Implications for the catalytic mechanism. **J. Struct. Biol.** 162: 491-499.
- Suginta, W. (2007). Identification of chitin binding proteins and characterization of two chitinase isoforms from *Vibrio alginolyticus* 283. **Enzyme Microbial Technol.** 41: 212-220.
- Suginta, W., Pantoom, S. and Prinz, H. (2009). Substrate binding modes and anomer selectivity of chitinase A from *Vibrio harveyi*. **J. Chem. Biol.** 2: 191-202.
- Suginta, W., Robertson, P. A. W., Austin, B., Fry, S. C. and Fothergill-Gilmore, L. A. (2000). Chitinases *Vibrio*: activity screening and purification of Chi A from *Vibrio carchariae*. **J. Appl. Microbiol.** 89: 76-84.
- Suginta, W., Songsiriritthigul, C., Kobdaj, A., Opassiri, R. and Jisnusaon, S. (2007). Mutations of Trp275 and Trp397 altered the binding selectivity of *Vibrio carchariae* chitinase A. **Biochim. Biophys. Acta.** 1770: 1151-1160.
- Suginta, W., Vongsuwan, A., Songsiriritthigul, C., Prinz, H., Estibeiro, P., Duncan, R. R., Svasti, J., and Fothergill-Gilmore, L. A. (2004). An endochitinase A from *Vibrio carchariae*: cloning, expression, mass and sequence analyses, and chitin hydrolysis. **Arch. Biochem. Biophys.** 424: 171-180.
- Suginta, W., Vongsuwan, A., Songsiriritthigul, C., Svasti, J and Prinz, H. (2005). Enzymatic properties of wild-type and active site mutants of chitinase A from *Vibrio carchariae*, as revealed by HPLC-MS. **FASEB J.** 272: 3376-386.

- Suzuki, K., Taiyoji, M., Sugawara, N., Nikaidou, N., Henrissat, B. and Watanabe, T. (1999). The third chitinase gene (*chiC*) of *Serratia marcescens* 2170 and the relationship of its product to other bacterial chitinases. **Biochem. J.** 343: 587-596.
- Suzuki, K., Sugawara, N., Suzuki, M., Uchiyama, T., Katouno, F., Nikaidou, N. and Watanabe, T. (2002). Chitinases A, B, and C1 of *Serratia marcescens* 2170 produced by recombinant *Escherichia coli*: enzymatic properties and synergism on chitin degradation. **Biosci. Biotechnol. Biochem.** 66: 1075-1083.
- Suzuki, K., Suzuki, M., Taiyoji, M., Nikaidou, N. and Watanabe, T. (1998). Chitin binding protein (CBP1) in the culture supernatant *Serratia marcescens* 2170. **Biosci. Biotechnol. Biochem.** 62: 128-135.
- Taira, T., Ohnuma, T., Yamagami, T., Aso, Y., Ishiguro, M. and Ishihara, M. (2002). Antifungal activity of rye (*Secale cereale*) seed chitinases: the different binding manner of class I and class II chitinases to the fungal cell walls. **Biosci. Biotechnol. Biochem.** 66: 970-977.
- Trudel, J. and Asselin, A. (1989). Detection of chitinase activity after polyacrylamide gel electrophoresis. **Anal. Biochem.** 178: 362-366.
- Tsujibo, H., Fujimoto, K., Tanno, H., Miyamoto, K., Imada, D., Okami, Y. and Inamori, Y. (1994). Gene sequence, purification and characterization of β -N-acetylglucosaminidase from a marine bacterium, *Alteromonas* sp. Strain O-7. **Gene.** 146: 111-115.

- Tsujibo, H., Fujimoto, K., Tanno, H., Miyamoto, K., Kimura, Y., Imada, D., Okami, Y. and Inamori, Y. (1995). Molecular cloning of the gene which encodes β -N-acetylglucosaminidase from a marine bacterium, *Alteromonas* sp. Strain O-7. **Environ. Microbiol.** 61: 804-806.
- Tsujibo, H., Orikoshi, H., Tanno, H., Fujimoto, K., Miyamoto, K., Imada, D., Okami, Y. and Inamori, Y. (1993). Cloning, sequence, and expression of a chitinase gene from a marine bacterium, *Alteromonas* sp. Strain O-7. **J. Bacteriol.** 175: 176-181.
- Uchiyama, T., Katouno, F., Nikaidou, N., Nonaka, T., Sugiyama, J. and Watanabe, T. (2001). Roles of the exposed aromatic residues in crystalline chitin hydrolysis by chitinase A from *Serratia marcescens* 2170. **J. Biol. Chem.** 276: 41343-41349.
- van Aalten, D. M., Komander, D., Synst, B., Gaseidnes, S., Peter, M. G. and Eijsink, V. G. (2001). Structural insights into the catalytic mechanism of a family 18 exo-chitinase. **Proc. Natl. Acad. Sci. USA.** 98: 8979-8984.
- van Aalten, D. M., Synstad, B., Burberg, M. B., Hough, E., Riise, B. W., Eijsink, V. G. and Wierenga, R. K. (2000). Structure of a two-domain chitotriosidase from *Serratia marcescens* at 1.9-angstrom resolution. **Proc. Natl. Acad. Sci. USA.** 271: 253-262.
- van Scheltinga, A. C. T., Armand, S., Kalk, K. H., Isogai, A., Henrissat, B. and Dijkstra, B. W. (1995). Stereochemistry of chitin hydrolysis by a plant chitinase/lysozyme and X-ray structure of a complex with allsamidin: evidence for substrate assisted catalysis. **Biochemistry.** 34: 15619-15623.

- van Scheltinga, A. C. T., Kalk, K. H., Beintema, J. J. and Dijkstra, B. W. (1994). Crystal structures of hevamine, a plant defence protein with chitinase and lysozyme activity, and its complex with an inhibitor. **Structure**. 15: 1181-1189.
- Watanabe, T., Ariga, U., Sato, U., Toratani, T., Hashimoto, M., Nikaidou, N., Kezuka, Y., Nonaka, T. and Sugiyama, J. (2003). Aromatic residues within the substrate-binding cleft of *Bacillus circulans* chitinase A1 are essential for hydrolysis of crystalline chitin. **J. Biochem.** (Tokyo) 1: 237-244.
- Watanabe, T., Ishibashi, A., Ariga, Y., Hashimoto, M., Nikaidou, N., Sugiyama, J., Matsumoto, T. and Nonaka, T. (2001). Trp122 and Trp134 on the surface of the catalytic domain are essential for crystalline chitin hydrolysis by *Bacillus circulans* chitinase A1. **FEBS Lett.** 494: 74-78.
- Watanabe, T., Ito, Y., Yamada, T., Hashimoto, M., Sekine, S. and Tanaka, H. (1994). The roles of the C-terminal domain and type III domains of chitinase A1 from *Bacillus circulans* WL-12 in chitin degradation. **J. Bacteriol.** 176: 4465-4472.
- Watanabe, T., Kanai, R., Kawase, T., Tanabe, T., Mitsutomi, M. and Miyashita, K. (1999). Family 19 chitinases of *Streptomyces* species: characterization and distribution. **Microbiology**. 145: 3353-3363.
- Watanabe, T., Oyanagi, W., Suzuki, K. and Tanaka, H. (1990). Chitinase system of *Bacillus circulans* WL-12 and importance of chitinase A1 in chitin degradation. **J. Bacteriol.** 172: 4017-4022.
- Wills-Karp, M. and Karp, C. L. (2004). Chitin checking-novel insights into asthma. **N. Engl. J. Med.** 351: 1455-1457.

Zakariassen, H., Aam, B. B., Horn, J. S., Vårum, M. K., Sørlie, M. and Eijsink, G. H. V. (2009). Aromatic residues in the catalytic center of chitinase A from *Serratia marcescens* affect processivity, enzyme activity and biomass converting efficiency. **J. Biol. Chem.** 284: 10610-10617.





APPENDIX A

SOLUTION AND REAGENT PREPARATION

A.1 Solutions for DNA cloning

A.1.1 0.5 M Ethylenediaminetetraacetic acid (EDTA) pH 8.0 (100 ml)

Dissolve 18.61 g (MW=372.3 g/mol) of EDTA in distilled water to a volume 80 ml and adjust pH to 8.0 with HCl, then add distilled water to a final volume of 100 ml. Sterilize the solution by autoclaving at 120°C for 15 min. Store the solution at 4°C.

A.1.2 50X Tris-acetate Electrode Buffer (1000 ml)

Dissolve 242 g Tris-base, 57.1 ml glacial acetic acid and 100 ml 0.5 M EDTA, pH 8.0 in distilled water to a volume of 80 ml and adjust pH to 7.6-7.8, then add distilled water to a final volume of 1000 ml and store at 4°C.

A.1.3 6X DNA Loading Dye (10 ml)

Dissolve 0.025 g Bromophenol Blue, 0.025 g xylene cyanol and 3 ml 100% glycerol in distilled water to a final volume of 10 ml and store at -30°C.

A.1.4 1 M CaCl₂ (100 ml)

Dissolve 14.7 g (MW=147.02 g/mol) of CaCl₂ in distilled water to a volume of 100 ml. Sterilize the solution by autoclaving at 120°C for 15 min. Store the solution at 4°C.

A.2 Solutions for bacterial culture

A.2.1) LB Medium (1000 ml)

Dissolve 10g Bacto Tryptone, 5g Yeast Extract and 5g NaCl in distilled water 950 ml. Stir until the solutes have been dissolved. Adjust the volume of the solution 1000 ml with distilled water. Sterilize the solution by autoclaving at 120°C for 15 min and store at 4°C.

A.2.2) LB Plate (1000 ml)

Dissolve 10g Bacto Tryptone, 5g Yeast Extract, 5g NaCl and 15g Bacto agar in distilled water 950 ml. Stir until the solutes have been dissolved. Adjust the volume of the solution to 1000 ml with distilled water. Sterilize by autoclaving the solution at 120°C for 15 min. Pour medium into petri dishes. Allow the agar to harden, and store at 4°C.

A.2.3) LB Medium containing ampicillin (1000 ml)

Dissolve 10g Bacto Tryptone, 5g Yeast Extract and 5g NaCl in distilled water 950 ml. Stir until the solutes have been dissolved. Adjust the volume of the solution to 1000 ml with distilled water. Sterilize by autoclaving the solution at 120°C for 15 min. Allow the medium to cool to 50°C before adding ampicillin to a final concentration 100 µg/ml and store at 4°C.

A.2.4) LB Plate containing ampicillin (1000 ml)

Dissolve 10g Bacto Tryptone, 5g Yeast Extract, 5g NaCl and 15g Bacto agar in distilled water 950 ml. Stir until the solutes have been dissolved. Adjust the volume

of the solution to 1000 ml with distilled water. Sterilize by autoclaving the solution at 120°C for 15 min. Allow the medium to cool to 50°C before adding ampicillin to a final concentration 100 µg/ml. Pour medium into petri dishes. Allow the agar to harden, and store at 4°C.

A.2.5) 100 mg/ml Ampicillin

Dissolve 1 g ampicillin in sterile distilled water to a volume of 10 ml. Sterilize by filter the solution through a 0.2 µm cut-off membrane disc, aliquot and store at -30°C.

A.3 Solutions and buffers for protein expression and purification

A.3.1) 30% (w/v) Acrylamide Solution (100 ml)

Dissolve 29 g acrylamide and 1 g *N,N'*-methylend-bis-acrylamide in distilled water to a volume of 100 ml, mix the solution by string until the solution is homogenous and filter the solution through Whatman membrane No.1 and store in a dark bottle at 4°C.

A.3.2) 10% (w/v) Sodium Dodecyl Sulphate (SDS) (100 ml)

Dissolve 10 g SDS in distilled water to a volume of 100 ml and store at room temperature.

A.3.3) 10% (w/v) Ammonium Persulphate (10 ml)

Dissolve 1 g of ammonium persulphate in distilled water to a volume of 10 ml and aliquot and store at -30°C.

A.3.4) 1.5 M Tris-HCl, pH 8.8 (100 ml)

Dissolve 18.17 g (MW=121.14 g/mol) of Tris-base in distilled water to a volume of 80 ml and adjust pH to 8.8 with HCl, then add distilled water to a volume of 100 ml and store at 4°C.

A.3.5) 0.5 M Tris-HCl, pH 6.8 (100 ml)

Dissolve 6.05 g (MW=121.14 g/mol) of Tris-base in distilled water to a volume of 80 ml and adjust pH to 6.8 with HCl, then add distilled water to a final volume of 100 ml and store at 4°C.

A.3.6) Staining Solution (100 ml)

Dissolve 0.1 g of Coomassie Brilliant Blue R-250 in 40 ml methanol and 10 ml glacial acetic acid and distilled water to a final volume of 100 ml. Mix the solution by string to be homogenous and filter through Whatman membrane No.1 and store in the dark bottle at 4°C.

A.3.7) Destaining Solution I (500 ml)

Mix 200 ml of methanol and 35 ml of glacial acetic acid. Add distilled water to a volume of 500 ml and store in the dark at room temperature.

A.3.8) Destaining Solution II (500 ml)

Mix 25 ml of methanol and 35 ml of glacial acetic acid. Add distilled water to a volume of 500 ml and store in the dark at room temperature.

A.3.9) 10X Tris-Glycine Electrode Buffer or Laemmli Buffer (1000 ml)

Dissolve 30.3 g Tris-base (MW=121.14 g/mol), 144.0 g glycine and 10.0 g SDS in distilled water to a volume 1000 ml, mix the solution by string to be homogenous and store in the dark bottle at room temperature.

A.3.10) 30% (w/v) Glycerol (100 ml)

Dissolve 30 ml glycerol in distilled water to a volume of 100 ml. Sterilize by autoclaving the solution at 120°C for 15 min, and store at dark bottle at 4°C.

A.3.11) 3X Gel Loading Dye (10 ml)

1. Glycerol	3 ml
2. 1 M Tris-HCl, pH 6.8	2.4 ml
3. 20% SDS	3 ml
4. Bromophenol Blue	0.006 g
5. β -mercaptoethanol	1.6 ml

Add distilled water to a volume of 10 ml; mix the solution until homogenous, aliquot and store at -20°C.

A.3.12) 12% Separating Gel SDS-PAGE 10ml

Mix the solution as follow:

1. Distilled water	3.3 ml
2. 1.5 M Tris-HCl pH 8.8	2.5 ml
3. 10% (w/v) SDS	0.1 ml
4. 10% (w/v) ammonium persulphate	0.05 ml

5. 30% Acrylamide solution	4.0 ml
6. TEMED	10 μ l

A.3.13) 5% Stacking Gel SDS-PAGE 5 ml

Mix the solution as follows:

1. Distilled water	3.0 ml
2. 0.5 M Tris-HCl pH 6.8	1.25 ml
3. 10% (w/v) SDS	0.05 ml
4. 10% (w/v) ammonium persulphate	0.025 ml
5. 30% Acrylamide solution	0.655 ml
6. TEMED	10 μ l

A.3.14) 1 M Isopropyl thio- β -D-galactoside (IPTG) (10 ml)

Dissolve 2.38 g (MW=238.30 g/mol) IPTG in sterile distilled water to a volume of 10 ml. Sterilize by filter the solution through a 0.2 μ M cut-off membrane disc, aliquot and store at -30°C.

A.3.15) 1 M Tris-HCl, pH 8.0 (200 ml)

Dissolve 24.23 g (MW=121.14 g/mol) Tris-base in distilled water to a volume of 150 ml and adjust pH to 8.8 with HCl, then add distilled water to a volume of 200 ml. Sterilize by autoclaving the solution at 120°C for 15 min. and store at 4°C.

A.3.16) 1 M NaCl (200 ml)

Dissolve 11.68 g (MW=58.443 g/mol) NaCl in distilled water to a volume 150 ml. Stir until the solutes have been dissolved. Adjust the volume of the solution to of 200 ml with distilled water. Sterilize by autoclaving the solution at 120°C for 15 min and store at 4°C.

A.3.17) 100 mM Phenylmethanesulphonylfluoride (PMSF) (10 ml)

Dissolve 0.17 g (MW=174.19 g/mol) PMSF in absolute isopropanol to a volume of 10 ml. Sterilize by filter the solution through a 0.2 µm cut-off membrane disc, aliquot and store at -30°C.

A.3.18) Extraction Buffer (100 ml)

To prepare 100 ml solution, mix the stock solution as follows:

- 2 ml of 1 M Tris-HCl pH 8.0 (final concentration of 20 mM)
- 15 ml of 1M NaCl (final concentration of 150 mM)
- 1 ml of 100 mM PMSF (final concentration of 1 mM)
- 0.1g of lysozyme 1mg/ml (add freshly before use)

Add sterile distilled water to a volume of 100 ml and store at 4°C.

A.3.19) Equilibration Buffer (1000 ml)

To prepare 1000 ml solution, mix the stock solution as follow:

- 20 ml of 1 M Tris-HCl pH 8.0 (final concentration 20 mM)
- 150 ml of 1M NaCl (final concentration 150 mM)

Add sterile distilled water to a volume 1000 ml and store at 4°C.

A.3.20) Wash Buffer I containing 5 mM imidazole (500 ml)

Dissolve 0.1702 g (MW=68.08 g/mol) imidazole in 500 ml of equilibration buffer and store at 4°C.

A.3.21) Wash Buffer II containing 20 mM imidazole (500 ml)

Dissolve 0.6808 g (MW=68.08 g/mol) imidazole in 500 ml of equilibration buffer and store at 4°C.

A.3.22) Elution Buffer containing 250 mM imidazole (500 ml)

Dissolve 8.51 g (MW=68.08 g/mol) imidazole in 500 ml of equilibration buffer and store at 4°C.

A.3.23) Bradford Reagent (100 ml)

Dissolve 0.01g coomassie Brilliant Blue G in 5 ml ethanol and 10 ml 85% orthophosphoric acid and distilled water to a final volume of 100 ml. Mix the solution by string to be homogenous and filter through Whatman membrane No.1 and store in the dark bottle at 4°C.

A.4 Reagents and buffers for enzymatic studies**A.4.1) 3, 5-Dinitrosalicylic Acid (DNS) Reagent (500ml)**

Dissolve 5 g (w/v) DNS in 100 ml of 2 M NaOH and add 250 ml of 60 % (w/v) sodium potassium tartrate makes total volume to 500 ml with distilled water and store in the dark at 4°C.

A.4.2) 1 M Sodium Acetate Buffer, pH 5.5 (100 ml)

Dissolve 13.60 g (MW=136.08 g/mol) sodium acetate in distilled water to a volume of 80 ml and adjust pH to 5.5 with HCl, then add distilled water to a volume of 100 ml and store at 4°C.

A.4.3) 3 M Na₂CO₃ (50 ml)

Dissolve 15.89 g (MW=105.97 g/mol) Na₂CO₃ in distilled water to a volume of 100 ml and store at 4°C.

A.4.4) Aniline-diphenylamine Reagent (200 ml)

Dissolve 4 g diphenylamine in 200 ml acetone and 30 ml 85% orthophosphoric acid, and then add 4 ml aniline, mix the solution by string to be homogenous and store in the dark bottle at room temperature.

A.5 Solutions of substrates**A.5.1) Preparation of Glycol Chitin**

Glycol chitin was obtained by acetylation of glycol chitosan (Sigma–Aldrich Co., USA), by method of Trudel and Asselin (1989). 0.5 Grams of glycol chitosan was dissolved in 10 ml of 10% acetic acid by grinding in a mortar. The viscous solution was allowed to stand overnight at 22 °C. Methanol (45 ml) was slowly added and the solution was vacuum filtered through the Whatman no. 4 filter paper. The filtrate was transferred into a beaker and 0.75 ml of acetic anhydride as added with magnetic stirring. The resulting gel was allowed to stand for 30 min at room temperature and then cut into small pieces. The liquid extruding from the gel pieces

was discarded. Gel pieces were transferred to a warning blender, covered with methanol, and homogenized for 4 min at top speed. This suspension was centrifuged at 15,000g for 15 min at 4 °C. The gelatinous pellet was resuspended in about 1 vol of methanol, homogenized, and centrifuged as in the preceding step. The pellet was resuspended in distilled water (50 ml) containing 0.02% (w/v) sodium azide and homogenized for 4 min. This was the final 1% (w/v) stock solution of glycol chitin.

A.5.2) Preparation of Colloidal Chitin

Colloidal chitin was modified the method of Roberts and Selitrennikoff (1988). Twenty grams of chitin power from crab shells (Seikagaku Corporation, Tokyo, Japan) was added slowly into 350 ml of concentrated HCl and left at 4 °C overnight with vigorous stirring. The mixture was added to 2 liter of ice-cold 95% ethanol with rapid stirring and kept overnight at -35 °C. The precipitate was collected by centrifugation at 5000g for 20 min at 4 °C. The precipitate was washed with sterile distilled water until the colloidal chitin became neutral (pH 7.0).

A.5.3) 100 mM Chitobiose (Di-N-Acetyl- Chitobiose)

Dissolve 0.42 g (MW= 424.4 g/mol) chitobiose in sterilize distilled water to a volume of 10 ml and store at -30°C.

A.5.4) 100 mM Chitotriose (Tri-N-Acetyl- Chitotriose)

Dissolve 0.63 g (MW= 627.6 g/mol) chitotriose in sterilize distilled water to a volume of 10 ml and store at -30°C.

A.5.5) 100 mM Chitotetraose (Tetra-*N*-Acetyl- Chitotetraose)

Dissolve 0.83 g (MW= 830.8 g/mol) chitotetraose in sterilize distilled water to a volume of 10 ml and store at -30°C.

A.5.6) 100 mM Chitopentaose (Penta-*N*-Acetyl- Chitopentaose)

Dissolve 1.03 g (MW= 1,034.0 g/mol) chitopentaose in sterilize distilled water to a volume of 10 ml and store at -30°C.

A.5.7) 100 mM Chitohexaose (Hexa-*N*-Acetyl- Chitohexaose)

Dissolve 1.23 g (MW= 1,237.2 g/mol) chitohexaose in sterilize distilled water to a volume of 10 ml and store at -30°C.

A.5.8) 100 mM *p*-Nitrophenyl *N*-Acetyl- β -D-Glucosaminide

Dissolve 0.34 g (MW= 342.31 g/mol) *p*-Nitrophenyl *N*-Acetyl- β -D-Glucosaminide in sterilize distilled water to a volume of 10 ml and store at -30°C.

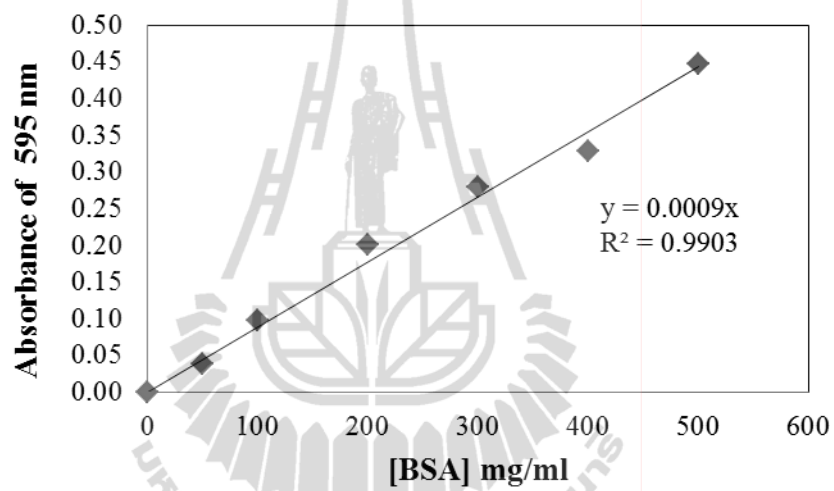
A.5.9) 100 mM *p*-Nitrophenyl Di-*N*-Acetyl-Chitobiside

Dissolve 0.54 g (MW= 545.5 g/mol) *p*-Nitrophenyl Di-*N*-Acetyl-Chitobiside in sterilize distilled water to a volume of 10 ml and store at -30°C.

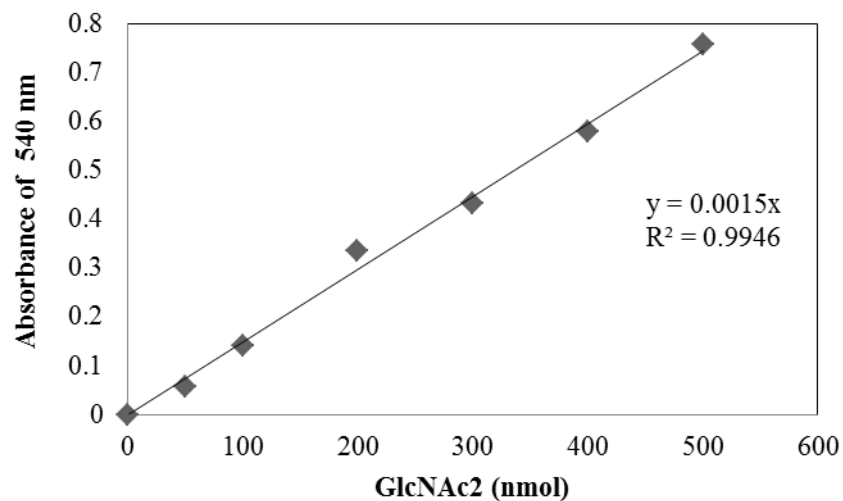
APPENDIX B

STRANDEDE CURVEDS

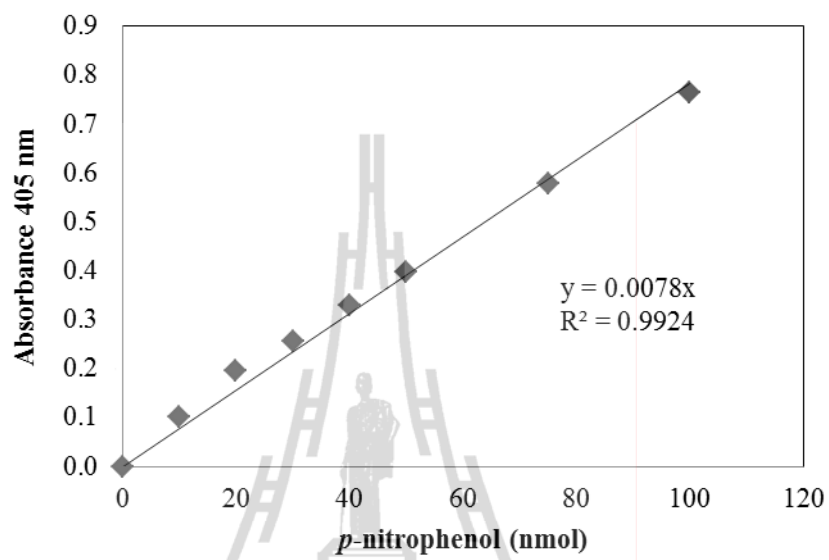
B.1 Stranded curve of BSA by Bradford's method



B.2 Stranded curve of GlcNAc₂ by DNS reagent



B.3 Stranded curve of *p*-nitrophenol



APPENDIX C

ABSTRACT SUBMIT

C.1 Sritho, N., Songsirittigul, C., and Suginta, W. (2008). Mutational analysis of the reducing-end binding residues of chitinase A from *Vibrio harveyi*. The 3th annual symposium of protein society of Thailand challenges in protein research in Thailand, Convention Center, Chulabhorn Research Institute, Bangkok, Thailand, Poster presentation.

C.2 Sritho, N., and Suginta, W. (2009). Mutational analysis of the active site residues Aspartate 313 and Tyrosine 435 of chitinase A from a marine bacterium *Vibrio harveyi*. 2nd SUT graduate Conference. Suranaree University of Technology, Poster presentation.

C.3 Sritho, N., and Suginta, W. (2009). Effects of active site residues aspartate 313 and tyrosine 435 in *Vibrio harveyi* chitinase A on chitin hydrolysis. The 4th annual symposium of protein society of Thailand, Protein research: From basic studies to applications in health sciences. Convention Center, Chulabhorn Research Institute, Bangkok, Thailand, Poster presentation.

C.4 Sritho, N., Pantoon, S. and Suginta, W. (2010). Role of aspartate 313 and tyrosine 435 of *Vibrio harveyi* chitinase A on chitin hydrolysis. The 5th Annual Symposium of Protein Society of Thailand, Protein research: From basic approaches to modern technologies. Convention Center, Chulabhorn Research Institute, Bangkok, Thailand, Poster presentation.

CURRICULUM VITAE

Name	Miss Natchanok Sritho
Date of Birth	9 December 1984
Place of Birth	Ubon-Ratchathani, Thailand
Education	<p>2003-2006, Bachelor of Science (Crop Production Technology), Suranaree University of Technology, Nakhon Ratchasima, Thailand.</p> <p>2007-2009, Master of Science (Biochemistry), Suranaree University of Technology, Nakhon Ratchasima, Thailand.</p>
Grant and Fellowship	<p>2009, Graduate Research Grant, Suranaree University of Technology, Nakhon Ratchasima, Thailand.</p>
Employment	<p>2008-2010, Biochemistry Teaching Assistant, Suranaree University of Technology, Nakhon Ratchasima, Thailand.</p>